Preparation and Characterisation of Polymer Microparticles with Varying Morphologies with Application in Drug Delivery

By Ana Letícia Braz de Sousa

Thesis submitted to the

University of Nottingham

for the Degree of Doctor of Philosophy

May 2019

Abstract

Polymer-based particles of varied porosity, roughness and morphology have been prepared by many different methods towards biomedical applications. One of their most important applications is as degradable and targeted drug delivery systems, with reduced toxicity and side effects compared to their solid counterparts. Polymeric carriers loaded with chemotherapeutic agents have been applied in the treatment of glioblastoma (brain cancer, GBM) in an attempt to overcome the systemic toxicity, low drug solubility and poor efficacy of current treatments.

In this work, polymeric microparticles (MPs) of poly(lactide) (PLA) and poly (lactide-*co*-glycolide) (PLGA) of various controlled morphologies have been developed with the capability to deliver a sustained release system loaded with cancer therapeutics against GBM cell proliferation and growth.

In experimental Chapter 2 a family of different porous polymeric microparticles with controlled size were produced *via* single emulsion processing, incorporating a porogen. The produced porous PLA and PLGA particles were determined to be in the size range 34 to 320 μm and exhibited homogeneous pore distribution throughout their particle structures. Particles encapsulated with dye exhibited encapsulation efficiency (EE) up to 21.6 $\pm$ 5.4%, whereas particles encapsulated with drug exhibited EE up to 56 $\pm$ 41%. Highly porous PLA particles (particle type C in this work) encapsulated with sodium chloride

methotrexate and non-porous PLA particles (particle type A) and non-porous PLGA particles (particle type A') encapsulated with docetaxel showed a significant difference in terms of therapeutic release in comparison to the other morphologies due the difference in the particle morphology and hydrophicility of the drug entrapped in the polymeric matrix($p>0.05$). Particles alone and free drug were subsequently tested *in vitro* to test their toxicity at 24h. Particles alone exhibited a lack of toxicity and drugs alone showed a limited specificity for GBM cells (U87 cell line). The multi-therapy paste formulations including therapy 2 (PLGA MPs, PLGA-PEG matrix and DTX) and therapy 5 (PLA MPS and ETP, PLGA-PEG matrix and DTX) showed a significant difference when compared with control 1(PLA MPs alone), control 2 (PLGA MPs alone) and control 3 (PLGA-PEG matrix alone) over the 30-day investigation period ($p<0.0001$).

In experimental Chapter 3, polymeric tablets were developed by mixing spherical PLA and PLGA MPs with non-spherical PLGA/polyethylene glycol (PEG) particles to achieve controlled and sustained release, and prolong the treatment against U87 cells. Mid porous PLA particles (particle type B) loaded with Nile Blue (NB) showed significant difference compared to non-porous PLA particles (particle type A), non-porous PLGA particles (particle type A') and mid porous PLGA particles (particle type B') ($p<0.0001$). Furthermore, these PLA and PLGA particles mentioned above exhibited controlled and sustained release over time, whereas the PLGA-PEG matrix exhibited burst release. U87 cells were

subsequently treated with therapy 5 (tablet formulations), which demonstrated continuous reduction in cell viability over a 30-day period ($p<0.0001$).

In conclusion, it is shown that polymeric MPs varying in their morphology have different surface areas and degradation rates, strongly influenced by the level of particle porosity. The release rate of active components is correlated with polymeric matrix composition and drug hydrophobicity. Porous polymeric carriers are a useful strategy for the controlled sustained release of active components such as chemotherapeutic drugs promoted by the slow release of dye and drugs. The development of polymeric paste and tablets herein prolonged the drug release from a PLGA-PEG matrix. Importantly, the tablet formulations (therapy 5) developed in this work can potentially control the proliferation and growth of U87 cells.

Acknowledgements

I would like to thank my main and co-supervisor, Dr Ifty Ahmed and Prof Derek Irvine for their assistance. I express my gratitude and appreciation to my co-supervisors, Prof Cameron Alexander and Dr Ruman Raman for all their valuable discussions with me, for challenging me, for their guidance and support, the provision of lab consumables and for providing me access to some of the best equipment available in the University of Nottingham. I also thank Prof David Grant for his support and assistance throughout my PhD.

I thank the post-docs, research fellows and technicians from the following: Advanced Materials Research Group; Division of Molecular Therapeutics and Formulation; Children Brain Research Group; Nanocenter and Slim laboratory for their assistance and valuable discussion. In particular, I thank Dr Reda Felfel, Dr Andy Parsons, Dr Claudia Conte, Dr Tatiana Lovato, Dr Giovanna Sicilia, Mr Paul Cooling, Mr Colin Rowe, Mrs. Julia Crouch, Mrs Carol Turrill, Dr Toby Gould, Dr Jonathan Rowlinson, Dr Maria Cebrero, Dr Rebecca Chapman, Mr Martin Roe, Mr Nigel Neate, Mr Ian Ward, Mr Christopher Gell and Mrs Denise Mclean.

I also give a special thanks to the students from Advanced Materials Research Group, Division of Molecular Therapeutics and Formulation, B15 lab and B28 office (Boots Building) for their support, valuable

discussion, friendship and good memories, both in and out of University. In particular I thank, Dr Uresha Patel, Dr Nusrat Sharmin, Miss Caitriona McCarron and Dr Patricia Monteiro for their support and friendship.

I am grateful to the University of Nottingham (UK) and Capes (Brazil) for awarding my PhD scholarship and sponsoring my studies (Grant number: 99999.003552/2014-04). I acknowledge the support of MeDe Innovation (UK) for sponsoring part of my project and the Royal Society of Chemistry – Materials Chemistry Division for awarding a travel grant that enabled me to present the finding from this work at the ICMAT conference in Singapore, June 2019.

Most importantly, I would like to express my gratitude to my British family, father-in-law and mother-in-law; Dr Joe Blaker and Mrs Juliet Blaker, my Brazilian family, mother, sister and grandmother; Mrs Virgínia Braz, Miss Ingrid Braz and Mrs Letícia Gonçalves for their care, love and support and last but not least, my husband; Prof Jonny Blaker for his unconditional support, love and for taking me on the best adventures in my life.

The results presented in this thesis have contributed towards the following paper and presentations:

Review Article:

Braz, A.L., Ahmed, I. *Manufacturing processes for polymeric micro and nanoparticles and their biomedical applications.* AIMS Bioeng, 4(1):46-72, 16 January 2017, DOI: 10.3934/bioeng.2017.1.46

Research Article:

Braz, A.L., Mautner, A., Ahmed, I., Rahman, R. and Alexander, C. *Multi-therapy agent against proliferation and growth of GBM cells.* (to be submitted)

Oral presentations (national and international) delivered by the author:

1. **Braz, A. L;** Mautner, A; Ahmed, I; Rahman, R; Alexander, C., "Polymeric Microparticles as a Dual Therapy for Glioblastoma Treatment". *10th International Conference on Materials for Advanced Technologies (ICMAT)*, Marina Bay Sands, Singapore. June 2019.
2. **Braz, A. L**; Ahmed, I; Rahman, R.; Alexander, C., "Development of controlled drug and gene therapy for brain cancer". *Advanced Materials Research Group Day Meeting*, University of Nottingham, UK March, 2018. 3 Minutes Thesis Presentation
3. **Braz, A. L**; Ahmed, I; Rahman, R., Alexander, C., "The challenges of polymeric particles development, their physical characterization and biological application". *Royal Society of Chemistry Annual Meeting*, University of Bradford, UK. January 2018
4. **Braz, A. L**; Ahmed, I; Alexander, C., "The main challenges of polymeric particles development and their physical characterisation". *Polymeric Advanced Technology Conference*, University of Manchester, UK. September 2017
5. **Braz, A.L**; Irvine, D.; Ahmed, I., *'Porous polymer microparticles for targeted delivery and release of pharmaceutical agents'. Advanced Materials Research Group Meeting*, University of Nottingham, UK. *September 2016*
6. **Braz, A.L**; Irvine, D.; Ahmed, I., *'Porous degradable polymer microspheres for drug delivery'* Brazilian consulate – **ABEP-UK (Associação de Brasileiros Estudantes de Pós-Graduação)*, Brazilian Consulate, London, UK. *May 2016*
7. **Braz, A.L**; Irvine, D; Hewakandamby, B; Ahmed, I., '*Porous polymer micro/nanospheres for targeted delivery and release of pharmaceutical agents and gene therapies derived from synthetic biology'. AMRG research day*, University of Nottingham, Nottingham, UK. *March 2016*
8. **Braz, A.L**; Ahmed, I., *'Controlling porosity of microspheres for drug delivery'. Medical Technology Meeting*, University of Nottingham, Boots Building, Nottingham, UK. *February 2016*

Poster presentations (national and international) under author supervision* and delivered by the author:

1. Affendy, F. N., Alrowili, D., **Sousa, A.L.B.**, Alexander, C., "Preparation and characterization of PLGA microparticles: non-loaded and loaded with dye". *Graduates Meeting*, Trent Senate Chamber, Trent Building, University Park, University of Nottingham, UK, April 2019.*
2. Alrowili, G; Affendy, F, **Braz, A.L.**, Alexander, C., "Preparation and characterization of non-loaded and dye-loaded PLGA microparticles with varying levels of porosity". *Graduates Meeting*, Trent Senate Chamber, Trent Building, University Park, University of Nottingham UK, April 2019.*
3. **Braz, A.L.**; Irvine, D; Hewakandamby, B; Ahmed, I., *'Controlling shapes, size and porosity for controlled drug delivery'. * Centre for Healthcare Technologies*, University of Nottingham, Jubilee Campus, Nottingham, UK. *February 2016*

List of Figures and Tables

List of Figures

CHAPTER 1

Figure 1.1: The chemical structure of some typical relevant natural and synthetic polymers used for drug delivery applications…….....6

Figure 1.2: Representation of the phase diagram of a polymer solution, spinodal and binodal behaviour [101]……...…...17

Figure 1.3: Behaviour of single and double emulsion within different compositions and transition points represented by the Winsor regions…….19

Figure 1.4: Micro size spheres produced without surfactant (A) and formulation with presence of surfactant (B) [37]……...20

Figure 1.5: Schematic representation of brain cancer, grade levels, current treatments to control the GBM cells proliferation, and perspective on local delivery treatment……29

CHAPTER 2

Figure 2.1: Polymeric microparticles of PLA and PLGA made with various levels of porosity via single emulsion process. Difference of porous structure between PLA particles (A, B, C, and E) and PLGA particles (A' B' and C'). High magnification cryo-SEM images (cross-

sections) of the PLA microparticle structure evidencing pore distribution and differences in pore sizes…….……69

Figure 2.2: Determination of the size distribution of the polymeric microparticles (PLA and PLGA MPs) by DLS (n=3)……..70

Figure 2.3: Particle size and pore size assessment of PLA and PLGA MPs by SEM and Cryo-SEM, respectively (n=3) (p<0.0001 ordinary one-way ANOVA: A *vs.* B, C, D and E; A' *vs.* B' and C')……71

Figure 2.4: Surface area and density of PLA and PLGA MPs measured by BET and helium pycnometry, respectively (n=3) (p<0.0001 ordinary one-way ANOVA: A *vs*. B, C, D and E; A' *vs.* B' and C')..72

Figure 2.5: Level of porosity of PLA and PLGA MPs represented by the quantity of gas adsorbed to the polymeric MPs determined by BET……..73

Figure 2.6: SEM analysis of the morphological changes of PLA particles as function of time exposed to buffered solution over 3 h (scale bars: 500 μm, 100 μm, 20 μm, 10 μm and 5 μm -insets)……..76

Figure 2.7: SEM analysis of the morphological changes of PLA particles as function of time exposed to buffered solution over 24 h (scale bars: 500 μm, 200 μm, 100 μm, 50 μm, 20 μm and 10 μm - insets)…….....77

Figure 2.8: SEM analysis of the morphological changes of PLGA particles as function of time exposed to buffered solution over 3 h (scale bars: 500 μm, 200 μm, 100 μm, 50 μm, 20 μm and 5 μm - insets)…….....78

Figure 2.9: SEM analysis of the morphological changes of PLGA particles as function of time exposed to buffered solution over 24 h (scale bars: 500 μm, 200 μm, 100 μm, 50 μm and 5 μm -insets)….. 79
Figure 2.10: SEM analysis of the morphological changes of PLA particles as function of time exposed to buffered solution over 7 days (scale bars: 500 μm, 200 μm, 100 μm, 20 μm and 10 μm - insets)…….....80
Figure 2.11: SEM analysis of the morphological changes of PLA particles as function of time exposed to buffered solution over 15 days (scale bars: 500 μm, 200 μm, 50 μm, 20 μm and 10 μm - insets)…….....81
Figure 2.12: SEM analysis of the morphological changes of PLGA particles as function of time exposed to buffered solution over 7 days (scale bars: 500 μm, 200 μm, 100 μm, 50 μm, 20 μm and 5 μm - insets)…….....82
Figure 2.13: SEM analysis of the morphological changes of PLGA particles as function of time exposed to buffered solution over 15 days (scale bars: 500 μm, 200 μm, 100 μm, 50 μm, 20 μm, 10 μm and 2 μm -insets)…….....83
Figure 2.14: SEM analysis of the morphological changes of PLA particles as function of time exposed to buffered solution over 30 days (scale bars: 500 μm, 200 μm, 100 μm, 50 μm, 20 μm and 10 μm - insets)…….....84
Figure 2.15: SEM analysis of the morphological changes of PLA particles as function of time exposed to buffered solution over 45 days

(scale bars: 500 μm, 200 μm, 100 μm, 50 μm and 20 μm - insets)…….....85

Figure 2.16: SEM analysis of the morphological changes of PLGA particles as function of time exposed to buffered solution over 30 days (scale bars: 500 μm, 200 μm, 100 μm, 50 μm, 20 μm, 10 μm and 5 μm -insets)…….....86

Figure 2.17: SEM analysis of the morphological changes of PLGA particles as function of time exposed to buffered solution over 45 days (scale bars: 500 μm, 200 μm, 50 μm, 20 μm and 10 μm - insets)…….....87

Figure 2.18: Schematic of the single emulsion process developed, showing organic phase into water phase (I) followed by the aggregation of molecules during the emulsification step (II) and formation of the porous particles (III). …….…...91

Figure 2.19: Polymeric microparticles exhibiting different levels of porosity, interaction between pores and gas flow (grey arrow and circle) between external and internal region. (A) Disconnected and/or non-porous structure showing monolayer adsorption), (D) connected pores show the gas flow along the internal region of microparticles and (E) particles with two size types of connected pores [1, 2].The gas starts to fill the particles surface as indicated by the red arrow while the gas inner particle adsorption in indicated by the grey arrow (particles D and E)……....95

CHAPTER 3

Figure 3.1: Diagram depicting the issues surrounding the use of synthetic polymers as biomaterials and features desirable to achieve an ideal local delivery system for brain cancer treatment……..……100

Figure 3.2: Summary of the local drug delivery systems investigated in this work as an initial screening study for localised therapy to overcome the poor prognosis of current GBM therapies……...106

Figure 3.3: Size distribution of PLA spherical microparticles with variable morphology encapsulated with Nile Blue, SMTX, ETP or DTX, as determined by DLS (n=3)……....119

Figure 3.4: Size distribution of PLGA spherical microparticles with variable morphology encapsulated with Nile Blue, SMTX, ETP or DTX, as determined by DLS (n=3)……....119

Figure 3.5: *In vitro* cumulative release profile of active agents encapsulated in PLA particles. Release study of spherical PLA microparticles encapsulated with Nile Blue, S.MTX, ETP or DTX over time. Error bars represent a confidence interval of 95% (n=3) ($p<0.05$: NB and ETP release, $p>0.05$: S.MTX and DTX release on-way ANOVA with Bartlett's test)……125

Figure 3.6: *In vitro* cumulative release profile of active agents loaded into PLGA microparticles. Release study of spherical PLGA microparticles encapsulated with Nile Blue, S.MTX, ETP and DTX over time. Error bars represent a confidence interval of 95% (n=3) ($p<0.05$: NB, S.MTX and ETP release; $p>0.05$ DTX release one-way ANOVA with Bartlett's test)……...126

Figure 3.7: *In vitro* cumulative release profile of active agents loaded into paste formulation. Release study of polymeric paste containing blank PLGA/PEG matrix and PLA microparticles loaded with Nile Blue, S MTX, ETP and DTX. Error bars represent a confidence interval of 95% (n=3) ($p<0.05$: S.MTX and ETP release; $p>0.05$: NB and DTX release one-way ANOVA with Bartlett's test)……128

Figure 3.8: *In vitro* cumulative release profile of active agents loaded into paste formulation. Release study of polymeric paste containing blank PLGA/PEG matrix and PLGA spherical particles of varying morphology loaded with Nile Blue, S MTX, ETP and DTX. Error bars represent a confidence interval of 95% (n=3) ($p<0.05$: S.MTX and ETP release; $p>0.05$: NB and DTX release one-way ANOVA with Bartlett's test)…….129

Figure 3.9: Multi-therapy system developed as a paste formulation for localised therapy against GBM cells proliferation and growth…….....130

Figure 3.10: Cytotoxicity evaluation of polymeric microparticles alone. U87 cells were assessed for viability after seeding onto non loaded particles. Error bars represent a confidence interval of 95% (n=3). ($p<0.05$: PLGA MPs *vs.* PLGA/PEG MPs one-way ANOVA with Bartlett's test)…….....131

Figure 3.11: Cell viability of free drug. U87 cells were assessed for viability after seeding onto free drug solution at 50 μg/mL. Error bars represent a confidence interval of 95% (n=3) (no significant difference was shown: one-way ANOVA with Bartlett's test)……...131

Figure 3.12: Cytotoxicity of active agents released from PLGA/PEG paste. U87 cells were assessed for viability after seeding onto pre-selected paste loaded with chemotherapeutic drug to determine cytotoxic properties of released agents over 24 h. Error bars represent a confidence interval of 95% (n=3) (****p<0.0001 one-way ANOVA with Bartlett's test)…….....132

Figure 3.13: Cytotoxicity of active agents released from PLGA/PEG paste. U87 cells were assessed for viability after seeding onto pre-selected paste loaded with chemotherapeutic drug to determine cytotoxic properties of released agents from 72 h up to 30 days. Error bars represent a confidence interval of 95% (n=3) (****p<0.0001 one-way ANOVA with Bartlett's test)……..……....132

Figure 3.14: Analysis of PLA and PLGA particles mixed with PLGA/PEG matrix forming a pharmaceutical tablet in buffered solution over 3 h by SEM (Scale bars: 1 mm, 500 μm and 200 μm-inset)…….....134

Figure 3.15: Analysis of PLA and PLGA particles mixed with PLGA/PEG matrix forming a pharmaceutical tablet in buffered solution over 7 days by SEM (Scale bars: 1 mm, 500 μm and 200 μm - inset)……...135

Figure 3.16: Analysis of PLA and PLGA particles mixed with PLGA/PEG matrix forming a pharmaceutical tablet in buffered solution over 30 days by SEM (Scale bars: 1 mm, 500 μm and 200 μm - inset)…….....135

Figure 3.17: *In vitro* cumulative release profile of active agents loaded into tablets formulation. Measurement of active components released from spherical microparticles (*i.e.* Nile Blue and S.MTX) and PLGA/PEG matrix (*i.e.* DTX) over 30 days of study. Error bars represent a confidence interval of 95% (n=3) ($p<0.05$: PLGA/PLA S.MTX and PLGA-PEG DTX release; $p>0.05$: PLGA/PLA NB release one-way ANOVA with Bartlett's test)…….....137

Figure 3.18: Multi-therapy system developed as tablets formulation for localised treatment against GBM cell proliferation and growth……138

Figure 3.19: Cytotoxicity of active agents released from tablet-based formulations. U87 cells were assessed for viability after seeding onto pre-selected tablets loaded with chemotherapeutic drug to determine cytotoxic properties of released agent over 24h. Error bars represent a confidence interval of 95% (n=3) (**** $p<0.0001$ one-way ANOVA with Bartlett's test)…….139

Figure 3.20: Cytotoxicity of active agents released from tablets formulation. U87 cells were assessed for viability after seeding onto pre-selected tablets loaded with chemotherapeutic drug to determine cytotoxic properties of released agent from 72 h up to 30 days. Error bars represent a confidence interval of 95% (n=3) (**** $p<0.0001$ one-way ANOVA with Bartlett's test)…….139

List of Tables

CHAPTER 1

Table 1.1: Applications of micro/nano particles for therapeutic delivery……...4

Table 1.2: Advantages and disadvantages of electrospray and electrospinning process to produce particles and fibres [78, 81-83]…13

Table 1.3: Summary of porogens used to form porous polymeric particles formulations and varyiance in their morphology……...25

CHAPTER 2

Table 2.1: Development of polymeric microparticles formulations under varied conditions such as type of polymer and PVA used, injection speed, porogen and energy applied to the system ……61

Table 2.2: Key formulation and production parameters for the families of non-porous and porous PLA and PLGA microparticles, their size ranges and yields …….....67

Table 2.3: Summary of the morphological changes of PLA (A,B and C) and PLGA (A', B' and C') microparticles, followed over a 45-day period, and determined using Image J analysis of electron microscopy images ……..…88

CHAPTER 3

Table 3.1: Schematic representation of the chemotherapeutic drugs used in this study and their log P…….109

Table 3.2: Amount of dye encapsulated in the spherical polymeric microparticles with variable morphology and dye concentration, determined using UV-Vis spectroscopy (n=1)……...121

Table 3.3: Amount of dye encapsulated in the spherical polymeric microparticles with variable morphology, determined using UV-Vis spectroscopy (n=3)……...122

Table 3.4: Amount of chemotherapeutic drug encapsulated in the spherical polymeric microparticles varying their morphology as determined using HPLC (n=3)……...……123

List of Symbols and Abbreviations

μL: Microlitres

μm: Micrometres

Å: Angstroms

BBB: Blood Brain Barrier

BCNU: Carmustine

BET: Brunauer-Emmett-Teller Theory

BTB: Blood Brain Tumour Barrier

CNS: Central Nervous System

Cryo-SEM: Cryo- Scanning Electron Microscopy

CS: Chitosan

DCM: Dichloromethane

DI: Deionised water

DLS: Dynamic Light Scattering

DMEM: Dulbecco's Modified Eagle Medium

DMSO: Dimethyl Sulphoxide

DNA: Deoxyribonucleic acid

DTX: Docetaxel

EPR: Permeability and retention effect

ETP: Etoposide

FBS: Fetal Bovine Serum

GBM: Glioblastoma

GSC: Glioblastoma stem cells

HLB: Hydrophilic-lipophilic balance

h: Hours

IOP: Intra ocular pressure

kg: Kilograms

m^2: Square metres

mg: Milligrams

mL: Millilitres

MPs: Microparticles

Mw: Molecular weight

NB: Nile Blue

nm: Nanometres

o/w: Oil-in-water

o/w/w: Oil-in-water-in-water

PCL: Poly(ε-caprolactone)

PEG: Polyethylene glycol

δ: Permeability

PLA: Polylactide

PLGA-PEG: poly(lactide-*co*-glycolide) and polyethylene glycol

PLGA: Poly(lactide-*co*-glycolide)

PMPs: Polymeric microparticles

PTFE: Polytetrafluoroethylene

PTX: Paclitaxel

PVA: Polyvinyl alcohol

RNA: Ribonucleic acid

s: Seconds

S.MTX: Methotrexate Sodium Salt

SBS: Solution Blow Spinning

SD: Standard deviation

SEM: Scanning Electron Microscopy

siRNA: Small interferin ribonucleic acid

TJs: Tight junctions

TMZ: Temozolomide

TOMAC: Trioctylmethylammonium chloride

VP: Verteporfin

w/o: Water-in-oil

w/o/w: Water-in-oil-in-water

Table of Contents

Abstract.....i

Acknowledgments.....iv

Contribution of the work to papers and presentations.....vi

List of Figures and Tables.....viii

List of Figures.....viii

List of Tables.....xvi

List of Symbols and Abbreviations.....xviii

CHAPTER 1 Introduction 1

1.1 Literature review 1

1.1.1 Methods to Produce Polymeric Microparticles 7

1.1.1.1 The spray-drying process and influence of parameters on particles formation 8

1.1.1.2 Electrospray and electrospinning technique.....10

1.1.1.3 Solution blow spinning/ atomisation method 15

1.1.1.4 Single and double emulsion 18

1.1.2 Porous Polymeric Microparticles 21

1.1.2.1 Shape, size and porosity 21

1.1.2.2 Delivery systems and biological applications ...26

1.1.3 Brain Tumour – Glioblastoma 28

1.1.3.1 The blood- brain- barrier and drug delivery systems.....33

1.1.3.2 Polymeric microparticles as a carrier for GBM treatment 37

1.1.3.3 Local delivery system: a pharmaceutical perspective 39

1.1.3.4 Glioblastoma and local delivery systems.....42

1.1.3.5 The future perspectives for GBM treatment.....47

1.2 Aim and Objective 48

1.3 Thesis structure 50

CHAPTER 2. Development of polymeric microparticles made with poly (lactide) (PLA) and poly (lactide-co-glycolide) (PLGA) with varying morphology 53

2.1 Introduction 53

2.2 MATERIALS AND METHODS 59
2.2.1 Materials 59
2.2.2 Microparticles preparation 60
2.2.3 Evaluation of Particle Morphology 61
2.2.4 Process Yield 62
2.2.5 Particle Size Distribution 62
2.2.6 Level of porosity and pores distribution 63
2.2.7 Particles density and Surface Area 64
2.2.7.1 Helium Pycnometry 64
2.2.8 Degradation study of PLA and PLGA microparticles 65
2.3 Results 66
2.3.1 Morphologically characterisation and particle size analysis 66
.....70
2.3.2 Level of porosity and particles density determination 70
2.3.3 Study of polymeric microparticles degradation behaviours *in vitro* buffered solutions over 45-day periods 73
2.4 Discussion 89
2.4.1 Morphological characterisation and particle size analysis 89
2.4.2 Level of particle porosity and particles density 91
.....95
2.4.3 Study of the morphological changes to the polymeric microparticles during *in vitro* assessment in buffered solution over 45-day period 95
2.5 Conclusions 97

CHAPTER 3. Development of a dual-therapy system for brain cancer treatment 100
3.1 Introduction 100
3.2 Materials and Methods.....108
3.2.1 Materials 108
3.2.2 Particle Size Distribution 108
3.2.3 Dye loaded into microparticles 108
3.2.3.1 Quantification of particles loaded with dye 109
3.2.4 Drug encapsulation into microparticles 109
3.2.4.1 Quantification and encapsulation efficiency of drug loaded particles 111

3.2.5 Polymer blend preparation 112
3.2.6 Paste formulation preparation..... 113
3.2.7 Tablet formulations preparation 114
3.2.8 Release study of loaded Nile Blue and chemotherapeutic drug 115
3.2.9 Cell culture 116
3.3 Results 118
3.3.1 Development and physicochemical characterisation of dye and drug-loaded polymeric microparticles with variable porosity 118
3.3.2 Development of a biodegradable polymeric paste formulation as a proof of concept for a local multi therapy system for GBM 127
3.3.3 Development of tablet formulations as a local multi-therapy system for GBM 134
3.4 Discussion 140
3.5 Conclusion 153

CHAPTER 4. Final Conclusions and Future Prospects 157
4.1 Technologies to develop spherical microparticles and the biological application..... 157
4.2 Local drug delivery systems and GBM treatment..... 158
4.3 Development of PLA and PLGA microparticles varying their morphology 159
4.4 Multi-therapy system and the efficacy of the local treatment 161
4.5 Future perspectives 164
REFERENCES..... 165

CHAPTER 1 Introduction

1.1 Literature review

Polymer-based particles have received considerable attention over the last few years for biomedical applications, especially when considering degradable materials for drug delivery. Polymeric micro- and nanoparticles of varying features such as particle porosity, roughness and morphology have been produced by different types of manufacturing processes (*i.e.* single and double emulsion systems, as well as spray drying) [3, 4]. The size of the particles also determines their applicability and has enabled use in controlled drug release against cancer, diabetes, malaria and many other disease indications [5].

Spherical polymeric micro and nanoparticles are the most common carriers used for many biomedical and pharmaceutical applications varying their size and morphology (*i.e.* level of porosity) [6]. It is well known that the level of porosity and interconnectivity between the pores found in the particles can modify drug release rate, in part due to access of drug diffusion and degradation from the polymeric matrix [7]. Release rates can also be tuned by addition of porogen into the organic phase [8, 9].

Microparticles have been used as drug delivery carriers to target specific sites in the body whilst protecting the drugs from physiological environments (*i.e.* drug metabolism), controlling their release rates (thereby improving the efficacy of conventional dosage

forms) and reducing toxicity and side effects [10, 11]. Furthermore, these drug delivery vehicles can help improve patient compliance and potentially control drug clearance, *e.g.* by the renal system [12].

World-wide, many researchers are interested in developing devices with improved chemotherapeutic drug solubility and diffusion rates through tissue and cells, and in developing mechanisms for local delivery systems (*i.e.* pharmaceutical formulations for local delivery) in order to improve patient outcome, and reduce toxicity and side effects caused by chemotherapy treatment [13]. Several biomedical materials have been investigated as microparticle carriers for drug delivery (*i.e.* PLGA, PLA, PEG and poly-ε-caprolactone: PCL) owing to their suitable chemical and physical properties. Some of these carriers have been translated to the market and used for pre-clinical studies and clinical treatments, such as Gliadel® wafers (*i.e.* GBM treatment), Corning® microcarriers (*i.e.* for cells expansion), SynBiosys® Merck (*i.e.* a biodegradable polymer platform for sustained release in the biological environment and as injectable formulations), Mobius® Merck (*i.e.* for growth of human mesenchymal cells), Cultispher® Sigma-Aldrich (*i.e.* for anchorage-dependent cells), Cytodex® Sigma-Aldrich (*i.e.* general microcarrier for culture), Foradil® Novartis and Bricanyl® AstraZeneca UK (*i.e.* asthma and pulmonary disease), Atridox® DenMat (*i.e.* for periodontal treatment), Sandostatin® Novartis (*i.e.* for acromegaly treatment) and Lupron depot® (*i.e.* for prostate cancer and endometriosis).

The characteristics of particles developed for biomedical applications must be carefully selected to determine their stability and efficiency. As well as considering the drug delivery aspect, it is also necessary to consider the residence time of the particles in the body, which tissues they will reside in, how they will be removed from the body, *e.g.* broken down and metabolised (enzymatic routes) or excreted [3] . Depending on the size of the particles, they can be used to specifically target channels on cell surfaces or be engulfed to deliver drugs from within the cell [14, 15]. They can also be delivered to specific vessels and capillaries in the bloodstream or even to the respiratory tract as an aerosol formulation [9, 14, 15]. Nanoscale materials in particular have been studied extensively as particulate carriers for several pharmaceutical and medical applications [12]. Table 2.1 provides an overview of the particles developed, their sizes and relevant target indications.

Sub-micron sized particles offer a number of distinct advantages over their microparticle counterparts. The principal advantage is the general relatively higher intracellular uptake of nanoparticles compared to microparticles due to their size. However, micro-sized particles can exhibit slow drug release profile due the surface area of the particles, decreased degradation rate and control the sustained release of drug over time from the polymeric matrix [3, 4, 16-18].

Spherical particles of both natural and synthetic biodegradable polymers, lipids and polysaccharides have been extensively studied

[19]. Some of the nanoparticles have been developed as injectable drug delivery systems, which require a size range between 5 nm to 250 nm. Their size is one of the most important physical parameters as this can alter the biological function of the injected particles and their circulation between veins and capillaries. In addition, these particles have the ability to flow in the blood stream and target pathological tissues such as tumours [20], whilst microparticles have been used for localized drug delivery [21].

Table 1.1: Applications of micro/nano particles for therapeutic delivery.

Tissue	Delivery Target	Particle size	Reference
Eye	Ocular	1µm	[22]
Lung	Respiratory tract	<3 µm	[23-25]
	Capillaries	2 and 13 µm	
	Tracheo-bronchial	≥10 µm	
	Alveolar region	<100 nm and 1 to 5 µm	
	Bronchioles	500 nm to 1 µm	
	Alveoli	< 250 nm	
	Capillary	< 15 to 25 µm	
Kidney	Endothelium fenestrate	< 60 to 80 nm	[25]
	Glomerulus	< 5 to 6 nm	
	Filtration diagram	< 4 to 6 nm	
	Perisinusoidal space	≤ 50 nm	
Liver	Biliary excretion	≤ 6 nm	[25]
	Sinusoidal sieve	≤ 200 nm	
Blood	Blood stream	< 100 nm	[25]

According to Rezman *et al* natural biomaterials can exhibit favourable biodegradability and biocompatibility with lower toxicity issues [26]. Some natural polymers can control the duration of active agent activity, improving their efficiency and reducing side effects under desired conditions, through modification of their pharmacokinetic profiles, which improve drug viability between tissue and cell channels choosing different routes to deliver chemicals signals in a specific site [27]. Natural polymers as well as synthetic polymers can control drug release and have biodegradability features. Lim *et al* demonstrated that natural polymer microspheres (*i.e*. chitosan and alginate) loaded with insulin showed better drug release profiles than PLGA, PLA, and PCL [28].

The most widely used synthetic polymers for drug delivery are PLA, PLGA and PEG; PLA and PLGA are also frequently used in tissue engineering scaffolds, and can generate acidic environments during their degradation processes [22, 26, 29, 30]. Natural and synthetic polymers show particular chemical structure and can influence the drug loading and polymer erosion as demonstrated in Figure 1.1. PLA is a linear aliphatic thermoplastic polyester, more hydrophobic than PLGA because of the presence of methyl groups in its chemical structure, and has suitable physical and mechanical properties for many biomedical applications, good biocompatibility and predictable kinetics of degradation [31, 32]. The hydrolytic degradation of PLA occurs by random cleavage of its ester bonds, and can completely degrade between 12 and 18 months [33], dependant on molecular

weight and degradation environment. Both PLA and PLGA carriers have been used for drug delivery systems against GBM cells, however they have not shown a sustained and prolonged treatment above 3 weeks of treatment. Therefore, the aim of this work was develop polymeric microparticles (PLA and PLGA) with controlled sustained release over time (30-day period).

PCL has been widely investigated to produce micro- -and nano-spheres for drug delivery applications and in general has a slower degradation rate (≈ 3 years eliminated from the body) and desirable mechanical properties [34, 35]. The mechanism proposed suggests hydrolytic ester cleavage of PCL with reduced diffusion of oligomeric species which can exhibit a neutral pH during *in vitro* drug release [26]. In addition, PCL has been explored for potential applications in bone and cartilage repair due to its elastic modulus and compressive strength which are similar to cancellous bone [26, 36] and demonstrated neutral pH over 6 months for protein encapsulation which demonstrated protein protection in acidic environments (*i.e.* stomach pH) [30, 37].

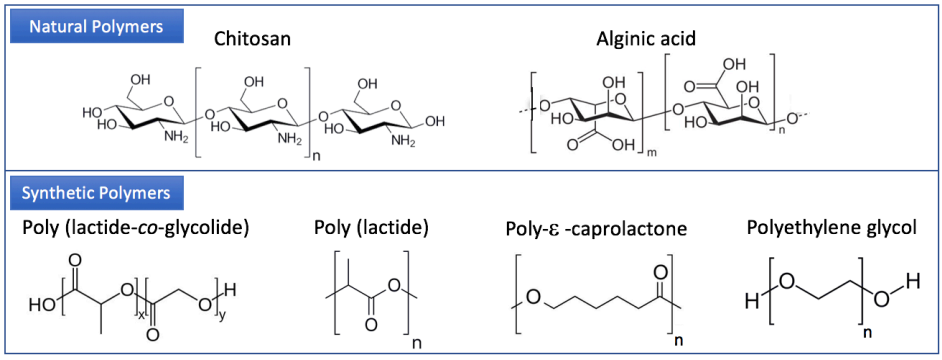


Figure 1.1: The chemical structure of some typical relevant natural and synthetic polymers used for drug delivery applications.

The above mentioned polymers can lead to production of non-toxic

degradation products that can be metabolised and excreted *via* normal physiological pathways [38]. PEG has also been heavily investigated for drug delivery applications, in part as a stealth coating to prevent the adsorption of plasma proteins and foreign body cascade, as well as stabilise micro particles as spheres in both gastric and intestinal fluids [39-41] .

1.1.1 Methods to Produce Polymeric Microparticles

The fabrication route used for polymeric micro- and nano particle production can significantly influence particle size and distribution, particle morphology, and importantly, the encapsulation efficacy of active components. The encapsulation of drugs and biological components, as well as their release rate can also be affected by the type of polymer, molecular weight, co/polymer composition and the nature of any excipients added to the particles [42].

Several methods have been developed to produce polymeric microspheres with different features for biomedical and pharmaceutical applications. These techniques have been developed to provide control over particle size and morphology, as well as expand the use of new materials and drugs [5]. Furthermore, some techniques used to produce microparticles and nanoparticles such as spray drying, electro spray/spinning, solution blow spinning/atomization and single and double emulsion have specific advantages and disadvantages, as discussed below. The single emulsion technique has been used worldwide as a direct method for incorporation of hydrophobic components, and is addressed in this thesis.

1.1.1.1 The spray-drying process and influence of parameters on particle formation

According to Fleming *et al* the spray drying process was developed by Robert Stauf for the drying of blood, milk and other highly complex organic liquids in 1901 [43]. Microparticles were formed by spraying droplets of fluid into a chamber followed by a drying process with hot air enhancing the rapid evaporation of the organic phase. The nozzle can be fed by solution, suspension, emulsion or paste formulation resulting in particle formation as powders, granules or/and agglomerates. Important parameters that alter particles features include the feedstock, feed temperature, melting temperature, abrasion, corrosion, specific gravity, solid content, surface tension and viscosity [44-46]. The parameters mentioned above can influence the form and density of the particles, as well as their morphology (*i.e.* porous or hollow particles). Moreover, particle sizes can be altered by changing atomisation energy, with smaller droplets formed by using higher atomisation energies [47-50].

The properties of the dried product formed depend on the physical and chemical properties of the feed and the dryer design, the operation of which is normally automatic with tightly looped control. There are a number of advantages in using this technique to produce powders, as follows: i) It is a fast, continuous, reproducible and single-step technique; ii) the ability to dry products which are heat-sensitive avoiding the degradation of their chemical components (*i.e.* essential

oil); iii) powders can be produced within predetermined particle size, morphology and moisture content; iv) some parameters can be adjusted very easily, such as solvent composition, viscosity, solute concentration, temperature and nozzle diameter; v) particles encapsulated with active components can attain high encapsulation efficiency; vi) powders obtained from this technique have better flow properties than other methods due particle sphericity and low density; and vii) this technique can improve the conservation and stability of products in dried solid forms [4, 44, 50-55].

Since spray drying is usually the end-point of an industrial process, it can also influence the quality of the final product. Moreover, the ability to encapsulate active compounds into micro- and nano-particles for use in pharmaceutical formulations, cosmetics and functional food preparation has attracted significant attention in past two decades [4].

Normally the particles generated in spray-dry systems exhibit a size range below 10 μm, which is essential for many pharmaceutical formulations, including powders for asthma inhalers, for diabetes control and multi-functional excipient tablet formulations. Furthermore, spray-drying is able to encapsulate drugs of various hydrophobicity and protect them from chemical interaction with other drugs [51, 56-59].

More recent developments have enabled the production of nano and micro size range particles between 100 nm to 5 μm by utilising vibrating mesh sprays with a narrower nozzle diameter than conventional spray dryers (500 to 700 μm in diameter) [23]. This

process avoids clogging of the spray nozzle and permits highly viscous solutions to be sprayed, with increased formulation homogenization, and reduced particle size, as well as improved powder properties [60]. This technique also enables encapsulation of active agents of various physicochemical properties within different polymeric matrices (*i.e.* synthetic, semi-synthetic, or those of natural origin) under very mild conditions with high encapsulation efficiency. Spray-drying technology is less dependent on drug solubility and polymers than other methods [61].

Another technique, which was introduced as an innovative process to produce submicron drug particles, is spray-drying technology incorporating vibrational atomization [62]. This equipment generates a fine aerosol of droplets of controlled size, which are fast drying and enables electrostatic deposition of the particles to surfaces. The advantages of this equipment are: i) Drying and collection of particles smaller than 2 µm, and ii) production of polymeric particles with a range of diameters between 300 nm to 5 µm. Spray-drying with a vibrational atomization system exhibits similarities with conventional spray-dry technology [63, 64].

1.1.1.2 Electrospray and electrospinning technique

Electrospinning processes have been reported since 1971, when fibres were produced from polyacrylonitrile in dimethyl formamide solution with diameters ranging from 50 nm to 1.1 µm [65]. Interest in this

technique has since increased exponentially due to its adaptability to a wide range of polymeric materials and applications [65].

Electrospraying uses constant liquid flow through a needle under constant pressure with high electrical potential to disperse the solution as fine droplets with solvent evaporation. The process is principally controlled by polymer solution viscosity, applied accelerating voltage, needle diameter, pressure and distance between the needle tip and collector plate. Droplets can be deposited individually or as an agglomeration of particles into a film or membrane form. Droplet sizes range from nanometres to micrometres, and films can be generated from 40 nm to 2 μm in thickness [61, 66].

The principles of electrospraying are similar to those of electrospinning, except that fibres are formed from typically more viscous polymer solutions in the latter case. Using the same polymer solution and equipment, either particles or fibres can be produced depending on the solution viscosity. This technique has the advantage that particles and fibres or a mixture (*e.g.*, beads-on-strings) can be produced without the use of surfactants [67]. Typically, high concentration of polymeric solutions can produce fibres, whilst lower viscosity solutions can produce solid, sub-micron particles [68, 69]. On the other hand, there are some disadvantages that limit the production of biomaterials as shown below in Table 1.2.

According to literature, particle morphology is dependent on chain entanglements, entanglement volume fraction ($Ø_{ent}$), overlap volume fraction ($Ø_{ch.ov}$), Rayleigh limit ($Ø_{Ray}$), Coulomb fission [70], applied

voltage, solution flow rate, temperature, humidity and the surface tension of the solution [71]. Chain entanglements are a direct consequence of chain overlap to produce fibres in electrospinning and Rayleigh limit is the rupture of the droplets during the last stage of solvent evaporation. Coulomb fission preserves the monodispersity and sphericity of the droplets [70, 72]. The parameters, $Ø_{ch.ov} < Ø_{Ray} < Ø_{ent}$ are important in preserving droplet integrity using the electrospray process [70].

Particles with size range down to 80 nm have been produced using polymeric solution at low flow rate and accelerating voltage, resulting in reduced jet formation and rapid volatilisation of organic solvent [72]. In addition, the applied electrical potential can affect the size and form of the droplets. A potential that generates sufficient electric charge is required to overcome the surface tension of the polymer solution to produce micro- and nanoparticles. Accelerating voltages (9 kV) have been reported to produce micrometric particles (400 μm) and an accelerating voltage of 15 kV has reportedly provided greater jet cone stability and enable particles of diameters between 3.4 μm and 10 μm to be formed. Collection distance is important, with sufficient distance allowing evaporation of the volatile organic solvent; films, porous membranes or conglutinated particles can be formed by controlling (typically increasing) collection distance [72] .

Table 1.2: Advantages and disadvantages of electrospray and electrospinning process to produce particles and fibres [78, 81-83]

Advantages	Disadvantages
• One step • High molecular weight polymers with high concentration of organic solution • Nanoparticles can be obtained • Does not require surfactants • Elimination of organic solvent: high speed of solvent evaporation • Monodisperse particles with high efficiency can be formed • Less shear stress than the emulsion technique • Narrow size distribution can be produced • Control over particle size • No heat required • Manufacture of porous fibres and spheres	• Low yields of particles obtained • Use cross-linking agent: reduced gelation time • Relative humidity and temperature of the spinning environment can affect particle morphology and need control for repeatability • Limited range of operation due to solution viscosity and surface tension

Particles produced via the electrospraying process are appropriate for a wide range of biological applications such as cell therapy (*i.e.* cell delivery to specific sites) using different cell lines (*i.e.* osteoblasts [73, 74], chondrocytes [75] and stem cells [76]), promotion of vascularisation and in bone repair [77], as well as drug delivery [78]. According to Kim *et al* silk fibroin particles have been produced for drug delivery applications by electrospray [68]. The shear viscosity and formulation concentration influenced particle formation; adhesive particles have even been produced. Their *in vitro* work demonstrated a that dense and compact cells layers could be formed after 4 days of incubation [68]. Almeria *et al* showed that PLGA particle morphology influenced the anchoring affinities of targeted cells, particles with large surface-to-volume ratios were preferred for targeting [70].

Lee *et al* demonstrated PLGA particles formed of multiple drug composite layers for tissue engineering and regenerative medicine applications [79]. These particles were produced in a tri-layered structure (*e.g.* core-shell-shell) with particle sizes ranging between 2.79 and 3.32 μm resulting from the electrospray system. Their work suggests that the particles with tri-layered structure can release multiple drugs with distinct kinetics and that the layered design can be controlled by varying the chemical composition of the polymers [79].

According to Gao *et al*, the electrospray process was able to form polymeric droplets *via* direct spray into a cooling system, which caused rapid evaporation of solvent and water [80]. This system was water-condensed, with phase separation (*i.e.* solvent evaporation),

imparting a porous morphology to the microspheres. Microspheres have also been produced using a non-solvent bath, or indeed a cryogenic liquid, to give spheres in the range 1 to 1000 μm in diameter [81].

Porous and non-porous fibres have been created by electrospinning into a cryogenic liquid to exploit thermally induced phase separation (TIPS) producing porous structure [82]. Porous fibres have also been produced via electrospinning using highly volatile solvents [82], as well as polymer blends followed by selective dissolution producing highly porous fibres [83] .

1.1.1.3 Solution blow spinning

Solution blow spinning can produce particles and fibres analogous to those of electrospinning/electrospraying, without the need for electric fields and uses very simple equipment [83]. The process is similar to air-brushing, and uses air pressure to disrupt surface tension. Polymer solutions are essentially atomised and the solvent evaporated leaving behind polymer spheres or fibres. Porous spheres and fibres can be produced by the technique, due to non-solvent induced phase separation (NIPS) and vapour phase induced phase separation (VIPS). Porous features present in the spherical particles have been attributed to phase separation in flight, solvent evaporation, and working distance between the nozzle and collector [84, 85]. Particle morphology is determined by several factors such as surface tension, polymer solution

viscosity, polymer molecular weight, solvent diffusion and polymer-solvent interaction.

According to Medeiros *et al*, porous polymeric microparticles were produced when the relative humidity was higher than 25% during solution blow spinning process [66]. They showed that pore formation was reduced due to high viscosity of the polymeric solution used, which resulted in well-defined porous structures. It is necessary to consider additional parameters such as type of porogen used, solvent evaporation rates and internal pressure to produce polymeric porous particles [66].

The phase separation mechanism can influence particle formation nucleation and growth. This correlates to the combination of liquid-liquid mixtures with crystallisation of the polymer (depending on the polymer), and the vitrification or crystallisation of the solvent, influencing the generation of porous structures. In addition, particle size and pore interconnectivity can be controlled by polymer-solvent concentration and cooling method applied [86].

Spinodal and binodal behaviour correlates with the formation of colloidal particles, as well as particle morphology and size [87]. In general, spinodal decomposition shows a rapid de-mixing of liquids under a predetermined thermodynamic phase whilst pores formation is attributed to phase separation [88]. The mechanism of particle formation occurs in the unstable region represented by the miscibility gap shown in the phase diagram (Figure 1.2) and is affected by the concentration of components (*e.g.* polymers) as well as interactions

between organic and non-organic phases and the solidification of polymers [74, 84, 86, 87, 89].

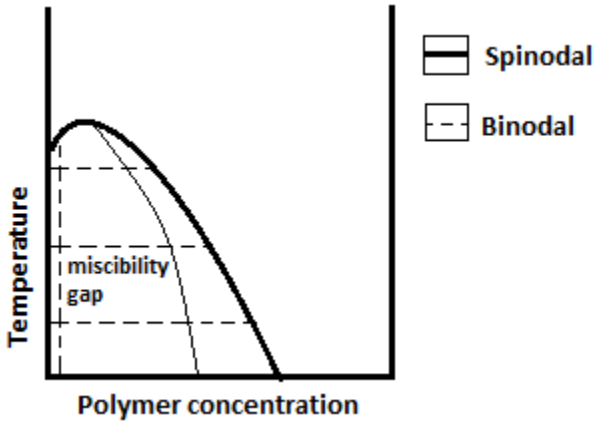


Figure 1.2: Representation of the phase diagram of polymer solutions, spinodal and binodal behaviour [101].

It has been shown that solution blow spinning (SBS) can produce non-porous and porous microspheres [91]. Rajendran *et al* produced sol-gel fibres by aqueous solution blow spinning process at reduced temperature. The gel fibres were converted to flexible ceramic fibres to produce orthoferrite ceramic fibres [90]. Behrens *et al* produced PLGA nanofibres using a commercial airbrush, the solvent evaporated rapidly, and fibres were produced. PLGA nanofibres have been deposited in multiple surgical resection models [85]. PLGA nanofibres were shown to support high cell viability and prevented the liver bleeding as well as air leakage when applied to the surface of the lung [85]. Medeiros *et al* developed porous polymeric microparticles with diameters in the range 500 nm to 75 μm, and fibres as a macroporous scaffolds using phase separation technique, combined with ice microspheres as *in situ* porosifiers by spraying polymer solutions and water through multiple nozzle directly into a cryogenic bath, followed

by freeze-drying to remove from frozen solvent/aqueous phases [91]. Daristotle *et al* produced PLGA/PEG/silica composite surgical sealants by solution blow spinning into a soft, conformal film after warming to body temperature [92]. The films were tested using an *ex vivo* model of intestinal anastomosis and an *in vivo* liver laceration model. The incorporation of silica particles improved the tissue adhesion through a nanostructured contact area and increased energy dissipation. Furthermore, the silica particles were shown not to modify the biodegradability of the films and did not increase the cytotoxicity and inflammation response [92].

1.1.1.4 Single and double emulsion techniques

This method uses disperse and continuous phases to produce micro and nano spheres. Different types of formulations can be processed such as i) single emulsions of water-in-oil (W/O) or oil-in-water (O/W) systems; and ii) double emulsions of water-in-oil-in-water (W/O/W) and oil-in-water-in-oil (O/W/O) systems. Oil droplets dispersed in a water phase are typically represented by O/W, whereas water phase dispersed in an oil continuous phase is represented by W/O [93]. Varying their combination, amount of oil and water phases in the system, can change the hydrophilic or lipophilic properties and the osmotic pressure of particles formation and influence the type of spheres produced as well as their size and shape [94].

Formulations with an excess of oil are typically considered macro-emulsions (O/W), and are represented by the Winsor I region as shown in Figure 1.3, which shows low hydrophile-lipophile balance (HLB).

On the other hand formulations with excess water are represented in the Winsor II region (W/O), which shows high HLB and the presence of micelles [95]. Winsor III regions represent a composition of oil, water and a "middle" bi-continuous micro-emulsion phase, coexisting in three-phase equilibrium as shown in Figure 1.3. This system represents the molecular behaviour near the interfacial limit between the oil (O) and water (W) phases [94, 96].

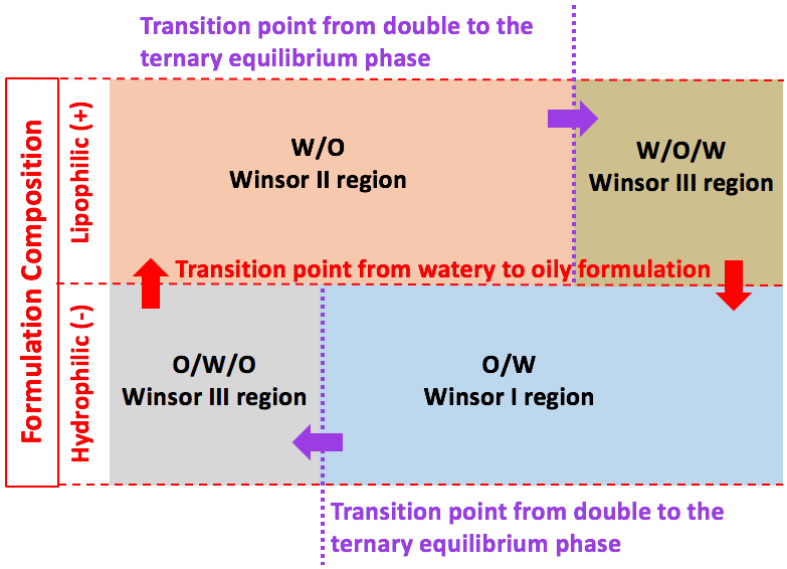


Figure 1.3: Behaviour of single and double emulsions within different compositions and transition points represented by the Winsor regions.

It is possible to produce different types of multiple systems where the dispersed phase contains even smaller dispersed droplets. In addition, surfactants can form a protective membrane on the surface of the droplet, reducing droplet coalescence [97]. On the other hand, when drops form in the oil phase, a new water-oil interface must be produced which increases the interfacial surface tension [98]. The physicochemical properties of single and double emulsion systems (*i.e.* rheology, stability and optical properties) are highly dependent on the hydrophobicity characteristics of the droplets. It is well known that the

droplet characteristics rely on the homogenization conditions (*i.e.* intensity and duration of energy input), as well as the system composition (*i.e.* concentration of emulsifier dispersed in the continuous phase) [93, 97].

Traditionally small-molecular weight surfactants have been used as stabilising agents for both the inner and the outer interfaces for double emulsion systems. In such systems, thermodynamically or physicochemical instability errors are corrected by the addition of a third component, which emulsifies the system and controls the release for drugs encapsulated in the micelles [99]. In addition, stable emulsions with small droplets are less prone to sedimentation and Brownian motion preventing flocculation of the droplets [93, 99] .

The size of the particles produced can be controlled by the velocity of stirring, type of stirrer used and the organic and water phase [99]. It should be noted that in this process it is necessary to use immiscible liquid phases to produce particles that can be micro- or nano- in size. According to Luciani *et al* single and double emulsion systems have been used to produce microspheres with varying diameter ranges from < 106 to 630 µm (see Figure 1.4) [37].

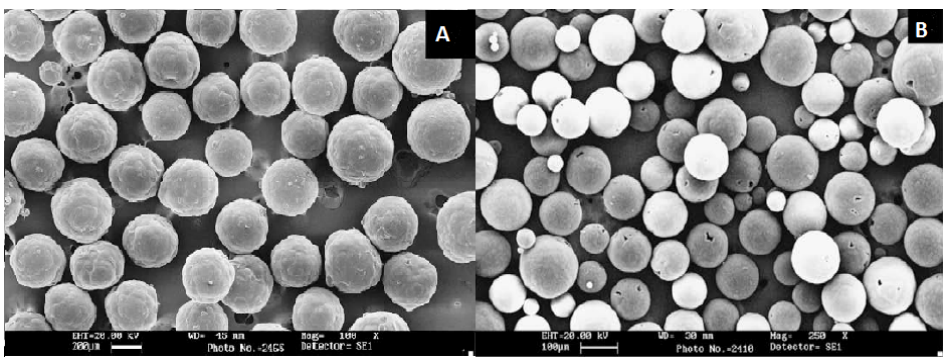


Figure 1.4: Micro-size spheres produced without surfactant (A) and formulation with presence of surfactant (B). Adopted from Luciani A et al (2008).

According to Rao *et al* [100] nanoprecipitation by the double emulsion system depends on some basic components such as: Type of polymer (*i.e.* synthetic, semi-synthetic or natural), the organic phase (polymer solvent) and continuous phase (non-solvent phase). Some organic solvents are miscible with water and can be removed by evaporation. Surfactants can influence particle formation and are necessary to prevent the nanoparticle suspension from agglomeration over long storage periods. The size of the spheres produced *via* the double emulsion technique has been reported to range between 63 to 560 nm [100].

Kumbar *et al* used an emulsion cross-linking method to prepare swollen chitosan microspheres to encapsulate diclofenac sodium using cross-linking agents (*i.e.* glutaraldehyde – GA and sulphuric acid – SA) and also explored the use of heat treatment [101]. This technique has been employed to produce particles with size ranges from 40 to 230 μm and exhibited encapsulation efficiencies of up to 30% for particles with SA [101, 102].

1.1.2 Porous Polymeric Microparticles

1.1.2.1 Shape, size and porosity

Porous polymeric microparticles have been developed since 1972 [113] and their physical features and application space have since been expanded. Control over particle morphology and size is one of the major challenges during particle formation and is critical for the

development of pre-clinical studies for drug delivery and targeting. According to the literature, particle formation is correlated to the type of methodology applied, type of polymer matrix (and use of surfactants), hydrophobicity and hydrolysis rate of the polymer matrix (if susceptible to hydrolytic degradation), interphase interaction (*i.e.* homogenisation process), surface stress and forces (*i.e.* due to van der Waals forces, Brownian motion) [103-106]. The forces applied in the formation of microparticles can alter the interphase interaction between the organic and non-organic phases, which also affect particle size [105, 107], multi-layer formation [105], sedimentation, migration and inertia of the particles [103].

Particle geometry can significantly alter behaviour in targeted drug delivery, due to influence on deposition at sites of therapeutic interest, permeation through biological barriers, interaction with cells and channels, and time required for the mechanism of uptake [108, 109]. The geometry and morphology of particles imparts distinctive properties and advantages depending on target application, [109-115] as follow:

- Spherical particles:

i) Improve particle flowability

ii) Reduce density

iii) Minimise macrophage uptake of pulmonary delivered drugs

iv) Can enable rapid uptake by the cell membrane

v) Can enable attachment of macrophages

vi) Can enable uniform matrix degradation and release of active components

vii) Are used for localised and systemic drug delivery

- Non spherical particles

i) Enable new designs for drug delivery systems

ii) Rotational property (*i.e.* influence the rheology of suspensions)

iii) Can move along complicated trajectories (*i.e.* tortuous veins)

iv) Can control clearance process (*i.e.* increase particles viability in serum)

v) Prolong circulation time (modification of particle geometry changes the time and mechanisms required for uptake)

vi) Can be used as vehicles to deliver drugs to various types of cells

vii) Can confound phagocytosis

Particle morphologies have been expanded over the years and a significant number of particles of varying shapes have been developed, including spherical particles (*i.e.* lipid-based beads), spheroidal particles [116], elongated and cylindrical microparticles [117, 118], discoidal particles [108, 119-121], virus-like particles [108, 122], red-blood-cell-like particles [123], core-shell and/or hollow particles [110, 124, 125] and nanopolypods [108]. According to Myerson *et al* particle shape and size are closely related with the biomedical application as

both characteristics are a limiting factor [108]. They reported that long worm-shaped PEG-polyethylene filomicelles manifest prolonged circulation time, avoid macrophage internalisation, and favour accumulation in tumours [108, 126, 127]. Disc shaped polystyrene particles have been reported to exhibit higher circulation half-lives over their spherical particle counterparts [108, 128].

It is well known that particle size can be affected by the method used to produce them (*i.e.* single emulsion formulation and processing parameters), polymer molecular weight, as well as their swelling behaviour [129]. Particle size is one of the limiting aspects towards biological applications [130, 131]. In general, microparticles show restricted application as a systemic delivery system through the blood stream for veins and capillaries of diameters below 30 μm; the drug administration sites changes as the particles become narrower or larger than the actual size of the sites [132]. Micron size particles are usually used for controlled sustained local therapy with high drug availability as well as matrix for scaffolds [133] and paste formulations [134]. Furthermore, these particles tend to accumulate in perinuclear and cortical regions [108, 134]. However, it is not known how the chemotherapeutic drugs can reach deeper areas of the brain cavity through localised and controlled sustained delivery systems and control cancerous cell proliferation. This presents an opportunity for exploration in the work in this thesis, addressing the challenge to develop polymeric formulations with controlled sustained release over

time to prolong the therapy efficiency of paste- and tablet-based formulations loaded with chemotherapeutic drugs.

Large particles of varying morphology can be obtained using porogen agents (*i.e.* volatile liquids, ammonium carbonate or bicarbonate) in the primary solutions or emulsions, as described in detail in Table 1.3 [9, 135]. The porogen tends to evaporate faster than the dispersion phase (*i.e.* non-organic phase) and can produce pores in the interior of the larger sized particles [9, 136, 137].

Table 1.3: Summary of porogens used to form porous polymeric particles formulations and varyiance in their morphology.

Types of porogen	Chemical and physical characteristics	How they work onto formulation	References
Dimethylformamide (DMF)	Colourless, odour: amine-like, melting/freezing point: -61°C, vapour density: 2.52, completely soluble in water	Organic phase and rapid evaporation (Electrospinning)	[66]
Toluene	Colourless, odour: aromatic, melting/freezing point: -93°C, vapour density: N/A, water solubility: 0.5 g/l at 15°C	Organic phase and rapid evaporation (Electrospinning)	[66]
Dimethyl carbonate (DMC)	Colourless to very faint yellow, melting/freezing point: 3°C, vapour density: N/A, water solubility: 13.9 g/100mL	Organic phase and rapid freezing producing crystals into the polymeric matrix (Solution Blow Spinning)	[91]
Ammonium bicarbonate	Crystalline, odour: N/A, Melting/freezing point: 60°C, vapour density: 2.73, water solubility: 79.1 g/l at 20°C	Aqueous solution and rapid sublimation during drying process (Spray-drying)	[135,56]
Ethanol	Colourless, odour: alcohol-like, melting/freezing point: -114°C, vapour density: 1.6, completely soluble in water	Organic phase and rapid evaporation (Spray-drying)	[136]
Dichloromethane	Colourless, odour: sweet, melting/freezing point: -95°C, vapour density: N/A, water solubility: 20 g/l	Organic phase and rapid evaporation (Single emulsion)	[373]

It has been challenging to produce different levels of porosity in large particles explored as alternatives for the encapsulation of active pharmaceutical ingredients [9]. Porous particles can exhibit different types of pore networks, such as interconnected porous structures that

can improve the diffusion of gas and fluids throughout their structures [138]. Furthermore, particles can exhibit different levels of porosity such as micro (<2 nm), meso (2 to 50 nm) and macroporosity (>75 μm) [139]. Hierarchical pores are also desirable in some cases, for example a porous interior can be protected by a denser skin region; the presence of hierarchical pore structures can improve the diffusive rates of physiological solution as well as increase the elimination rate of polymer matrix degradation products from the target site [139].

1.1.2.2 Delivery systems and biological applications

The release rates of drugs and fragile chemical structures including proteins and nucleic acids can be controlled by embedding them in micro and/or nano carriers [42]. Drugs and fragile chemical structures (*i.e.* RNA, DNA) can be destroyed when exposed to extreme pH conditions such as those in the gastrointestinal tract [42]. Furthermore, polymer molecular weight can influence particles degradation rates and particles morphology, which in turn can affect cell internalisation, phagocytosis and circulation in the blood stream [42, 68, 140].

Various delivery systems have been developed in order to improve the therapeutic dosage at specific body sites and improve patient compliance and outcome. These delivery systems are applicable in ophthalmology [22], inhalation systems [141] (*i.e.* insulin delivery), cell delivery [15] (*i.e.* cells encapsulated within the particles) and cell growth and proliferation [142]. Moreover, polymeric carriers can deliver antigen presenting cells, chemotherapeutic drugs to the brain cavity, protect DNA/RNA against acidic environment and prevent their

degradation [5, 22, 134, 140, 143, 144]. Kim *et al* [145] showed that cells (*i.e*. rat adrenal pheochromocytoma-derived cell line – PC-12) attached in PCL porous microspheres, which had been modified with growth factors and gelatin to coat the particles, exhibited potential applicability for neuronal tissue regeneration[146].

Polymeric microparticles have been applied to aerosolisation systems to achieve enhanced and deeper reach within the lungs for local drug delivery [147, 155-157]. Interest in this type of system has been driven significantly by the pharmaceutical industry as a non-invasive approach for therapeutic treatment of lung disorders [147] (*i.e.* asthma [148], tuberculosis [149], pulmonary fibrosis [150], lung cancer [151]) and endocrine disease [152] *(i.e.* diabetes [141, 153, 154]).

Natural and synthetic polymeric materials have been used to protect drugs against the low pH environment of the stomach, to avoid rapid clearance and enable controlled drug release. According to Sai *et al* [158] chitosan (CS) particles demonstrated antibacterial activity against *Staphylococcus aureus* and *Escherichia coli*, showing a relevant bacteriostatic effect due the sustained release of iodine, is a broad-spectrum fungicide. Furthermore, Mukhopadhyay *et al* showed that alginate nanoparticles (100-200 nm) could be encapsulated with insulin followed by CS polyelectrolyte complexation [29]. These particles were developed for oral insulin administration and revealed sustained delivery within the intestinal tract. High concentrations of CS increased the particle size and the positive charge on the surface of

these particles facilitated the encapsulation of insulin and prolonged drug activity at least up to 9h within the gastro-intestinal site [29].

Degradable nanoparticles have been produced from PLGA, PCL and poly-alkyl-cyanoacrylates, loaded with different types of anticancer drugs and applied in drug delivery applications [13, 22-25]. Kumari *et al* showed the release profile of drugs (*i.e.* 9-Nitrocamptothecin, Paclitaxel, Cisplatin, Xanthones, Rose Bengal, triptorelin and Dexamethasone) in PLGA nanoparticles with anti-cancer activity for various types of tumours [11]. PLGA have been blended with alginate, chitosan, pectin poly (propylene fumarate), poly (vinyl alcohol) and poly (ortho ester) to overcome the acidic nature of PLGA in some biological environments [11]. PLGA nanoparticles are effective against some diseases when entrapped with drugs and have demonstrated improved physical stability, up to 3 to 4 months higher when compared with other types of polymers [11]. Nagy *et al* developed hybrid aerogel microparticles functionalized with methotrexate against tumour cells growth [159]. The microparticles showed a promising controlled release system and showed a lack of toxicity in the cancerous cells [159].

1.1.3 Brain Tumour – Glioblastoma

Cancer is one of the major causes of human deaths worldwide. GLOBOCAN, a project of the international agency for research on Cancer, in 2018 estimated about 64,601(21.8%) cases of brain and central nervous system (CNS) cancer occur in Europe, 9,040 (14%)

cases occurred in Northern Europe and 5,760 (63.7%) cases occurred in UK for both sexes [160]. According to literature, brain tumours do not show specificity to age and gender. However, tumour recurrence and death remain on the increase (in part due to improved diagnosis) and is related to the high rates of hypercellularity, mitosis, cells proliferation and necrosis, as shown in Figure 1.5 [160].

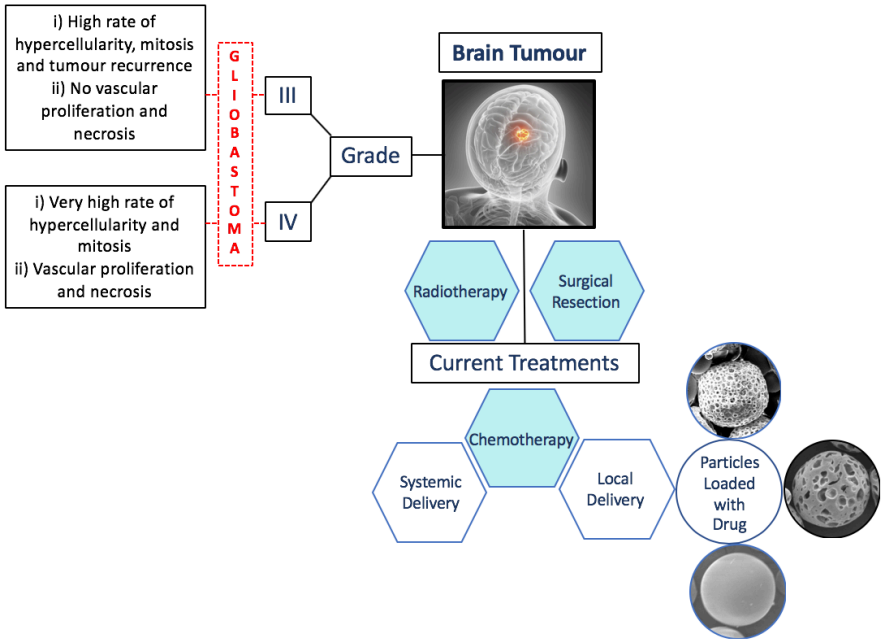


Figure 1.5: Schematic representation of brain cancer, grade levels, current treatments to control glioblastoma (GBM) cell proliferation and perspective on local delivery treatment.

Glioblastoma (GBM) is an aggressive in adults, and has a direct impact on the patient's life in terms of their physical, psychological and neurological conditions [161], it is also one of the most feared by researchers and oncologists [161-163]. According to GLOBOCAN 2018, the incidence of malignant brain tumour is 5 per 100k males with very high Human Developed Index (HDI) and 4 per 100k females [164-166]. Glioma accounts for 29% of all primary brain and central nervous system (CNS) tumours and 80% of malignant brain tumours

[167]. Common signs and symptoms of GBM patients include edema, haemorrhage, high intracranial pressure, headaches, seizures, focal neurological deficits and changes in mental status [161, 168].

The median overall survival of patients with GBM is less than 2 years after current multimodal treatment; combined surgical intervention, with radiotherapy and chemotherapy [164, 169, 170]. Current brain cancer chemotherapy treatment alone does not show a significant control of cancer proliferation and tumour cell recurrence [171]. Furthermore, there is a range of side effects due to the toxic chemotherapeutic drugs. These therapeutic agents are usually non-specific in targeting cancer cells and kill healthy cells albeit in lower proportion, resulting in systemic toxic effects [171].

The capacity of GBM cells to mutate, migrate (*i.e.* clonal and sub-clonal evolution) and resist current treatment makes the therapeutic treatment extremely difficult and is predominantly fatal. Even after tumour resection the cells are highly invasive, specifically given the presence of GBM cells away from the tumour resection site [172-176]. At present, there is no standard treatment established for brain cancer, especially for GBM, which is a highly aggressive brain cancer. However, the scientific community is focused on the development of new devices and many different strategies to deliver therapeutic agents to the tumour resection site, effectively reducing possible side effects and accumulation of drug in normal brain and peripheral tissues caused by the administration of drugs [161, 177]. Polymeric drug containing

microparticles can be locally delivered in an effort to reduce the side effects of chemotherapeutic drugs via systemic administration and control of tumour cells post-surgical resection [178]. However, several aspects, such as histological, genetic and drugs delivery systems need to be investigated further in order to improve treatments.

GBM has been classified as grade IV astrocytoma, arising from astrocytes or supportive brain tissue [161, 177] and exhibits histological homogeneity despite the clinical heterogeneity of GBM sub-types, directly affecting disease prognosis [172, 179]. According to the literature, GBM can be divided into primary GBM (90%), in which the tumour arises without previous lower grade pathology and/or symptoms, and secondary GBM, which derives from the progression and mutation of lower grade cells (*i.e.* astrocytomas) and normally affects younger patients [172]. Both subtypes of GBM show a high rate of recurrence, tumorigenic ability, genetic heterogeneity and capacity for multipotent differentiation due the self-renewing of GBM stem cells (GSC) [172, 180-182]. Furthermore, the GSC spend most of the time in G0 phase (metabolically active cells and fully differentiated) of their cell division cycle and can exhibit resistance to chemotherapy due to the activation of DNA repair regulatory systems and high expression of ABC transporters [164, 183, 184]. GBM subtypes are clinically indistinguishable and can be only be assessed using microscopy [185], and genetically by specific cell markers [161, 186].

Cancerous cells usually recur for GBM tumour treated with the first line therapy which can include surgical resection, radiotherapy and drugs therapy such as nitrosoureas, temozolomide (TMZ), bevacizumab, or tyrosine kinase inhibitors [187, 188]. Second line treatments have been under *in vitro* and *in vivo* investigation and depend on factors such as tumour size and location, patient age, time from initial diagnosis and previous treatments [187]. Even though, the present GBM knowledge in terms of genetic and molecular modifications as well as therapeutic systems has not increased the number of patients with long term survival status above 8% [161, 185].

Recent studies have questioned the clinical efficacy of chemotherapeutic agents against GBM due to systemic chemotherapy toxicity and drug delivery limitations [175, 176], which results in treatment failure. Several factors are involved with the failure of current treatment available such as blood-brain-barrier (BBB) limitations (described in the following section) and high intratumoral pressure gradients, which restrict drug penetration [175, 189, 190]. The monotherapies established so far have achieved limited success with rare exceptions and for this reason combinatory drug systems such as multi-therapy systems are developed in this thesis. Other multi-therapy systems explored include double covered particles [21], the combination of radiation followed by chemotherapy [185, 191, 192], prodrug conjugated with self-assembled targeted nanoparticles [193]

and localised drug delivery technologies [134, 194] have been developed to overcome the issues cited above related to GBM treatment.

1.1.3.1 The blood- brain- barrier and drug delivery systems

The blood-brain-barrier (BBB) is a dynamic and flexible membrane between the body and brain and is well known for nutrient transport and homeostasis between them, which can prevent permeation of toxic molecules to the brain [187]. Paul Ehrlich and Edwin Goldman observed the injection of water-soluble dyes through the blood stream and did not find dye presence in the cerebrospinal fluid (CSF) [195]. Later, Friedemann demonstrated that lipid dyes were able to cross the BBB [195, 196]. The physiology of BBB is an important aspect for drug development and delivery systems [187]. Further BBB research has demonstrated that passage into the brain of peripherally injected dyes is impeded. It has been proven that small molecules such as a wide range of lipid-soluble molecules can diffuse through the BBB [197, 198].

Nutrients and small molecules, including several drugs can be transported in and out of the brain by various methods such as i) passive diffusion, ii) carrier-mediated transport, iii) endocytosis and iv) active transport, however the types of transport across the brain can more likely to be P-glycoprotein substrates or be taken up by

peripheral tissues [187, 199]. Some factors can limit the entry of molecules into the CNS, such as high surface area and a tendency to form more than six hydrogen bonds, which increases the free energy between an aqueous phase in contact with lipid environment of the cell membrane [197, 200]. The permeability of molecules is also affected by the presence of hydrogen bonds and the molecular weight bigger than 450 Da) [197, 201]. Even though small molecules have higher permeability feature at the tumour site due the absence of BBB [187, 202].

The BBB is created by endothelial cells, which is formed by the capillaries combined with the micro vessels and then creates the largest interphase exchange between blood stream and brain. The surface area of the micro vessels directly depends on anatomical region and gives a total area between 12 and 18 m^2 for exchange in the brain. The BBB exhibits a combination of specific ion channels and transporters essential for drug delivery systems as well as provides a stable and safe environment for neural function away from neurotoxic molecules/drugs present in the blood [197]. It has been proven that the adult central nervous systems (CNS) does not have a regenerative capacity when damaged, which is affected directly by the non-regeneration property of the neurons [203]. It is important to highlight that CNS tumours usually compromise the structural integrity of the BBB causing a leak at the tumour core and breakdown of the physical barrier [187, 204].

Tight junctions (TJs) are part of the BBB structural support and are located between the cerebral endothelial cells, the choroid plexus epithelial cells and the cells of the arachnoid epithelium. The TJs can significantly reduce the permeation of molecules through the BBB, consequently, disruption of the TJs causes disruption of the BBB [164, 197, 205]. CNS tumours cause the loss of the TJs and GBM can be evident by loss of claudin-3, which is directly correlated with loss of BBB integrity and functional properties such as permeability and selectivity of toxic molecules [197, 206]. Indeed, the permeability of molecules through the BBB is linked with the severity of the disease [197, 207].

The enhanced permeability and retention effect (EPR) is exploited in passive drug delivery systems targeting tumours and is enhanced by low lipophilic drug and brain matrix with cancerous cells. EPR takes advantage of the tumour nature such as high vascular density and leaky vasculature of the brain, high pressure of interstitial fluid and inefficient lymphatic drainage as well as the diffusion of drugs through the brain due poor outcome and insufficient drug concentrations at the tumour site due the reduced drug concentration systemically [203, 208]. To overcome the limitations of passive targeting and damage to BBB caused by the GBM cells, active targeting approaches have been developed using localised delivery systems [161]. The BBB is not the only membrane present in the brain that can prevent drug diffusion,

increase the resistance to chemotherapy and recurrence of cancer cells; the blood brain tumour barrier (BTB) is also correlated with the advantages of EPR cited above [203, 209]. At the early stage of cancer cell proliferation, the BBB supplies the brain with the necessary nutrients and maintains normal physiological function. However, when the tumour cell clusters grow to a certain volume, the BBB is damaged and a BTB is formed [164].

The proliferation of cancer cells, the deterioration, angiogenesis and gradual impairment of the BBB and BTB increase the difficulty in delivering nano systems as well as systemic delivery platforms efficiently to the tumour site due to the heterogeneity of micro vessels which makes malignant gliomas even less permeable [164, 210]. The pharmacological treatment for GBM is limited mainly for two reasons, the ineffectiveness of the delivery platforms that can transport across the BBB and the infiltrative nature of gliomas that utilise the available brain vasculature [164, 211, 212]. There are however several transport pathways that can mediate the diffusion of therapeutic agents across the BBB, for example receptor mediated transcytosis, lipoprotein receptors, integrin receptors and transferrin receptors [211, 213]. Pharmacological pathways can be used as an alternative resource to improve the systemic delivery and the dose response of the patients to the treatments by active targeting. Another strategy that can be adopted to overcome the high toxicity of the chemotherapeutic drugs, avoid the systemic side effects and increase the drug dose able to reach the

remaining infiltrative cells is the use of localised delivery systems in particular micro carriers, developed in this thesis.

1.1.3.2 Polymeric microparticles as a carrier for GBM treatment

Temozolomide (TMZ) is the most used drug for GBM treatment, however there is no established treatment so far due the infiltrative and proliferative nature of GBM cells, remaining in the affected tissue after tumour resection and the small area removed from the original neurosurgery lesion [170, 178]. Current treatments available focus on the improvement of patient survival as well as their quality of life. Polymeric microparticles (PMPs) are becoming a standard carrier for cancer treatment and one of the go to choices for development of devices for GBM treatment. PMPs can have satisfactory biocompatibility, biodegradability and loading capacity for hydrophobic drugs [130].

PMPs of varying morphology, size and loading capacity have been developed in order to improve some aspects of the drug delivery systems and control of GBM cell proliferation, such as reduction of the systemic toxicity of chemotherapeutic drugs [178], improve drug bioavailability and half-life [214], develop mouldable devices [134], achieve the therapeutic dosage at the tumour resection cavity [169] and improve patient compliance. There is a critical need to develop more effective treatments for GBM due to the low and short survival times

of the patients. The possibility to create micro carriers loaded with toxic drugs gives the opportunity to create a safe standard treatment, which can directly affect GBM cell recurrence. Technologies for PMP development have advanced creating more multifunctional particles and researchers have started to take advantages of different particle morphologies and functions [215], and further explored in the current thesis.

PMPs can affect the capacity of drug loading as well as the release rate due the interactions between the polymer and drug and their hydrophilic/hydrophobic features [216, 217]. The types of matrix used to develop the PMPs, water diffusion into the matrix and the loading capacity influence the release rate. According to the literature, Siepmann *et al.* found that micro particles size can improve the initial loading capacity of PLGA microparticles formed with a solid-in-oil-in-water emulsion technique [219]. The size of the microparticles also determines the degradation rate of polymeric microparticles [218, 219]. PMPs can avoid the rapid diffusion and degradability of chemotherapeutic drugs in brain tissue when compared with polymeric nanoparticles [5,142].

Shah *et al* developed PLGA microparticles loaded with verteporfin (VP) and assessed them *in vitro* and *in vivo* using patient derived GBM cells [220]. VP is a small hydrophobic molecule with poor solubility in aqueous solution and can potentially cause severe side effects in

patients. The VP carrier developed in their study reduced cell viability by 50% after 24h of treatment radiosensitizing primary patient-derived GBM and other CNS-and non CNS-derived tumour cells [220]. The *in vivo* treatment showed a significant reduction in tumour volume from day 8 through day 21 in a xenograft model suggesting that PLGA micro carriers can be effective local therapeutic strategies for a variety of solid tumours including GBM [220].

The success of PMPs for GBM treatment relies on the selection of appropriate matrix (*i.e.* polymer) to address the physicochemical limitations of free drug such as solubility and stability, and to overcome the biological difficulties in reaching the target which include the infiltration of drug through the BBB, body and immune clearance, cell entry and off-target deposition. Treatment efficacy depends on the nature of the drug and the route of administration, for example, oral, injection, transdermal, inhalation and local delivery [215]. It has been shown that PMPs developed for local delivery treatments can achieve maximal therapeutic efficacy with minimal systemic toxic effects [221]. PMPs can also decelerate tumour growth compared to single-drug treatment controls [215].

1.1.3.3 Local delivery system: a pharmaceutical perspective

Over the last century localised delivery systems have been studied and their medical devices improved. Each year these drug delivery medical

devices increase the quality of life of millions of patients affected with a wide range of diseases. Local therapies present common advantages regarding their effect in pre-clinical and clinical studies, as follows [222-225]:

i) Regulation of dose-dependent activity

ii) Reduced dosage required

iii) Reduction of side effects and systemic toxicity

iv) Improvement of drug bioavailability and half-life

v) Avoid rapid metabolisation and clearence of the drug

vi) Increase the therapeutic effect targeted directly to the required site

vii) Reduction of drug variability from patient to patient with narrow therapeutic index

viii) Avoid high-dose requirement

ix) Improve drug response and solubility in aqueous environment

x) Better pharmacokinetic and pharmacodynamic profiles of the drug

xi) Higher selectivity, efficiency and safety of drug administration

xii) Reduction of irritation and/or nuisance to the patient

xiii) Not altering normal physiological functions

xiv) Higher effectiveness of the therapeutic treatment

Local drug delivery has gained great attention specially for the type of formulations developed to improve drug delivery system and the clinical conditions of the patients. Formulations include solid forms (*i.e.* tablets, capsules, troches, discs, wafers, lozenges, powders,

microparticles and nanoparticles), semisolids (*i.e.* gels, hydrogels, soft chewable gelatin capsules, pastes, cream emulsions, ointments, films, biofilms, foam, suppositories and patches) and liquids (*i.e.* sprays, solutions, emulsions and mouthwashes). Formulations for localised delivery have been developed to overcome some limitations with the systemic delivery systems such as high drug toxicity, inefficiency of therapeutic response, low drug availability at tissue site and undesirable side effects [222, 226-231].

Localised drug delivery includes formulation approaches that facilitate the entry and passage of therapeutic compounds in the body. They can provide more effective treatment, show controlled and sustained drug release/diffusion from the polymer matrix in long term period , up to 30 days, as proposed in this thesis, and can reduce resistance and recurrence, as well as avoid high intracranial pressure [169, 225, 232]. Local delivery systems have been applied to different disorders, for example i) musculoskeletal disorders to deliver therapeutic agents to the desire site of action [226, 227, 233], ii) ovarian and brain tumour treatment to control the proliferation and growth of cancer cells directly and improve drug penetration in the cell environment [134, 234, 235], iii) spinal cord injuries to improve the intraspinal delivery with degradable polymeric devices [236], iv) antimicrobial therapeutics for bone infection [237], v) fungal or bacterial infections which affects mucosal membrane [231, 238, 239], and vi) diabetes [240].

Local drug delivery strategies are adopted in general to reduce the detrimental effects of systemic drug delivery systems which are applied for encapsulation of drugs as well as protection of proteins, nucleic acids, enzymes and genes against enzymatic degradation avoiding the rapid clearance from the body [225, 226, 241]. Furthermore, localised therapy systems can maintain drug availability longer in superficial peritoneal surfaces, CNS (*i.e.* the brain cortex) [5], intraspinal regions [243], knee joints [244], and the intracavity of the tooth [246].

1.1.3.4 Glioblastoma and local delivery systems

Therapeutic local delivery strategies developed to treat GBM demonstrate survival periods of up to 14 months. Even though, the majority cases reported in the literature of patients treated with aggressive tumour resection, radiotherapy and local treatments have minimal survival rates. Some factors involved with the short term survival of GBM patients correlat with the rapid rate of GBM cell proliferation due to constant genetic modifications [174, 242], nonspecificity of the current drugs due the high resistance of primary tumours to the chemotherapic drugs [175, 190], and the rapid clearance of those drugs [243]. The heterogeneity of tumour cells and individual tumours correspond with resistance to current treatments

[175, 244]. Furthermore, there is no established chemotherapy regimen available and patients are best treated within clinical investigation protocols [161, 245]. There is a critical need for the development of efficient and specific drug delivery systems for GBM treatment.

Treatment of GBM is complex in terms of genetic modifications, histopathological aspects, properties of chemotherapeutic drugs and type of the delivery systems developed to influence the treatment site. Some of the main issues and considerations are listed below, following [130, 161, 164, 172, 174, 221, 246]:

i) High proliferation and recurrence of GBM cells

ii) Activation of DNA repair

iii) Proliferation of cancer cells in deep areas of the brain

iv) Calcification in different areas of the brain

v) Post-therapy resistance (*i.e.* DNA damage checkpoints, hypoxia, acidic and metabolic stresses, oncogenese and transcription factor)

vi) Evidence of edema and haemorrhage

vii) Location of the tumour and loss of brain functional tissue (*i.e.* tissue resection)

viii) Intracranial pressure

ix) Lipophilicity and specificity of the chemotherapeutic drug

x) Half-life of the drugs

xi) Mono or combination of therapies

xii) Sustained and controlled release of the drugs

xiii) Drug administration route

xiv) Biocompatibility and (bio)degradation of the materials (*i.e.* carriers, devices)

xv) pH of tumorous cells

A brain catheter implant was reported in the literature as one of the earliest strategies to control the proliferation and recurrence of GBM with minimal systemic toxicity, however the depth of distribution of the drug from the injection site is very limited (<3mm) and repeated surgeries are needed, leading to an increased risk of local side effects (*i.e.* intracranial haemorrhage and infections) [161, 247]. Another device with the same purpose that has been widely studied, is based on a micro-catheter connected to a pump to create a pressure gradient, allowing the drug to permeate further in the brain tissue (2-3cm), however this intra-arterial infusion was not shown to improve patient survival [209].

Current treatment for post-surgical tumour resection are Gliadel® wafers, approved by the FDA and developed from co-polymeric microparticles encapsulated with carmustine (BCNU). Gliadel® wafers are placed into the brain cavity (*e.g.* 8 discs) to reach the therapeutic dosage of BCNU locally [161]. The wafers present some inconvenient factors, such as poor drug diffusion and fast drug release in the first 5-7 days, rapid drug clearance (*i.e.* "sink effect"), they are single chemotherapeutic agent delivery systems, the implants are prone

to dislodge, the cytotoxicity of BCNU is compromised by the development of drug resistance, cell recurrence and tumour growth. Survival of patients who receive Gliadel® wafers has been reported to be some 2 months longer than the patients that do not receive the wafers [21, 161, 175, 248, 249]. Development of local delivery systems, such as Gliadel® wafers has been shown to improve the efficiency of the treatment against GBM using varied types of chemotherapeutic drugs in combination and separately such as paclitaxel [161], mitoxantrone [250], taxol [251], doxorubicin [252], minocycline [253], riluzole and memantine [161, 254]. Unfortunately, the therapeutic effect of Gliadel® wafers with drugs in combination has not improved patient survival so far and GBM remains incurable. A key opportunity and motivation in this thesis is the development of implantable delivery systems with chemotherapeutic drugs in combination and prolonged drug release to control GBM cells proliferation over a 30-day period.

Recurrence of GBM cells usually occurs along the resection cavity borders and a second option of treatment such as local delivery devices can possibly reduce the risk of tumorous cells recurrence [169, 255]. Rahman *et al* showed a sustained release *in vitro* study of Trichostatin A (TSA), Etoposide (ETP) and Methotrexate (MTX) from PLGA/PEG based microparticles [134]. Blended microparticles were applied to the brain cavity of sheep in the form of paste system. A gradual release of therapeutic agent was reported over 3-4 weeks and the short-term

survival study demonstrated that the drug diffused approximately 1mm from the original resection cavity [134]. Shapira-Furman *et al* developed polymeric microparticles double encapsulated with TMZ and BCNU and compressed these into wafer-like disc shapes [21]. A rodent glioma model was treated with both TMZ and BCNU disks and demonstrated long-term survivals rates of 87.5%, which was extended by 25% over TMZ and BCNU alone [21]. Both of these reports [31,144] represent proof-of-concept pre-clinical studies that can be applied to solid and GBM tumour treatment by local co-administration of chemotherapeutic drugs, however the nonspecificity and short half-life of the chemotherapeutic drugs (≈ 1.8h for TMZ) remain as challenges for GBM patient treatment.

Semi-solid (*i.e.* paste, hydrogels) or/and solid formulations (*i.e.* discs, tablets, nanofibrous membranes) delivered to the brain cavity post-surgical resection can reduce the recurrence of GBM cells [164, 169, 175]. Recent findings suggest that combination therapies show synergistic effects in terms of drug efficacy and appear some of the most promising treatments methods for GBM [187]. The Johns Hopkins Oncology Center, USA, treated 15 patients with GBM (83%) [256]. BCNU (40mg/sqm/die) and cisplatin (40mg/sqm/die) were administered concurrently for 3 days every 3-4 weeks in combination with radiotherapy (45 Gy plus a 15-Gy). This sequential chemo radiotherapeutic regimen appears to have significant antitumor activity in adults with newly diagnosed high-grade gliomas [256]. Kozielski *et*

al developed poly-beta-amino ester nanoparticles combined with multiple siRNA molecules (Robo 1, YAP1, NKCC1, EGFR and survivin) delivered to human GBM in *vitro* and *in vivo* [257]. *In vitro* data demonstrated inhibition of cancer cell growth and migration and the animal models presented a tumour weight reduction over time. The therapy proposed is promising for the treatment of GBM and other solid tumours [257].

Despite the efforts of the research community to improve the delivery systems, develop more stable chemotherapeutic drugs, combination therapies, and improve patient survival, GBM remains incurable. There is a significant scope for research focussed on combinatorial drug and genetic delivery systems and localised therapy against GBM, explored in this thesis.

1.1.3.5 Future perspectives for GBM treatment

GBM cell resistance and recurrence, tumour growth post-surgical resection and chemotherapy is related to the infectiveness of established treatments. The difficulty in developing a highly effective localised delivery system goes beyond the issues discussed previously, and must address the continuous genetic modifications of the cancer cells and resistance of the patients to the highly toxic drugs.

The scientific community has focused on the development of new strategies including development of local delivery systems, specific drugs, multi-therapy agents, more stable materials (*i.e.* polymers, functionalised polymers with chemotherapeutic drugs), and targeting genetic defects to reduce the proliferation and recurrence of GBM cells, however it is not clear how these strategies combined can promote outstanding panorama for GBM treatment. Effective use of mathematical models is also required to describe theoretical aspects correlating drug diffusion in the brain tissue, the behaviour and migration of GBM cells under certain conditions, drug clearance, interaction of the chemotherapeutic drugs with the cells, and many other aforementioned aspects.

Technologies, delivery systems and innovations applied to GBM treatment will expand the understanding around treatment failure, interaction between the devices and brain tissue, development of pharmaceutical formulations, improve the release profile of the chemotherapeutic drugs, pharmacological pathways, genetic modifications and combination of therapies to improve patient survival.

1.2 Aim and Objective

The overarching aim is to produce polymeric microspheres that have the capability to deliver a payload of cancer therapeutics directly to cells; release of the payload will then be triggered by raising the temperature to body physiological temperature, which will act to

change the conformation of the polymers exposing the therapeutics to the cells that internalise them. This project will act as a springboard for the development of targeted drug delivery in the brain cavity post-surgical intervention.

There are four cascading objectives to this thesis:

Objective A. Production of non-porous and porous polymeric microsphere carriers and their physical characterisation

The single emulsion process was used to produce non-porous and porous polymeric microspheres (target diameter size range 5 - 200 μm). The physical properties of the polymeric micro-spheres were fully characterised with an objective to control their size, morphology and level of porosity. A porosity target of 70-90% is desirable as this provides sufficient mechanical integrity for local delivery and sufficient payload surface area. The micro-particles produced have a wide range of biomedical applications beyond cancer treatment, including tissue engineering.

Objective B. Incorporation of active components into the polymeric microsphere carriers

Microparticles with three different levels of porosities were produced and loaded with active components (*i.e.* dye and toxic drugs) using the single emulsion process. The physical properties of the loaded microparticles were fully characterised in terms of their size and

porosity, as well as chemical composition and quantification of active components.

Objective C. Development of a multi-therapy system for local drug delivery and assessment of drug release

A local delivery system is developed towards treatment of GBM cells using polymeric formulations loaded with multi-therapeutic agents to control cancer cell proliferation. PLGA-PEG matrix was mixed with a water solution of Docetaxel (DTX) and the resultant spherical particles were encapsulated with methotrexate sodium salt (S.MTX), etoposide (ETP) and DTX. The paste and tablet formulations developed herein as multi-therapy delivery system were characterised in terms of their physical properties during an *in vitro* degradation study, loading efficiency of active components and release study at physiological temperature.

Objective D. Assessing the Activity of the multi-therapy delivery system

The release of chemotherapeutic drugs from the local delivery system containing spherical particles evaluated in Objective C (above) was assessed using U87 cells to investigate the toxicity of the particles and the therapeutic efficiency of the multi-therapy delivery systems.

1.3 Thesis structure

The objectives described above are divided into respective chapters as follows:

Chapter 2

The chapter is focussed on the development of the polymeric microparticles with varying morphology as described in Objective A. The hypotheses bulleted below were tested and the particles were fully characterised in terms of their size distribution, pore sizes, porosity, interconnectivity, surface area, density and degradation behaviour *in vitro*.

Hypotheses tested:

a) Particles with controllable shape and size can be achieved via single emulsion process
b) Particles with controllable morphology and porosity can be achieved using porogen in the organic phase (*i.e.* single emulsion)
c) Particles with superior level of porosity will show a higher gas adsorption and diffusion of fluids in their structure than the non-porous particles

Chapter 3

This chapter is focussed on the development of non-porous and porous microparticles loaded with chemotherapeutic drugs via the single emulsion process, their characterisation and quantification. The release of active components (*i.e.* dye and chemotherapeutic drugs) was assessed *in vitro* under physiological conditions as function of time. Paste and tablets formulations were developed using a mixture of

PLGA-PEG matrix with solution of Docetaxel (DTX) and PLA/PLGA spherical particles loaded with this drug (DTX). A tablet formulation study was conducted to assess their *in vitro* behaviour under physiological conditions as function of time. The drug release behaviour and profile of a multi-therapy system including more than one drug in the polymeric formulations followed over a 30-day period. Particle toxicity and localised therapeutic efficiency was assessed in during this *in vitro* study.

Hypotheses tested:

a) PLGA will enable higher drug loading than PLA
b) Particles with higher levels of porosity will show a faster release rate
c) The multi-therapy system developed with PLGA and PLA spherical particles will enable sustained controlled release rate
d) The multi-therapy formulations (*e.g.* paste and tablets) will prolong the GBM therapy against tumorous cell proliferation

Chapter 4

This chapter reports the conclusion of each experimental chapter and presents future perspectives correlated with the treatments against GBM.

CHAPTER 2. Development of polymeric microparticles made with poly (lactide) (PLA) and poly (lactide-*co*-glycolide) (PLGA) with varying morphology

2.1 Introduction

The fabrication method for micro and nano sized polymer particles is one of many factors to be considered for encapsulation and release of therapeutics, depending on the end application. This is further affected by a complicated array of factors including the type of polymer, molecular weight, co/polymer composition and nature of any excipients added to the particles [42]. Several methods have been developed to produce polymeric microspheres for biomedical and pharmaceutical applications. These techniques have been established to provide control over particle size, morphology and to enable the use of new materials and drugs [5].

Polymeric microparticles developed by colloidal emulsion or suspension techniques have been produced with particle sizes ranging between a few nanometres to several micrometres. The type of formulations (emulsion and/or suspension) and concentration of components (organic and non-organic phase) influence particle

formation, their physical and/or spontaneous aggregation, stability, as well as concentration of the active components [130, 258-260]. Generally, suspensions can be divided into three categories: i) Solid particles in a liquid medium, ii) liquid droplets in a liquid medium (*i.e.* emulsion systems) and iii) gas in liquid systems (foams) [129]. According to Royer J R *et al*., the synthesis of colloidal systems are affected by several factors such as rotary Brownian motion, non-Brownian behaviour, shear thinning, hydrodynamic forces such as repulsion and attractive forces (*i.e.* van der Waals force) [129] and the varying equilibrium phase behaviours of materials [261, 262]. The formation of microparticles, their physical properties, such as morphology and size can be affected by repulsive and attractive intermolecular forces during formation [261, 263, 264]. Furthermore, interfacial forces have dominant roles in determining the behaviour of many complex fluids such as emulsion system, polymer blends, the fusion of vesicles and production of polymeric nano- and micro-particles [265-267].

Other aspects relate to the physical properties of particles, which can include the presence of pores in their structure. The level of porosity of polymer microparticles is associated with the type of porogen used in the organic phase, the rate of porogen evaporation [91] and type of formulations [130, 268]. Furthermore, particle morphology factors, which include different levels of porosity and particle size, can be affected by: i) The type of polymers used in the formulation, their chemical structures and molecular weight (M_W) [131, 269], ii) the type

of surfactant in emulsion processing (*i.e.* purity, hydrophilic-lipophilic balance and Mw), iii) types of solvents [270], iv) the energy put into the system (*i.e.* stirring method and rate) [99, 130], and v) concentrations and removal of porogen used in the organic phase (*i.e.* polymeric solution) [130, 271].

An important challenge in the production of polymeric microparticles, when incorporating hydrophobic and hydrophilic agents in a single emulsion process, is the fine control of their morphology [272-275]. Many techniques have been used to control the physical properties of particles, including their size, shape [276, 277], particle yield, suspension homogeneity and stability [270]. Some of the pharmaceutical formulation methods used to make porous particles include single emulsion (*i.e.* oil [o] and water phase [w] - o/w) and double emulsion (*i.e.* o/w/o, w/o/w). These techniques rely on the hydrophobicity and hydrophilicity of the active components, and types of polymers to produce spherical microparticles, which can encapsulate different types of agents such as hydrophobic or hydrophilic drugs [278-281].

Polymeric microparticles have been used for applications such as chromatography [282, 283], sensing and detecting [282, 284, 285], tissue engineering, as drug delivery carriers [42, 68, 130], and for other biomedical applications [10, 130]. Polymeric carriers have been developed using natural and synthetic polymers such as chitosan, alginate, poly(lactide) (PLA) and poly(lactide-*co*-glycolide) (PLGA) [28, 39]. The type of material used to develop polymeric microparticles

can influence the loading and encapsulation efficiency of drugs ranging from small molecule therapeutics to biomacromolecules. In general, relatively low drug loadings are achieved, typically 5% (and usually less than 10%), this issue is even worse for those drugs with poor aqueous solubility [286-289]. Synthetic materials and particles have been developed over the last few years for various biomedical applications, in particular towards translational work from pre-clinical to clinical. According to Park *et al.* polymeric microparticles (*i.e.* PLGA-PEG) were loaded with dorzolamide to control ocular hypertension and glaucoma [12]. They found that the polymeric microparticles named as MUCO_NM decreased the intra ocular pressure (IOP) by almost 25% whilst the commercial eye drop solution (Trusop®) reduced the IOP by only 10% [302]. Furthermore, they tested the dosage frequency of Trusop® and MUCO_NM, which showed that Trusop® had been administered 4 times during 2 h to reach the same efficacy as MUCO_NM [302]. Park C G *et al.* suggested that MUCO_NM as a potential carrier could enhance the efficacy of dorzolamide when topically delivered to the eye [290].

According to Smith *et al*, PLGA/PEG microparticles loaded with Etoposide were developed in order to control the growth and proliferation of GBM cells (astrocytoma grade 4) [271]. The PLGA/PEG particles formed a paste formulation, which fused together at body temperature and demonstrated release of the active chemotherapeutic drug over a period of 3 weeks [271]. The paste was placed into the resection cavity and the tumour growth was measured

by imaging techniques. The paste remained in the resection cavity after 28 days of *in vivo* study, and did not cause cytotoxic adverse effects in the absence of drug, suggesting no significant systemic effect from the localised drug delivery. Furthermore, reduction of tumour growth was observed with the higher dosage of PLGA/PEG particles loaded with Etoposide (160 mg/kg), which persisted up to 21 days following implantation of the polymeric system. These authors suggested that the PLGA/PEG system is a safe and effective way to release chemotherapeutic agents as well as control the growth of GBM cells and extend patient survival [291].

As evidenced from the literature, there are many advantages of porous particles in terms of application compared to non-porous particles, such as reduced amounts of material (*i.e.* degradation products) to be eliminated from the body, and better distribution of biological factors within the particles. Porous particles can also impart control over drug release rates via increased surface area [131, 292, 293] and over the degradation rate of the polymeric matrix [294]. Hierarchical pore systems are also advantageous as such particles can feature high pore volumes, as well as tailored drug diffusion rates, controlled by judicious pore structure design [295, 296]. There are many kinds of pore networks, in which the individual pores may vary both in size, shape, interconnectivity and tortuosity. A feature of special interest for varying purposes is the *width (w)* of the pores, *i.e.* diameter of a cylindrical pore, or/and the distance between the sides of pores with different morphologies [297].

Classification of pore structures can be related to the size ranges and their characteristic adsorption, as manifested effects in the isotherm represented by the linear graphs of gas adsorption. As an example, in microporous structures that have a pore size less than 20 **Å** (2 nm), the potential interaction is significantly higher than in wider pores owing to the proximity of the walls and the amount of gas adsorbed versus a given relative pressure, enhanced during the gas analysis. Mesoporous structures have pore sizes between 20 and 500 **Å** (2 and 50 nm), while the macropore range is more than 500 **Å** (50 nm). The macropore range are so wide that it is virtually impossible to map out the isotherm in detail because the relative pressure increase is faster than the mesoporous features and are close to the maximum limit range of gas adsorption [297].

Ni *et al.* produced polymeric non-porous and porous particles (*i.e.* PLGA) loaded with cinaciguat (a heart failure drug) via single emulsion and solvent evaporation methods [308]. Porous particles were made using different concentrations of porogen in the formulation [308]. They found that particles with porous structures exhibited a burst release profile during the initial 2 h of drug release; this release was associated with particles that had a high degree of porosity, and reported to be a far higher rate than for non-porous counterpart particles. Particles with porogen concentrations between 20% and 40% exhibited a burst release profile of up to 87% of the drug incorporated during the first 7 hours, whilst non-porous particles exhibited a burst release of 15% followed by a plateau region [298].

These results evidence that porous microparticles are a useful vehicle to control drug release [298].

This chapter describes the types of polymeric microparticles achieved by single emulsion system, varying and controlling their morphology, size (and size range) as well as their pore structures using an organic phase porogen. The main focus of this study was to show the difference between non-porous and porous particles by imaging techniques, to determine their size by dynamic light scattering (DLS), determine particle porosity by BET surface area analysis, and to investigate how the produced polymeric particles behaved in buffered solution over a 45-day period of *in vitro* investigation, followed by SEM.

PLA microparticles (MPs) were used as a proof-of-concept study in order to develop a range of microparticle morphologies, as PLA is a robust and slowly-degradable polymer which can be readily prepared, stored and analysed. However, the advantages of stability can in fact also be a disadvantage for some drug delivery applications, therefore formulation strategies for drug encapsulation and release were developed and applied using PLGA with similar porosity features to the PLA microparticles but with faster hydrolysis kinetics.

2.2 MATERIALS AND METHODS

2.2.1 Materials

Polylactide (PLA) beads were purchased from Nature Works LLC (Ingeo^{TM} Grade 3251D average M_W ~ 90,000 to 120,000 g mol^{-1},

density 1.24 g/cm^3, PDI: 1.636) (NW PLA) were used as a matrix for the spherical microparticles formulation. Poly(lactide-*co*-glycolide) (PLGA-medical grade) was purchased from EVONIK (average M_w ~ 65,900 g mol^{-1}, PDI: 1.7. Dichloromethane (DCM) (Grade HPLC ≥ 99.8%) and cyclohexane (porogen) were purchased from Sigma-Aldrich. Polyvinyl alcohol (PVA) 86.5 – 89% hydrolysed, M_n 6.7 x 10^{4}Da) was donated by Nippon Gohsei, Japan. Polyvinyl alcohol (Mowiol® 4-88) 86.7 - 88.7 mol% hydrolysis, M_w ~31,000 g mol^{-1} was purchased from Sigma Aldrich, UK.

2.2.2 Microparticles preparation

A single emulsion method was used for development of spherical PLA and PLGA microparticles [268, 274, 299]. The organic phase containing PLA or PLGA and organic solvent (DCM) at 5% (w/v) was dropped into aqueous PVA solution at 0.5% (w/v) using a syringe driver (World Precision Instrument) under constant magnetic stirring (IKA RCT basic) during 4 h (speed 500 rpm) at room temperature as demonstrated in Table 2.1. Some of formulations were developed using both stirrer and ultrasonic probe sonicator (Apex Instruments Co.) as described in the table below. The suspension of particles was washed 3 times with deionised water (DI) and centrifuged (Jouan CR4-22) at 500 rpm for 10 min. After the washing process, the particles were kept in a Falcon tube® and dried under vacuum at room temperature for 24 h. The porous microparticles were produced by addition of cyclohexane (porogen - 5% w/v) solution in the organic

phase. The difference in particles morphology were achieved according with the method demonstrated below in Table 2.1. Formulations were produced in triplicates and each batch was characterised separately.

Table 2.1: Development of polymeric microparticles formulations under varied conditions such as type of polymer and PVA used, injection speed, porogen and energy applied to the system.

Type of polymer	Type of PVA	Injection Speed (mL/min)	Porogen (Cyclohexane)	Energy into the system	Sample Code
PLA	NG-PVA-383 Gohsei	0.4	No	Stirring	A
		0.8	Yes	Stirring	B
		1.6	Yes	Stirring	C
		4.4	Yes	Stirring	D
		4.4	Yes	Stirring and sonication	E
PLGA	NG-PVA-383 Gohsei	0.4	No	Stirring	A'
		0.4	Yes	Stirring	B'
	Mowiol 4-88 Sigma Aldrich	4.4	Yes	Stirring and sonication	C'

2.2.3 Evaluation of Particle Morphology

Scanning Electron Microscope (SEM)

The microparticles were sputter-coated with platinum, to avoid image distortion due to charging, and examined using a Philips XL-30 (FEI, USA) scanning electron microscope (SEM) with an accelerating voltage of 10kV in secondary electron mode and a working distance of 10 mm. The sizes of particles and their distributions were further analysed with Image J software (32-bit Java 1.6.0_24). The known scale bar featuring in each SEM image examined was used to calibrate subsequent measurements on that image using Image J software and

based on pixel number. Representative particles (n = 50) were measured manually using Image J per SEM image and their average diameter and standard deviation reported.

2.2.4 Process Yield

Process yield was defined as the mass of polymer material recovered after centrifuging the micro particle suspension and drying for 24 h. Dried material was accurately weighed and the process yield was calculated using equation 1:

Equation 1

$$\text{Process Yield (\%)} = \frac{(\textit{mass of dry MP}) \times 100}{(\textit{mass of polymer used in MP preparation})}$$

2.2.5 Particle Size Distribution

Dynamic Light Scattering (DLS)

Particles in suspension were loaded in a small cell (10 mL) with ultrapure water. Particle suspensions were auto diluted by adding ultrapure water to the cell until the suspension reached a concentration between 8 and 12%, according to a standard operating procedure established at Boots Building (University of Nottingham). The samples were measured via laser diffraction using a Coulter LS230 with white

light filtered (30s – 450, 600 and 900 nm) and polarised 2 angles – (90° apart).

Hydrodynamic radii of the polymeric microparticles were measured from standard auto correlation functions, the measured diffusion coefiencients were related to particle hydrodynamic radius *via* the Stokes-Einstein equation as shown in equation 2,

$$R_H = \kappa T/6\pi\eta D$$

Equation 2

where R_H is the hydrodynamic radius, κ is the Boltzmann constant, T is the temperature, D is the diffusion coefficient, and η is the viscosity of the solvent. Additionaly it was assumed that the particles were spherical and non-interacting.

Results are reported as mean of three separate measurements of three different batches (n = 9) $\pm$ standard deviation (SD).

2.2.6 Level of porosity and pores distribution

Cryo – Scanning Electron Microscopy (Cryo-SEM)

Microparticles were mixed with polyvinyl acetate (PVAc)-based glue, frozen with liquid nitrogen and placed into a cryo-scanning electron

microscope (cryo-SEM) pre-chamber, fractured with a blade *in situ*, coated with gold and placed into the cryo-SEM chamber. Cross sections of the particles were examined using a Jeol 6060LV (The Oxford CT 1500) with an accelerating voltage of 6 kV. Pore size analysis was further evaluated with Image J software (32-bit Java 1.6.0_24). The scale bar on Image J software was calibrated as described above (in section 2.2.3) per image, and representative particles (n = 100) were measured manually, results are presented as average and standard deviation.

2.2.7 Particles density and Surface Area

2.2.7.1 Helium Pycnometry

The absolute density of specimens was obtained by measuring the volume of powder excluding the pores as well as the void spaces between particles using a Micrometrics AccuPyc 1340 helium pycnometer (Norcross, GA, USA). Measurements were taken in triplicate for each sample type. Measurements were conducted at room temperature and relative humidity of 50%.

2.2.7.2 Surface Area - BET

The specific surface area was automatically carried out by computing the multipoint BET analysis method as shown in equation 3. The linear region selected for the BET analysis was within P/P_0 = 0.05 to 0.30 range of relative pressure. The average area a_m (molecular cross-

sectional area calculated from the liquid density of the adsorbate) occupied by a single nitrogen molecule in the complete monolayer, a_m = 0.162 nm^2 at 77K n^a_m is the monolayer capacity, where n^a is the amount adsorbed at a relative pressure P/P_0, and L is the number of entities per mole, also called Avogadro's number, normally accepted as 6.022 x 10^{23} [294, 300, 301].

$$SSA = n^a_m a_m L$$

Equation 3

2.2.8 Degradation study of PLA and PLGA microparticles

Dried microparticles (1 mg) were dispersed in Dulbecco's phosphate buffered solution (1 mL) at 37°C in eppendorf tubes under constant shaking in triplicates. Samples (10 µL) of the suspension were removed from the eppendorfs at predermined time intervals and an equal amount of fresh buffer was replaced. The samples were placed on SEM stubs at room temperature for 24 h to dry prior to analysis by SEM as described in section 2.2.3 .

2.2.9 Statistical analysis

Each test was performed in triplicate. The values are expressed as mean and standard deviation (SD). Statistical significant differences between the treatments were evaluated with analysis of variance (ANOVA) and Bartlett's test significant difference (LSD) using GraphPad Prism, with alpha < 0.05 and <0.0001 being the probability of error .

2.3 Results

2.3.1 Morphologically characterisation and particle size analysis

Solid spherical PLA MPs were produced *via* the single emulsion process to vary their level of porosity and porous features as described in the methods chapter 2. Various levels of controlled porosity were achieved when the porogen was mixed with the organic phase in the emulsion process. A family of five different PLA MPs were successfully developed, varying in their morphology and porous structure and subsequently investigated for drug release in this thesis. The method developed for non-porous and porous PLA particles was also applied for PLGA particle production. A family of three different PLGA MPs were produced, which are nominated as non-porous, medium porosity and highly porous particles.

The sizes and morphologies of the PLA and PLGA MPs were determined by SEM and image analysis, and the level of porosity assessed using cryo-SEM, as shown in Figure 2.1. The particles produced under varied conditions, particle size and yield range are reported in Table 2.1. The non-porous PLA spherical particles (Type A) exhibited an average diameter of 34 $\pm$ 5 μm. The family of PLA porous particles produced are shown in Figure 2.1 (Types B – E) and represent the various morphologies, porosity levels and exhibited diameter ranges attained, at 100 $\pm$ 15 μm; 64 $\pm$ 10 μm; 48 $\pm$ 8.5 μm; 14

± 4.5 µm, all respectively. The non-porous PLGA spherical particles (Type A') had an average diameter of 101 ± 32 µm, whereas medium porosity (Type B') and highly porous PLGA particles (Type C') had diameters of 110 ± 28 µm and 30 ± 17 µm, all respectively as shown in Figure 2.1. Non-porous PLA particles represented in Figure 2.1A and porous particles represented in Figure 2.1B - E had yields of 24 ± 1.5, 60 ± 0.8, 60 ± 2.2, 80 ± 1.2 and 30 ± 1.4%, all respectively. The non-porous PLGA particles represented by 1A' and porous particles represented in Figure 2.1B'-C' had a yield of 85 ± 1.3, 60 ± 0.6 and 40 ± 1.3%, all respectively.

Table 2.2: Key formulation and production parameters for the families of non-porous and porous PLA and PLGA microparticles, their size ranges and yields.

Type of polymer	Porogen (Cyclohexane)	Energy into the system	Sample Code	Particle size (µm)	Particle yield
PLA	No	Stirring	A	34 ± 5	24 ± 1.5
	Yes	Stirring	B	100 ± 15	60 ± 0.8
	Yes	Stirring	C	64 ± 10	60 ± 2.2
	Yes	Stirring	D	48 ± 8.5	80 ± 1.2
	Yes	Stirring and sonication	E	14 ± 4.5	30 ± 1.4
PLGA	No	Stirring	A'	101 ± 32	85 ± 1.3
	Yes	Stirring	B'	110 ± 28	60 ± 0.6
	Yes	Stirring and sonication	C'	30 ± 17	40 ± 1.3

The morphology and particle size are crucial determinants for the application of polymeric microparticles as drug delivery vehicles. Particle size can be a limiting factor for biological applications and determine suitability for local or systemic drug delivery due to the diameter of the veins and capillaries, as well as delivery of the particles through the blood stream and respiratory tract [14, 15, 91, 130]. The

diameter (μm) range of the PLA and PLGA MPs produced was confirmed by DLS, as shown in Figure 2.2. Particles nominated as A, exhibited a broad peak at 50 μm and a second peak between 50 and 300 μm whilst particle E exhibited a peak below 50 μm as shown in Figure 2.2. Furthermore, particles B and C exhibited narrow peaks with a diameter range between 50 and 100 μm, and two peaks above 100 μm; between 180 and 320 μm; particles nominated as D exhibited a distinct narrow peak at 50 μm as shown in Figure 2.2 (PLA MPs size distribution). PLGA MPs exhibited a single peak between 50 and 70 μm for sample A' and particles B' and C' exhibited a broad peaks between 50 and 80 μm and between 30 and 50 μm, respectively as shown in Figure 2.2.

Inner particle porosity features as well as pore geometry assessed by Cryo-SEM, which revealed similar levels of porosity between their external and internal regions, as shown in Figure 2.1 (B-E). Particle diameters were determined based on 2-dimensional (2D) SEM images, and are summarised in Figure 2.2. Both the PLA and PLGA particles exhibit circular cross-sections, the electron microscopy observations reveal that particles A and A' (Fig 2.1) do not exhibit any porous structure in their internal region, whereas particles B, C, D and B', C' revealed continuous and interconnected pores (Fig 2.1), matching closely to the surface pores observed for the particles, with pore diameters determined as 2.71 $\pm$ 0.7 μm, 6.00 $\pm$ 1.63 μm, 7.40 $\pm$ 1.4 μm, 5.22 $\pm$ 3.9 μm and 5.35 $\pm$ 3.0 μm, all respectively. Furthermore,

particles nominated as E exhibited hierarchical pore structures, with two different pore sizes, determined as 0.36 ± 0.09 µm, represented by red arrows and 5.23 ± 0.64 µm represented by a red circle as shown in Figure 2.1(E).

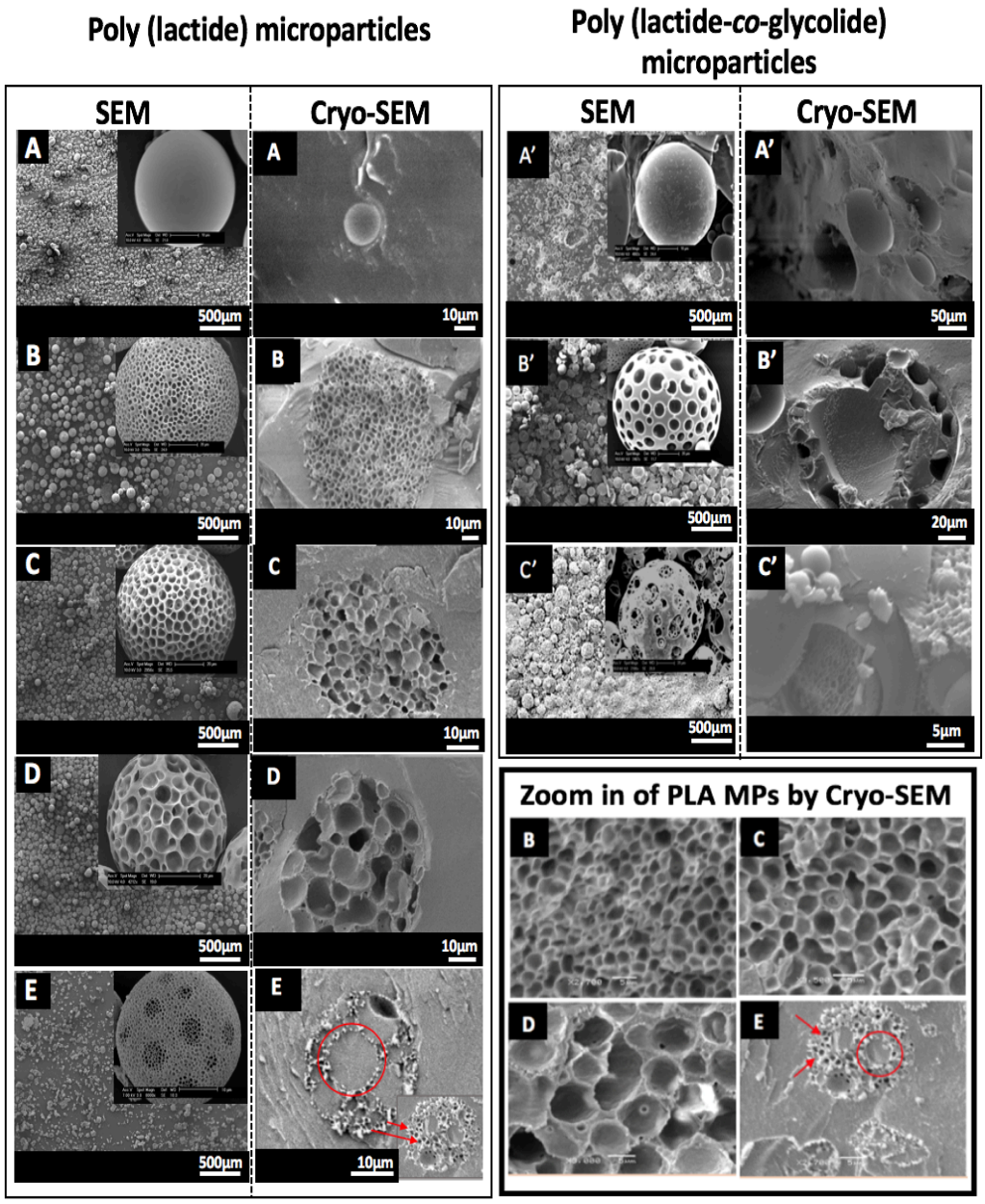


Figure 2.1: Polymeric microparticles of PLA and PLGA made with various levels of porosity, produced via single emulsion process. Differences in pore structures between PLA particles (A, B, C, and E) and PLGA particles (A' B' and C'). High magnifications cryo-SEM images (cross-sections) of the PLA microparticles structure evidencing pore distributions and differences in pores size (Scale bars: 500µm, 50µm, 20µm, 10µm and 5µm – insets).

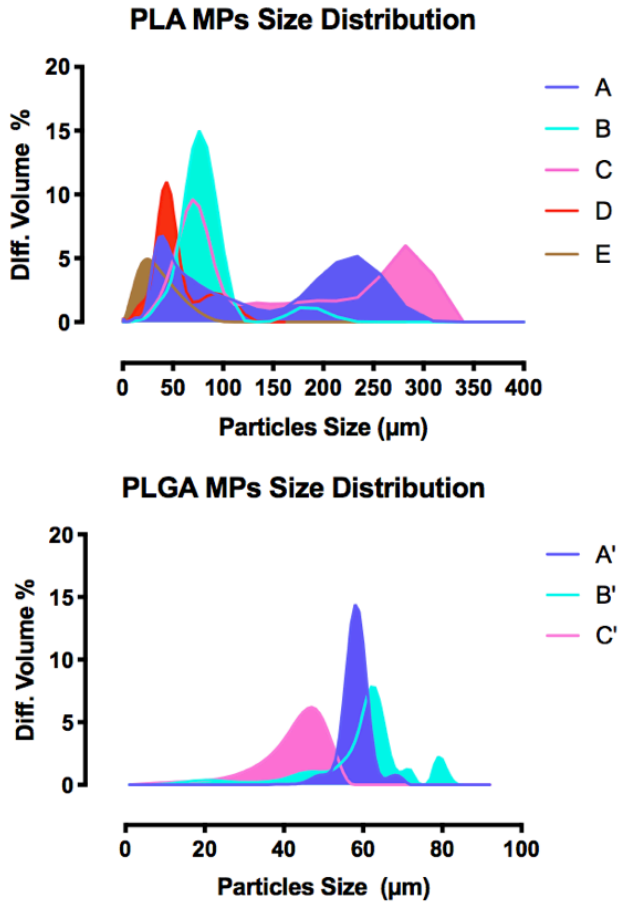


Figure 2.2: Determination of the size distribution for the polymeric microparticles (PLA and PLGA MPs), determined by DLS (n=3).

2.3.2 Level of porosity and particle density determination

Pore size distributions of PLA and PLGA MPs were determined from measured cross-sections of Cryo–SEM images, as shown in Figure 2.1. Particles nominated C and D exhibited larger pore diameters in comparison to particle type B. However, particle type E exhibited a bimodal diameter range, as shown in Figure 2.3. Furthermore, particle type A' did not exhibit any inner porosity features, whereas particles B' and C' exhibited pore diameters of 5.22 $\pm$ 3.85 µm and 5.35 $\pm$ 3.01 µm, respectively. Particles A and E exhibited lower densities compared to particle types B, C and D, as shown in Figure 2.4 (PLA MPs

measurement). Furthermore, particles A' exhibited higher densities than B' and C', as shown in Figure 2.4 (PLGA MPs measurement). The surface area of spherical MPs was determined using BET, as described in the previous chapter (section 2.2.7.2). Particles B, C and D exhibited similar surface area values, determined as 5.2, 5.8 and 4.9 m^2/g, respectively. Whereas particles A and E exhibited surface areas of 6.72 and 1.7 m^2/g, respectively. Particles A' had a surface area value of 0.67 m^2/g, whilst particles B' and C' exhibited a surface areas of 2.26 and 1.57 m^2/g, respectively, as shown in Figure 2.4.

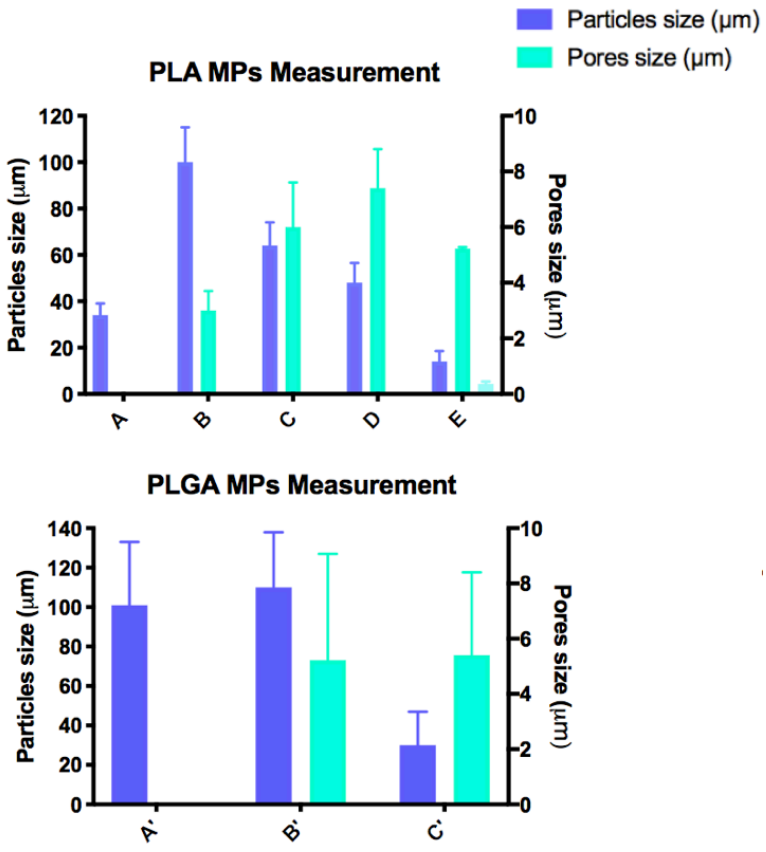


Figure 2.3: Particles size and pores size assessment of PLA and PLGA MPs measured by SEM and Cryo-SEM images, respectively. (n=3) ($p<0.0001$ Ordinary one-way ANOVA: A vs. B, C, D and E; A' vs. B' and C').

The BET technique was used to determine surface area, and the rates of gas diffusion into particles, indicative of pore interconnectivity and the different levels of porosity found in particles features. Figure 2.5 shows the relative pressure (P/P_o) as function of gas adsorbed into the particles produced. The gas isotherm for particles A exhibits a negative gas adsorption, reaching -4 cm^3/g, and particle E reached gas adsorption at 2.25 cm^3/g; whilst, particles B, C and D exhibited similar gas adsorption profiles. Furthermore, particle type A' exhibited gas adsorption at 5.28 cm^3/g whilst particles B' and C' exhibited gas adsorption at 15.37, 11.50 cm^3/g, respectively.

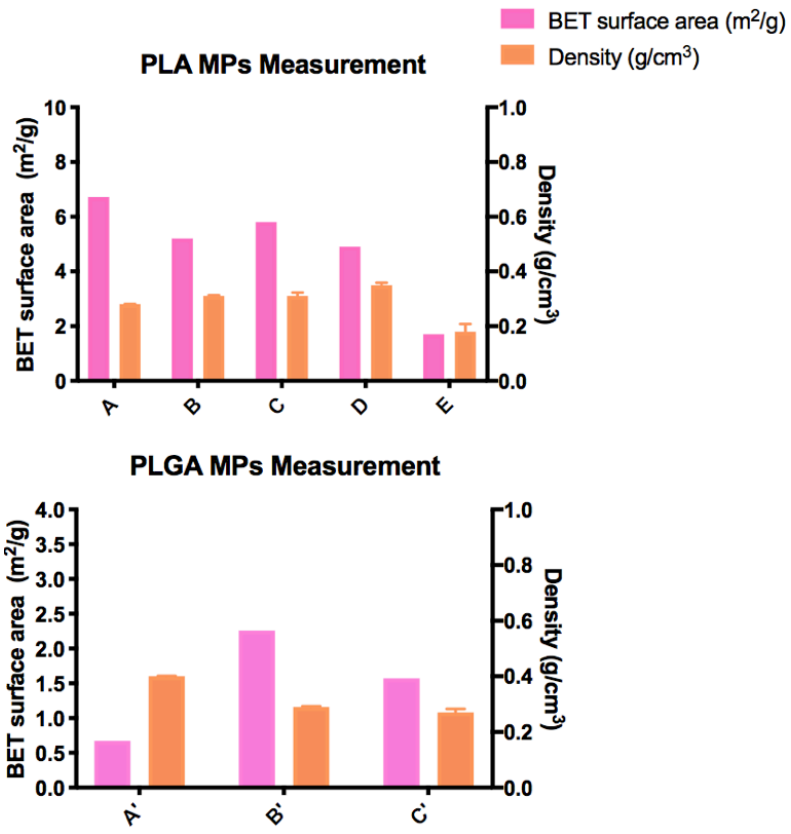


Figure 2.4: Surface area and density of PLA and PLGA MPs measured by BET and helium pycnometry, respectively. (n=3) ($p<0.0001$ Ordinary one-way ANOVA: A vs. B, C, D and E; A' vs. B' and C').

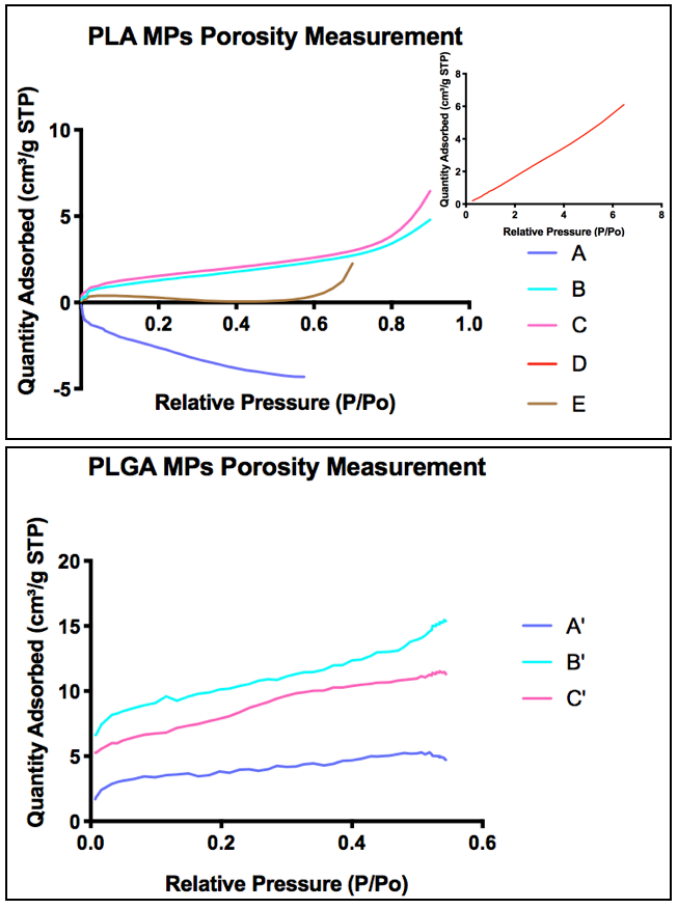


Figure 2.5: Level of porosity of PLA and PLGA MPs represented by the quantity of gas adsorbed to the polymeric MPs, determined by BET.

2.3.3 Study of polymeric microparticle degradation behaviours in *in vitro* buffered solutions, over a 45-day period

An *in* vitro study was conducted to assess the hydrolytic degradation of the polymeric microparticles over a 45-day period under controlled conditions, as described in section 2.2.8. Morphological changes to the polymeric microparticles were assessed by SEM and analysed using Image J, shown in Figures 2.6-2.17, and summarised in Table 2.2. PLA and PLGA microparticles exhibited three distinct morphologies, designated, non-porous, medium porosity and highly porous, depending on particle type. These morphologies were targeted in order to assess differences in their behaviour in buffered solution under

continued agitation at 37^{o}C, over time period relevant to controlled drug delivery for GBM.

PLA and PLGA particles were initially analysed at early time points, 3 h and 24 h as shown in Figures 2.6 to 2.9; PLA particle types B and C exhibited some erosion and fragility after 24 h, as indicated by the red arrow in Figure 2.7. PLGA microparticle types A' and B' showed evidence of particle rupture and the presence of large pores after 3 h and 24 h degradation, as indicated by red arrow in Figure 2.8 and Figure 2.9.

Progression of PLA microparticle degradation is shown at 7 days for particles A, B and C and at 15 days for particles B and C, significant differences are indicated by the red arrows in Figures 2.10 and 2.11. Particles type A exhibited significant deformation as opposed to rupture at days 7 and 15, as shown in Figures 2.10 and 2.11. PLGA microparticle types A' and B' exhibited increased particle degradation, as well as particle rupture, over this same period, as shown in Figures 2.12 and 2.13 (red arrow). Whereas, particle type C' tended to shrink in size, evident at 7 and 15 days in comparison to 3 h and 24 h. PLA and PLGA microparticles degraded for 30 and 45 days exhibited different degradation behaviours, with particle type A exhibiting deformation behaviour, and particles B and C showing evidence of rupture and increase in pore size, compared to 3 h, as shown in Figures 2.14 and 2.15 (red arrows). Furthermore, particle type A' exhibited

deformed morphology, with evidence of pore closure at particle surfaces, whereas particles B' and C' exhibited marked rupture and degradation compared to 3 h, as shown in Figures 2.16 and 2.17.

PLA and PLGA microparticles were assessed over a 45-day period by SEM and Image J. PLA particles B and C exhibited particle size ranges from 67.00 ± 18.14 μm to 86.70 ± 19.00 μm and 5.15 ± 1.37 μm to 77.56 ± 15.38 μm, respectively, and pores sizes from 4.41 ± 1.37 μm to 3.86 ± 1.70 μm and 2.19 ± 0.72 μm to 10.13 ± 3.30 μm, both respectively. However, PLA particle type A exhibited size reduction from 52.22 + 13.00 μm to 12.34 ± 3.20 μm with an absence of pores in their surface (summarised in Table 2.3). PLGA particle types A' and C' exhibited particle size reduction from 52.22 ± 12.76 μm to 14.00 ± 6.00 μm over the 45-day period, and 3.15 ± 1.00 μm to 1.03 ± 0.15 μm over the 30-day period, both respectively, whilst particle type B' exhibited a size range from 117.30 ± 31.71 μm to 132.41 ± 24.51 μm and pores size from 4.60 ± 1.11 μm to 5.60 ± 1.60 μm over the 45-day period (summarised in Table 2.3). Furthermore, particle type C' exhibited pore size reduction from 1.80 ± 0.64 μm to 0.41 ± 0.19 μm over a 30-day period (summarised in Table 2.3).

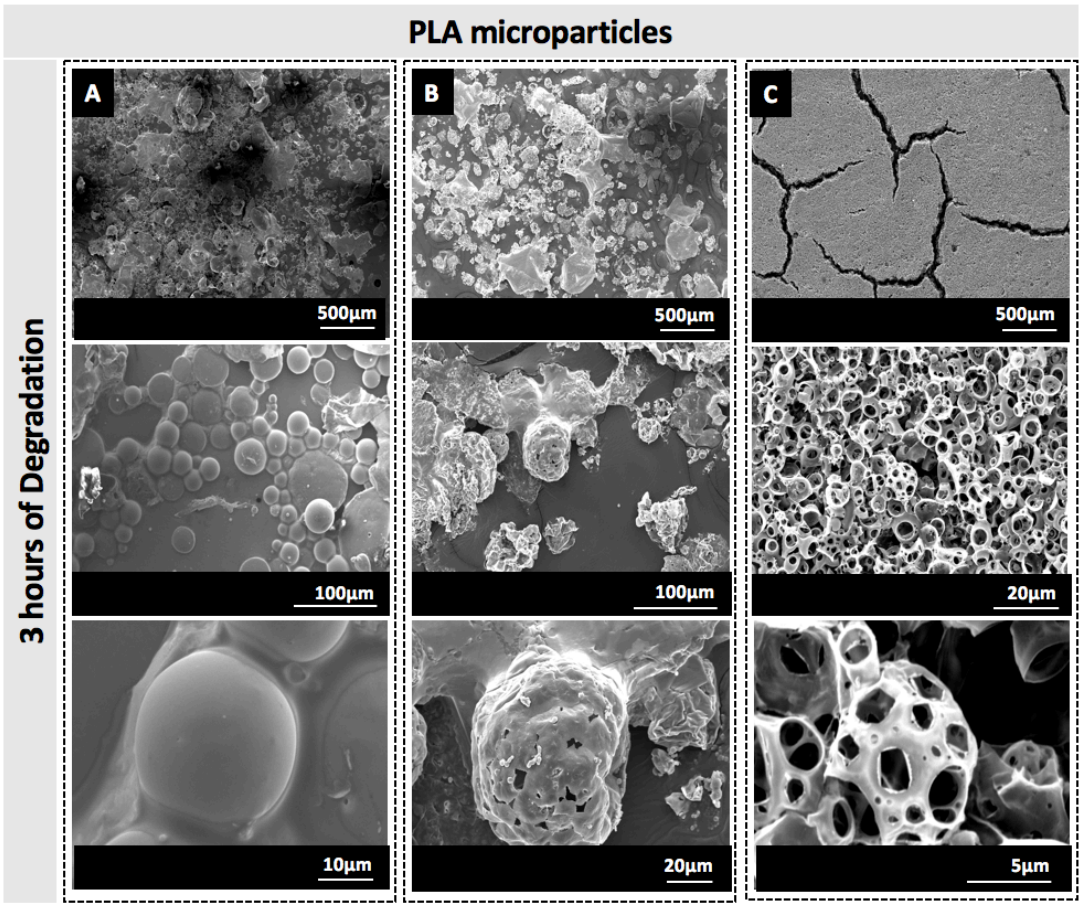


Figure 2.6: SEM analysis of the morphological changes of PLA particles as function of time exposed to buffered solution over a 3 h period (scale bars: 500 µm, 100 µm, 20 µm, 10 µm and 5µm -insets).

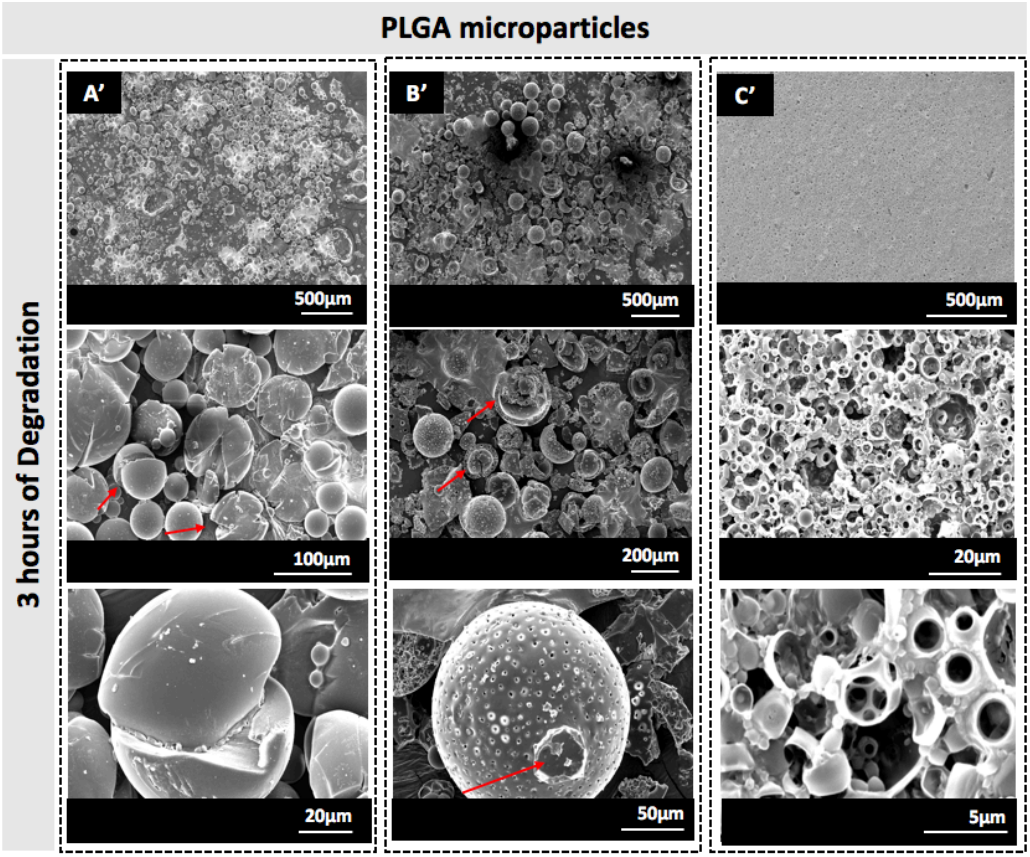


Figure 2.7: SEM analysis of the morphological changes of PLA particles as function of time exposed to buffered solution at 24h (scale bars: 500 µm, 200 µm, 100 µm, 50 µm, 20 µm and 10 µm -insets).

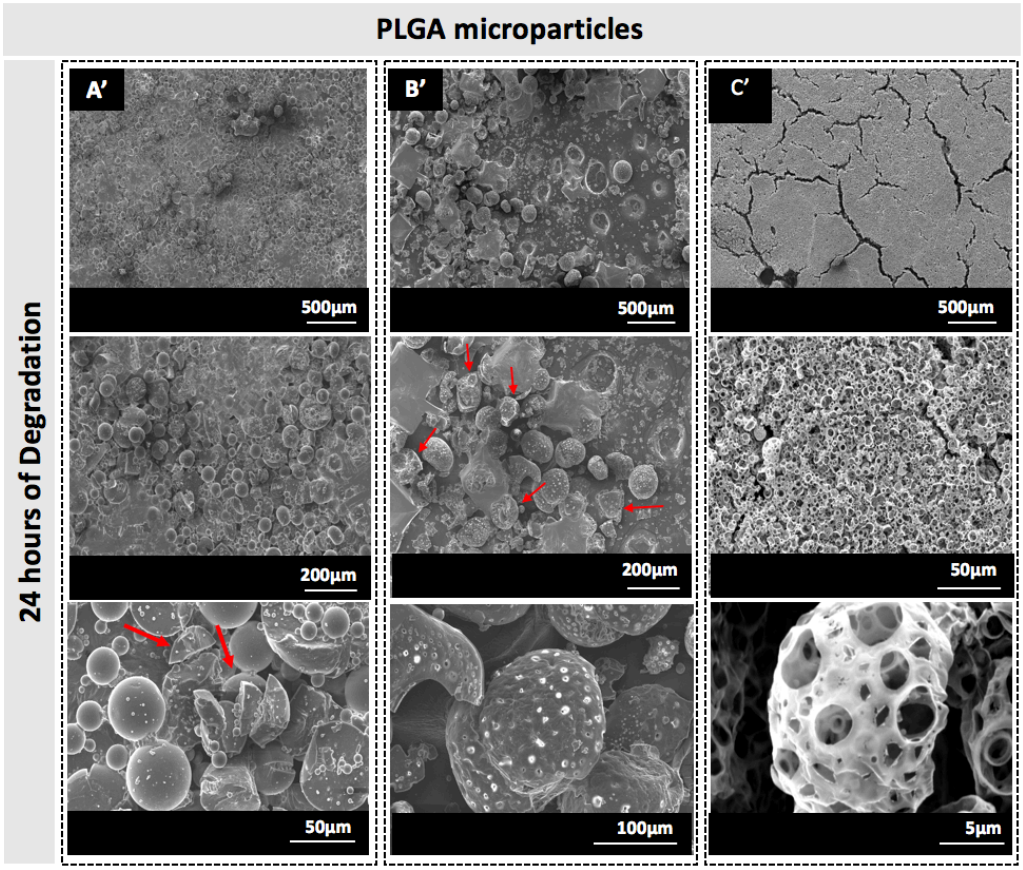


Figure 2.8: SEM analysis of the morphological changes of PLGA particles as function of time exposed to buffered solution at 3h (scale bars: 500 µm, 200 µm, 100 µm, 50 µm, 20 µm and 5 µm -insets).

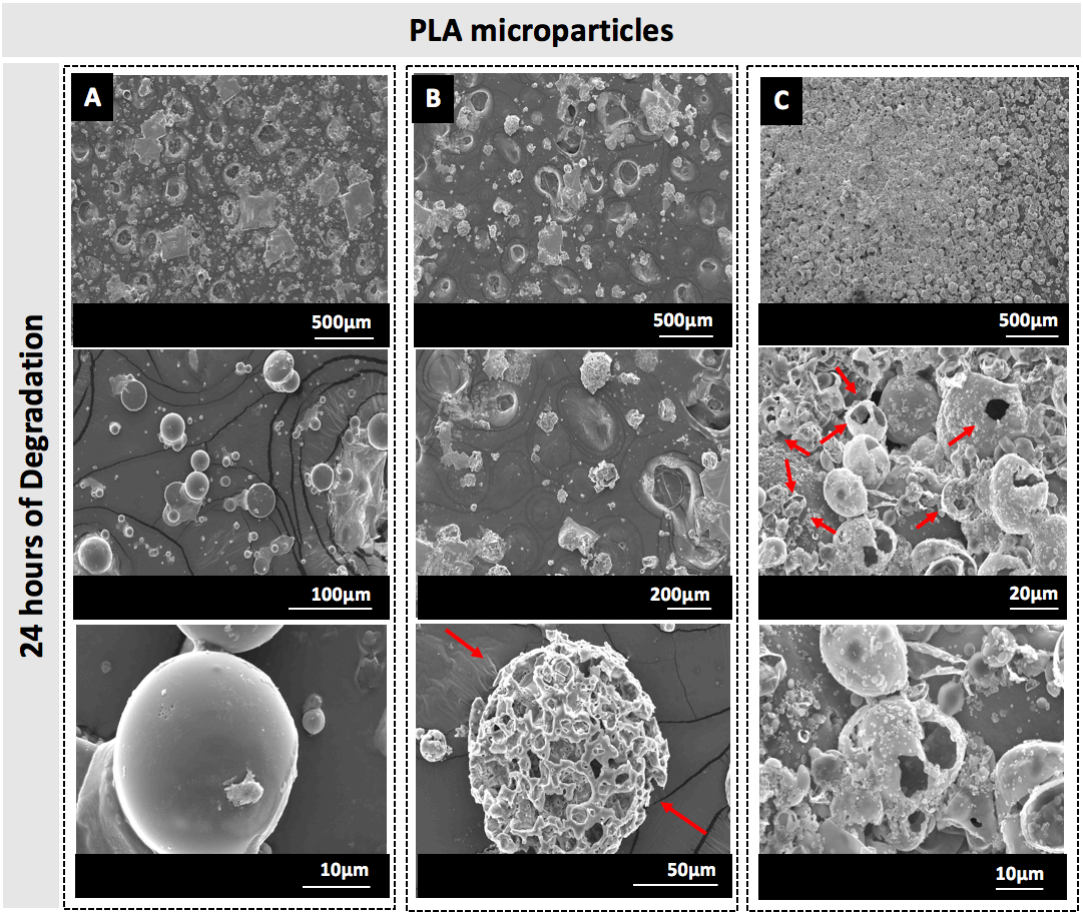


Figure 2.9: SEM analysis of the morphological changes of PLGA particles as function of time exposed to buffered solution at 24h (scale bars: 500 µm, 200 µm, 100 µm, 50 µm and 5 µm-insets).

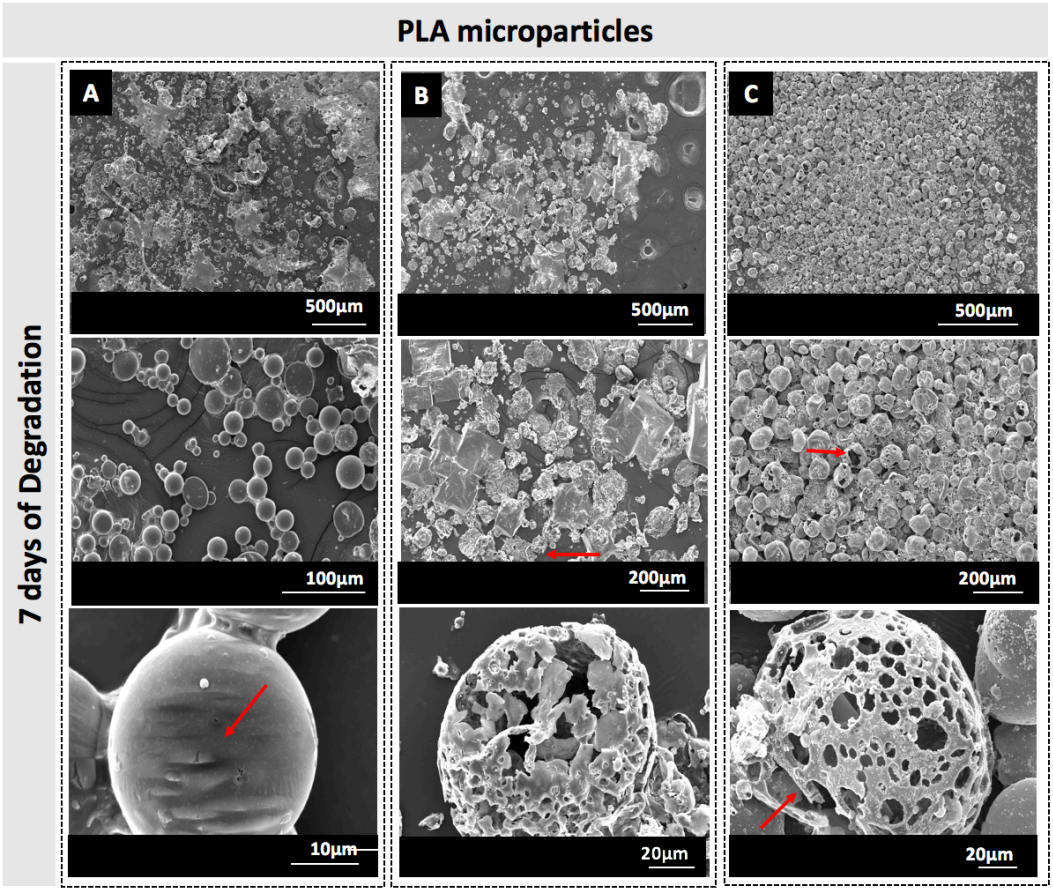


Figure 2.10: SEM analysis of the morphological changes of PLA particles as function of time exposed to buffered solution at 7 days (scale bars: 500 µm, 200 µm, 100 µm, 20 µm and 10 µm -insets).

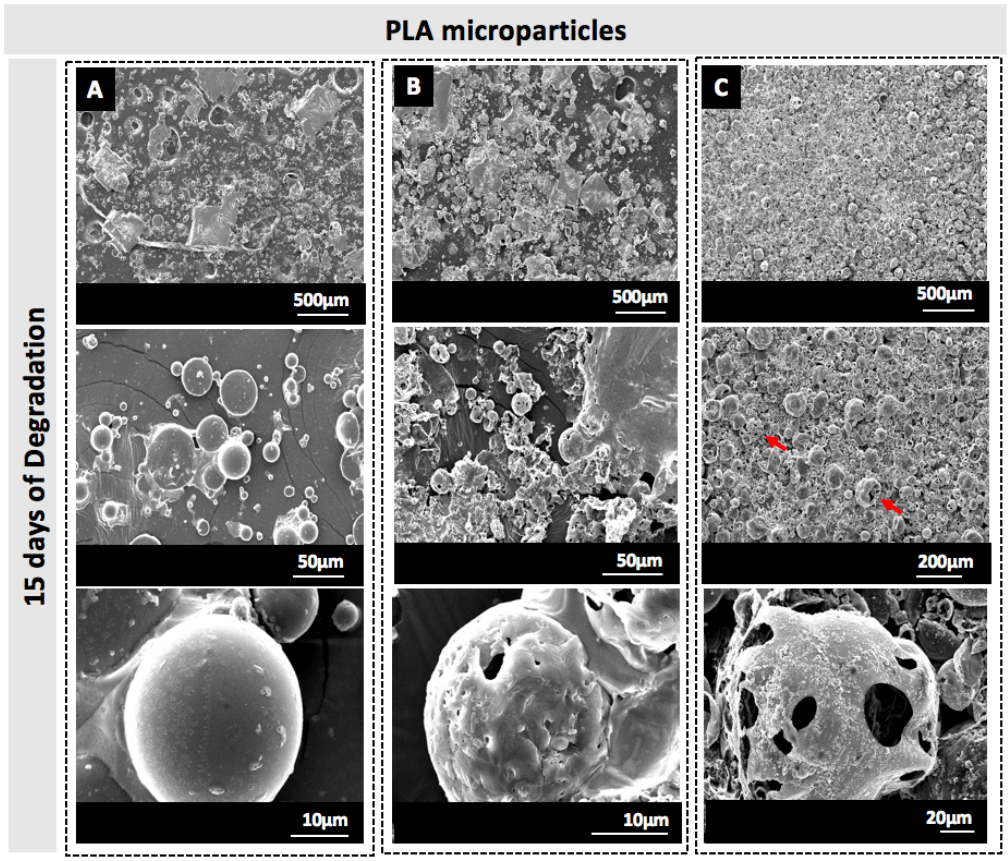


Figure 2.11: SEM analysis of the morphological changes of PLA particles as function of time exposed to buffered solution at 15 days (scale bars: 500 µm, 200 µm, 50 µm, 20 µm and 10 µm-insets).

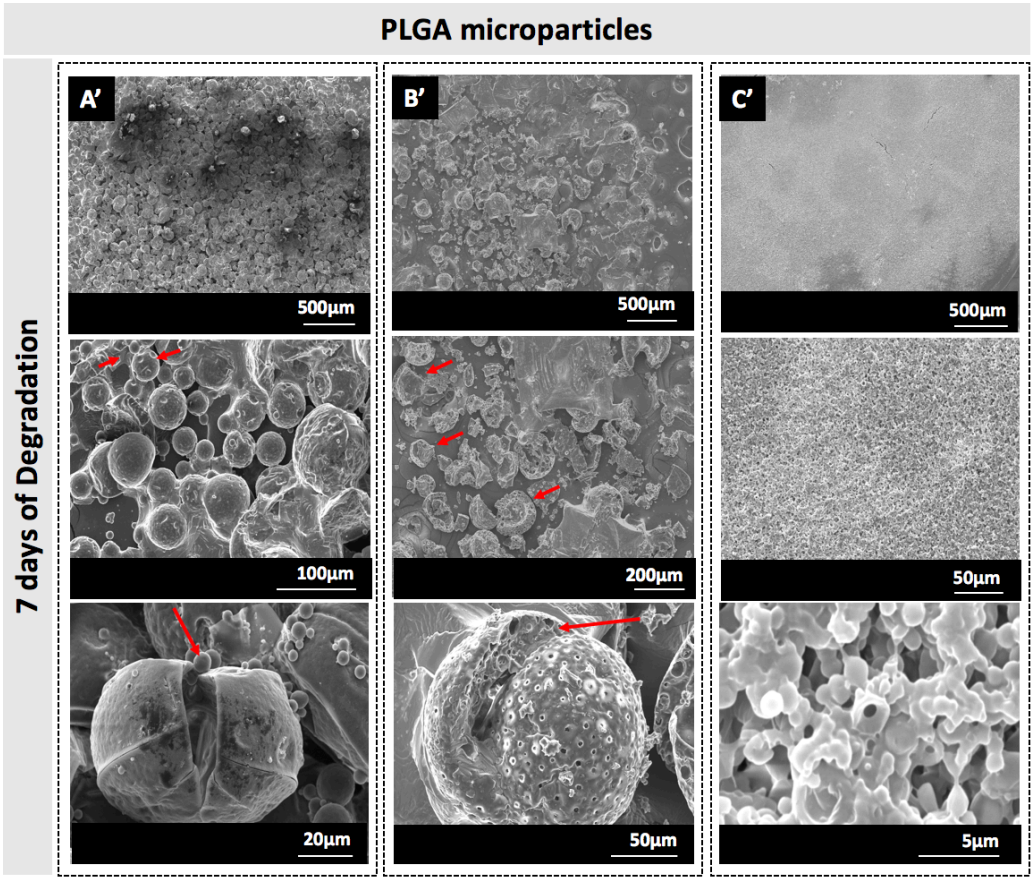


Figure 2.12: SEM analysis of the changes in morphologies of PLGA particles as function of time exposed to buffered solution at 7 days (scale bars: 500 µm, 200 µm, 100 µm, 50 µm, 20 µm and 5 µm-insets).

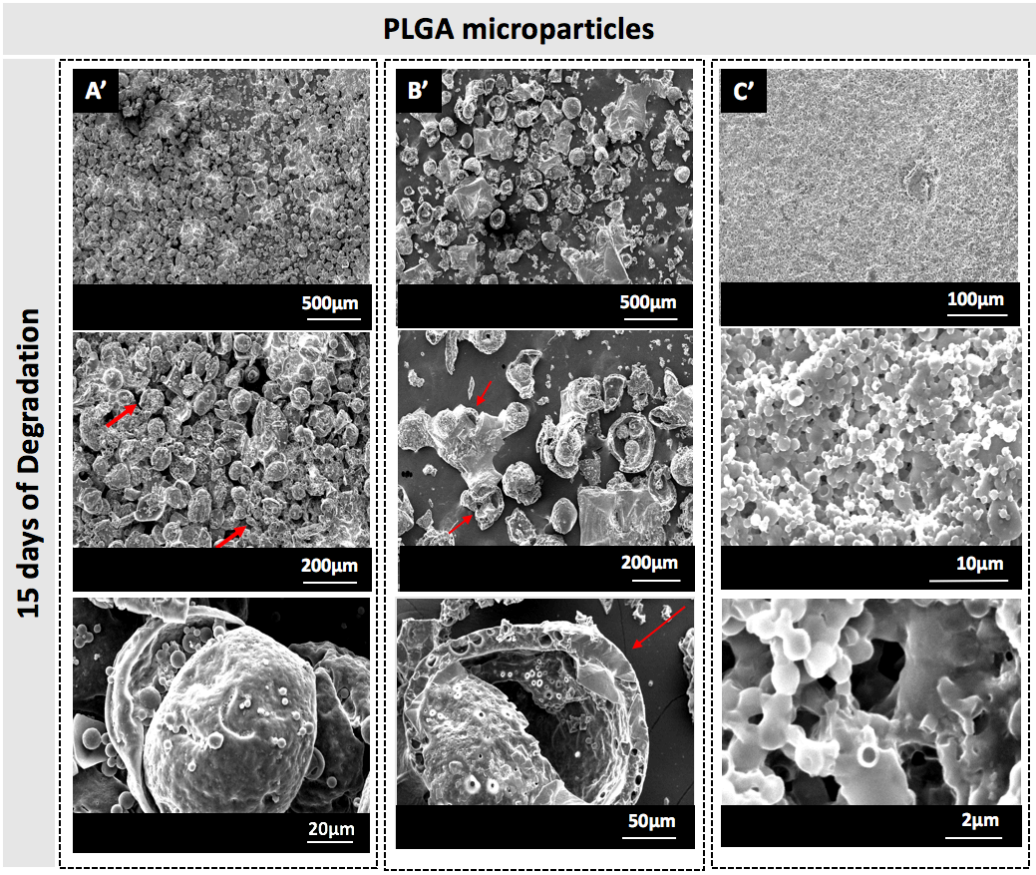


Figure 2.13: SEM analysis of the morphological changes of PLGA particles as function of time exposed to buffered solution at 15 days (scale bars: 500 µm, 200 µm, 100 µm, 50 µm, 20 µm, 10 µm and 2 µm-insets).

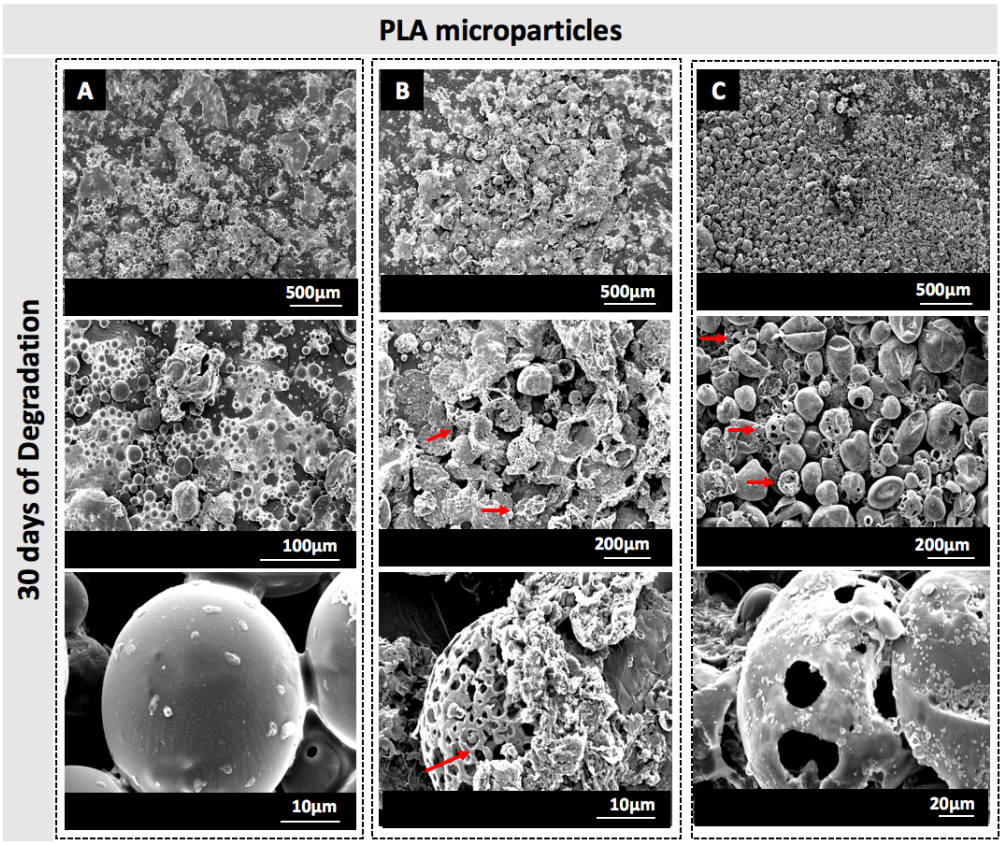


Figure 2.14: SEM analysis of the changes in morphologies of PLA particles as function of time exposed to buffered solution at 30 days (scale bars: 500 µm, 200 µm, 100 µm, 20 µm and 10 µm-insets).

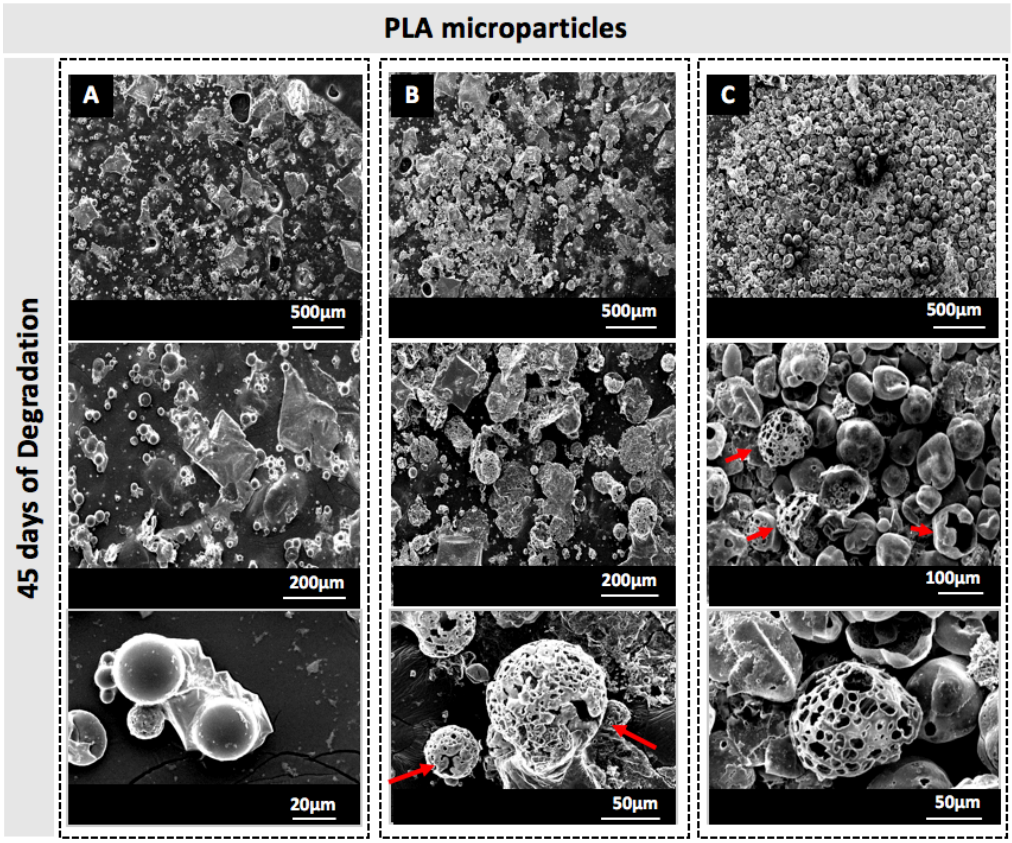


Figure 2.15: SEM analysis of the morphological changes of PLA particles as function of time exposed to buffered solution at 45 days (scale bars: 500 µm, 200 µm, 100 µm, 50 µm and 20 µm-insets).

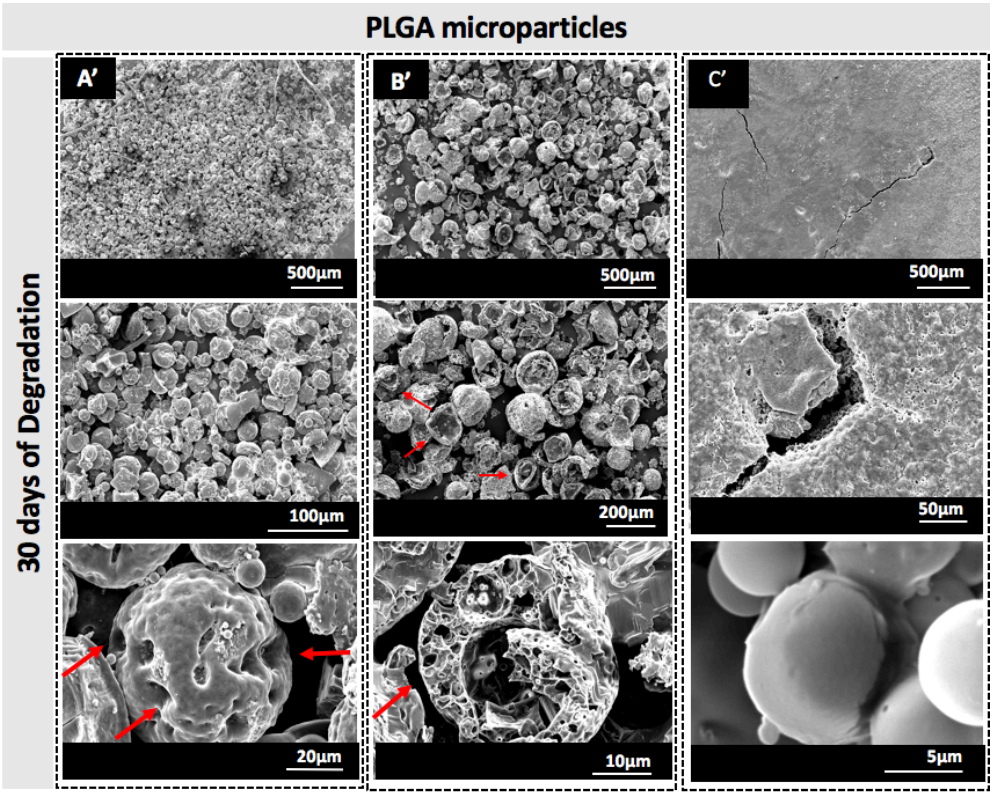


Figure 2.16: SEM analysis of the changes in morphologies of PLGA particles as function of time exposed to buffered solution at 30 days (scale bars: 500 µm, 200 µm, 100 µm, 50 µm, 20 µm, 10 µm and 5 µm -insets).

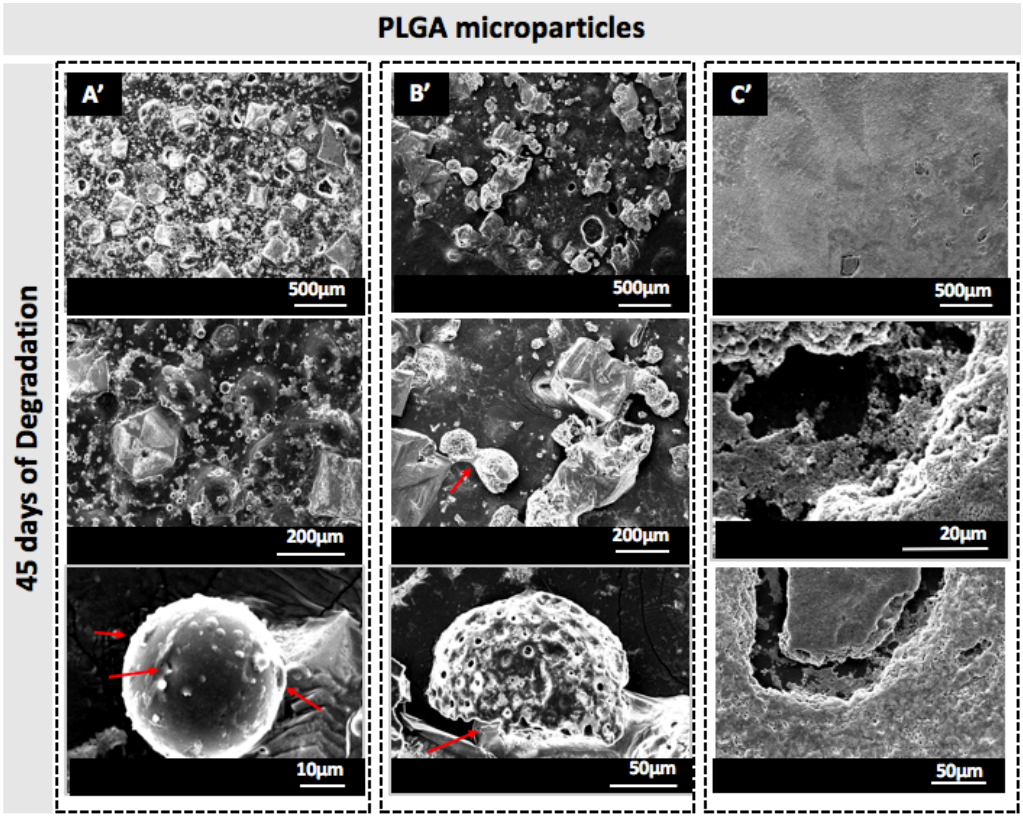


Figure 2.17: SEM analysis of the changes in morphologies of PLGA particles as function of time exposed to buffered solution at 45 days (scale bars: 500 µm, 200 µm, 100 µm, 50 µm, 20 µm and 10 µm -insets).

Table 2.3: Summary of the morphological changes of PLA (A, B and C) and PLGA (A', B' and C') microparticles, followed over a 45-day period, and determined using Image J analysis of electron microscopy images.

Particles Type	Time points	Particles size (µm)	Pores size (µm)
A	3h	52.22 ± 13.00	Non-porous
	24h	42.00 ± 12.00	Non-porous
	7 days	56.64 ± 15.32	Non-porous
	15 days	63.05 ± 12.37	Non-porous
	30 days	14.00 ± 6.00	Non-porous
	45 days	12.34 ± 3.20	Non-porous
B	3h	67.00 ± 18.14	4.41 ± 1.37
	24h	88.53 ± 21.50	7.76 ± 1.75
	7 days	81.21 ± 40.61	3.70 ± 1.46
	15 days	25.68 ± 10.01	3.34 ± 2.08
	30 days	62.32 ± 7.23	3.53 ± 1.15
	45 days	86.7 ± 19.00	3.86 ± 1.70
C	3h	5.15 ± 1.37	2.19 ± 0.72
	24h	19.24 ± 5.77	7.60 ± 3.00
	7 days	61.21 ± 16.24	7.09 ± 2.45
	15 days	39.92 ± 11.80	7.75 ± 3.34
	30 days	65.12 ± 3.44	8.42 ± 2.11
	45 days	77.56 ± 15.38	10.13 ± 3.30
A'	3h	52.22 ± 12.76	Non-porous
	24h	42.00 ± 11.51	Non-porous
	7 days	56.64 ± 15.32	Non-porous
	15 days	63.05 ± 12.37	Non-porous
	30 days	23.42 ± 14.53	Non-porous
	45 days	14.00 ± 6.00	Non-porous
B'	3h	117. 30 ± 31.71	4.60 ± 1.11
	24h	130.00 ± 31.20	3.00 ± 1.00
	7 days	136.28 ± 12.14	2.9 ± 0.77
	15 days	130.00 ± 21.62	4.05 ± 2.00
	30 days	128.34 ± 12.35	4.20 ± 1.23
	45 days	132.41 ± 24.51	5.6 ± 1.60
C'	3h	3.15 ± 1.00	1.80 ± 0.64
	24h	7.12 ± 2.44	1.88 ± 0.83
	7 days	1.50 ± 0.31	0.77 ± 0.34
	15 days	1.10 ± 0.27	0.41 ± 0.19
	30 days	1.03 ± 0.15	Not measurable
	45 days	Film formation	Not measurable

2.4 Discussion

2.4.1 Morphological characterisation and particle size analysis

The major focus of this chapter was to understand the differences in levels of porosity achieved from the polymeric microparticles through different formulations and emulsion techniques, and to determine how the level of porosity could affect particle degradation behaviour *in vitro*, in buffered solution over a 45-day period. Physical properties including particle morphology, porosity and size can affect particle application [261, 262, 302, 303]. Control over morphology and uniformity of size are amongst some of the major challenges in drug delivery systems, these properties depend on factors such as, i) type of formulation (*i.e.* single or double emulsion), ii) working distance between liquid injection and collector in the case of the electrospray technique [130], iii) types of polymers and their chemical properties such as molecular weight (Mw), iv) type of surfactants (*i.e.* level of hydrolysis, purity and Mw) [131, 269]; and v) energy input to the system during formation [99, 130].

As can be seen in Figure 2.1(A-E and A'-C'), the polymeric microparticles showed the same level of porosity between their external and internal regions and particle size varied up to 320 μm for

PLA microparticles, and between 20 and 80μm for PLGA microparticles, as determined by DLS. Furthermore, PLA and PLGA particles exhibited a size range between 14 to 101 μm as determined by analysis of SEM images (Figure 2.2). Non-porous and porous particles were produced *via* a single emulsion process where the organic phase interacted with an aqueous phase, as shown in Figure 2.18 (I). The various pore morphologies were achieved by addition of porogen in the organic phase and rapid evaporation of the porogen during the development of spherical particles [304]. These findings corroborate with the hypotheses described in this work in section 1.4 (Chapter 1). Furthermore, the development of particles with controllable shape and size requires continuous drop wise system whilst the shear force removes the organic solvent by evaporation, as shown in Figure 2.18 (II). The energy into the system during the particles formation (*i.e.* shear force) [305] was modified to achieve particles with different sizes (see Figure 2.18-III). The level of porosity achieved was also influenced by van der Waals and intermolecular forces [306]. Following the process described above, it was possible to achieve similar particle sizes as well as uniformity in porosity between the internal and external region of the particles due the type and amount of porogen added to the polymeric solution, as shown in Figure 2.1.

The level of porosity of the porous polymeric microparticles was confirmed by analysis of Cryo-SEM images, which evidence various

pores sizes up to 7.6 µm for the PLA microparticles and up to 5.8 µm for PLGA microparticles. Porous microspheres have several advantages over bulk (solid) particles, including a lower amount of polymer to be eliminated from the body [307], attachment of cells is possible, and importantly enable a further level of control to tailor the release profile of encapsulated therapeutic agents [308, 309].

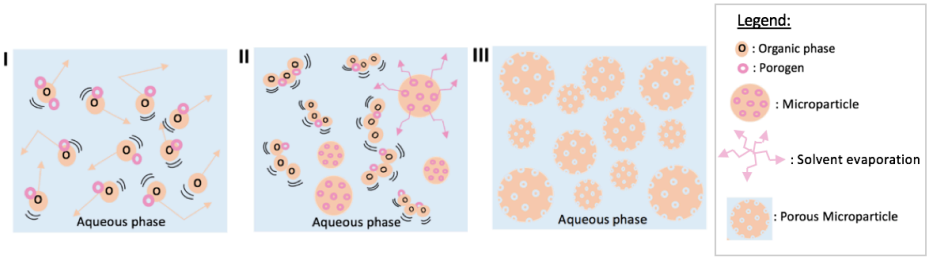


Figure 2.18: Schematic of the single emulsion process developed, showing organic phase into water phase (I) followed by the aggregation of molecules during the emulsification step (II) and formation of the porous particles (III).

2.4.2 Level of particle porosity and particle density

The spherical shape of the particles and their low density should impart better flowability of particles, for delivery to the respiratory system (*e.g.* inhalers) and avoid particle agglomeration. This property is also related to the small van der Waals force between the organic and water phase in order to produce particles with controllable shape [310]. As seen in Figure 2.4, PLA particle types B, C and D exhibit a density range between 0.18 and 0.35 g/cm^3, whereas particles A and E exhibit a density range between 0.28 and 0.18 g/cm^3. The non-porous and porous PLGA particles have a density range between 0.40 and 0.27 g/cm^3, with particle type C' exhibiting lower density than particles A'

and B', as shown in Figure 2.4. These results demonstrate that particles with high levels of porosity have reduced density values in comparison with bulk (non-porous) particles. According to the literature, particles with closed pores (shown in Figure 2.1) can exhibit thicker pore wall structures, influencing microparticle density [311]. Polymeric microparticles with uniform shape and pore sizes are a particular feature achieved with this work, as shown in Figure 2.1(B-E and B'-C').

Pore size and particle density are important for biomedical applications, such as aerosol formulations. Furthermore, the pore size influences the amount of liquid and gas adsorbed to the microparticles. The level of porosity of the microparticles is related to the gas adsorption to the microparticles and the resistance force between adsorbent and adsorbate, which includes the amount of gas adsorbed during gas expansion into the system, and influenced by phenomena such as: i) type of material; ii) particle geometry; iii) the geometry and interconnectivity of the pore network (permeability, δ); iv) monolayer or multilayer formation; v) adsorption interaction (*i.e.* repulsive forces); vi) strength of gas-wall and gas-gas interactions; vii) the state and thermodynamic stability of gas confined to narrow pores related to gas flow interaction [1, 2, 301, 303, 312].

As seen from Figure 2.3 the differences in microparticle pore diameters correlate well with Figure 2.1 (B-E and B'-C'),

corroborating that the porosity observed between the surface and internal regions of the microspheres produced were near identical. The gas adsorption to the microparticles cited above influenced the BET surface area analysis of the particles and resulted in the family of PLA microparticles with different surface areas: 6.7, 5.2, 5.8, 4.9 and 1.7 m^2/g (summarised in Figure 2.4), and a family of PLGA microparticles with surface areas 0.67, 2.26 and 1.57 m^2/g (Figure 2.4 A'-C'). Control over particle morphology, porosity and surface area of those particles was achieved by controlling the type of formulation and chemical components, as previously described in section 2.2.1.

Varying the type of formulation and type of polymer enabled alteration of the physical properties of the resultant particles, in terms of their morphology, particle size, pore sizes and structure. The different levels of porosity of the polymeric microparticles produced can alter particle density, trajectory of gas diffusion (*i.e.* multilayer diffusion through particle walls and/or diffusion through the pores) [313] and gas resistance filling the pores [314]. Furthermore, particle porosity was conducted by gas adsorption analysis *vs.* relative pressure and measured the level of porosity of PLA and PLGA microparticles by filling the pores up to the maximum pressure.

The difference in the levels of porosity of particles (2.1A-E) was evidenced by their different isothermal behaviour, as shown in a Figure 2.5(PLA MPs Porosity Measurement). Microparticles A and A' did not

possess porous structures, as confirmed by reduced gas adsorption (Figure 2.5). These results suggest that the non-porous PLA particles (2.5A) had been compressed during the gas adsorption cycle due the monolayer gas adsorption; PLGA particles (Figure 2.5A') also showed a reduced gas adsorption when compared to porous PLGA particles. Moreover, results for non-porous particles suggest that gas adsorption, was restricted to monolayer adsorption, likely due to the absence of pores [311] as shown in Figure 2.19 (A) represented by red arrows. Porous PLA and PLGA particles (B, C, D and B') exhibited similar isotherm profiles, which indicate that gas adsorption was higher than particles E and C', as shown in Figure 2.5. This result suggests that particles with interconnected pores have multilayer adsorption, in which the external layer has been covered with the gas in the first instance, and subsequently gas adsorption occurs in particles, as shown in Figure 2.19 (D), corroborating with mathematical theory developed by Brunauer, Emmet and Teller (BET). Whereas, particles E and C' present higher gas resistance and an ascendant isothermal curve, indicating that monolayer adsorption completes and then multilayer adsorption progresses as a result of hierarchical pores structure, as shown in Figure 2.19(E) [1, 295, 315-317], corroborating with the hypotheses established in this study where particles with superior level of porosity would exhibit a higher gas adsorption when compared with the non-porous particles.

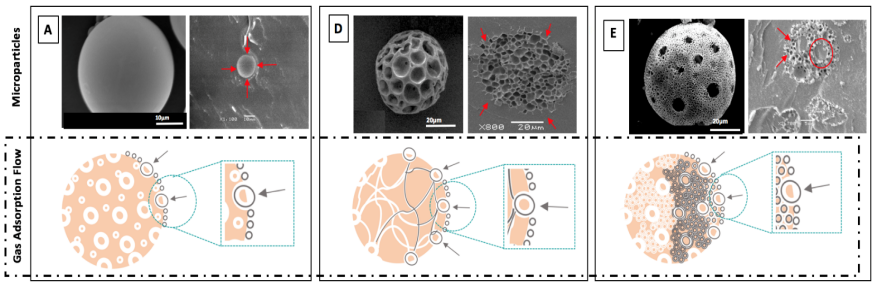


Figure 2.19: Polymeric microparticles exhibiting different levels of porosity, and depicted interactions between the pores and gas flow (grey arrows and circles) between the external and internal regions. (A) Disconnected and/or non-porous structure with monolayer adsorption), (D) connected pores allowing gas flow with the internal region of microparticles and (E) particles with two sizes connected pores [1, 2].The gas starts to fill the particles surface as indicated by the red arrow while the gas inner particle interior is indicated by the grey arrows (particles D and E).

2.4.3 Study of the morphological changes to the polymeric microparticles during *in vitro* assessment in buffered solution over a 45-day period

PLA microparticles exhibited similar behaviour between 3 and 24 h of *in vitro* study and PLGA microparticles (A' and B') exhibiting initial morphological fragility over 3 h of study as shown in Figure 2.6 and Figure 2.8. These results suggest that changes in particle degradation behaviour can be correlated with the polymer type (PLA or PLGA), attributed to hydrolytic attack, and acidic oligomeric degradation products causing accelarated degradation [318-320].

Particle hydrolysis increased substantially over the time points 30 and 45 days of study, which showed a larger pore formation for particles B and C, in comparison with PLA particles at the 3 h early time point. These data corroborate well with the literature where the presence of pores in the particle morphology improves autocatalytic processes due

the presence of liquid between the external and internal areas of the polymeric particles [321]. As the polymers degrade, their molecular weight decreases, the particles become increasingly porous due the physical erosion of the polymeric matrix, which also increase the fragility of polymeric particles [321].

Non-porous PLGA microparticles (A') exhibited pores formation after 30 days of degradation, mainly caused by polymeric erosion, whilst medium porous PLGA particles (B') and highly porous PLGA particles (C') exhibited significant changes in their porous structure, higher particle fragility and high levels of degradation in comparinson with particles assessed over 3 h and 24 h of study due the fast diffusion of media through the porous strucuture, as shown in Figure 2.16. Furthermore, particle types A, A' and C' exhibited reductions in their particle sizes over the 45-day degradation study, corroborating with the literature where particles with higher surface area exhibit rapid degradation rate, as shown in Table 2.3. Particle types B and B' (medium porosity) exhibited increasing pore sizes over the 45-day period, corroborating with the literature where the hydrolytic degradation occurs homogeneously depending on the thickness of the particle's surface and initially occurs faster on surface than at the particle core [322]. Bulk erosion occurs when the hydrolytic degradation rate of the surface of particles is not so high in comparison to the diffusion rate of water/buffered solution. Furthermore, the rate of particle degradation is influenced by a set of factors including, the

chemical composition of the polymers, pH, water uptake and the nature of the chemical bonds of the polymers. Although, all these factors can have a substantial effect on the degradation rate of the polymeric particles, the initial polymer molecular weight governs degradation time [323].

PLA and PLGA particles degrade by simple hydrolysis of the ester linkages a process, which can be both acid and base catalysed [226]. Polymer composition can influence particles degradation as well as particle size; the degradation products formed within smaller particles can diffuse more easily to the surface, compared to larger particles, where the degradation products have a longer path to the surface, and can result in autocatylic degradation [219, 321].

2.5 Conclusions

A range of PLA and PLGA microparticles with controlled size and various porosities have been produced and their structure characterised. The degradation behaviour and change in particle morphology, size and pore structure was followed by *in vitro* study in buffered solution over a 45-day period. The morphology of particles was followed using SEM and images analysis, particle size was also assessed using DLS. Non-porous (A, A') and porous (B-E, B'-C') spherical particles with similar levels of porosity between their internal and surface region have been produced. The particles could be made in

controlled sizes, in the range 24 to 320 μm. The non-porous spherical PLA particles (A) developed, have higher density than their hierarchically porous conterpart PLA microparticles; PLGA non porous particles (A') also exhibited a higher densities than their porous counterpart particles (B'-C'), also confirmed by surface area analysis. The level of porosity in the particles can alter gas adsorption behaviour. Non-porous PLA particles (A) exhibited negative gas adsorption whilst porous particles (B-E) exhibited positive gas adsorption profiles. Furthermore, the non porous PLGA particles (A') showed a reduced gas adsorption in comparinson with their porous counterpart PLGA particles (B'-C'). This result suggests that the non-porous particles (A and A') had been compressed during the gas adsorption cycle due the absence of pores in the particle's surface; whereas, porous particles (B-E and B'-C') exhibited a higher rate of gas adsorption indicative of less resistance to gas adsorption. The degradation study undertaken for the produced particles evidenced the initial fragility of particles over a 24 h period, formation of pores in non-porous particles, as well as pore size increase over time. This result suggests that particle degradation depends on the presence of pores in particle's surface as well as pores size, surface area of polymeric microparticles and the level of polymeric hydrolysis.

The physical properties of non-porous and porous polymeric microparticles has been determined in this study and these particles could be utilised for several applications downstream, including local drug delivery and tissue engineering. Their application as a dual-

therapy system for brain cancer treatment is further investigated in Chapter 3.

CHAPTER 3. Development of a dual-therapy system for brain cancer treatment

3.1 Introduction

Biomaterials are a key component of local delivery systems for central nervous system (CNS) tumours. One of the main advantages of biomaterials for biomedical applications is their biocompatibility with the body, other advantages include: i) low toxicity, ii) low immune response, iii) modulation of the materials according to the application, iv) encapsulation of drugs with different hydrophobicities and capability for sustained release, v) safe localised drug delivery to the brain, and vi) reduced side effects [324-327]. Furthermore, some biomaterials in the form of polymeric microparticles have proven ability to prolong the half-life of drugs to achieve a sustained drug release, increase the stability of the drugs in the blood and plasma, overcome poor drug solubility, improve the transport of drugs through the blood-brain-barrier (BBB) and brain-tumour-barrier (BTB), and improve patient compliance and outcome [324, 328, 329].

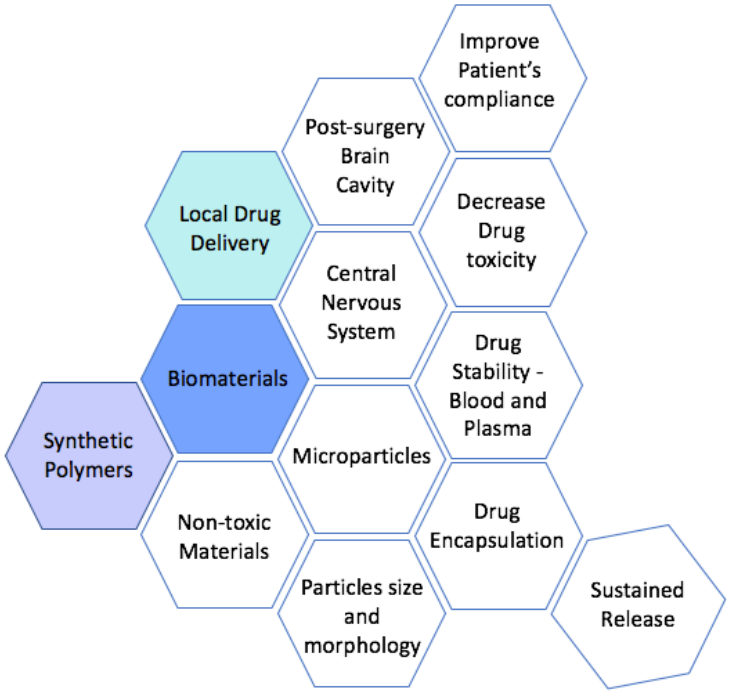


Figure 3.1: Diagram depicting the issues surrounding the use of synthetic polymers as biomaterials and features desirable to achieve an ideal local delivery system for brain cancer treatment.

The factors highlighted above correlate to the development of standard treatments for drug delivery to the CNS, as shown in Figure 3.1. PLGA is used worldwide in the development of biomaterials for local drug delivery in the form of nano- and micro- carriers. PLGA and PLA have been approved by the FDA and applied in therapeutic devices due to their physical properties, biocompatibility and degradability. PLGA is an aliphatic polyester, its crystallinity can be tuned from fully amorphous to fully crystalline depending on block structure and LA:GA ratio. However, PLGA with high GA content can exhibit rapid degradation rate at body temperature [335]. PLA has D and L stereoisomers forms and can be semi-crystalline or amorphous depending on composition. Semi-crystalline PLA has reportedly presented a degree of crystallinity of around 37% and can exhibit a

slow degradation rate under physiological conditions [330]. These poly(α-hyroxyesters) have been applied to several delivery systems, including those towards treatment of solid tumours [273, 322, 324]. According to Jun *et al* poly(ethylene glycol)-poly(lactide) (PEG-PLA) loaded with paclitaxel (PTX) has been used as a carrier for brain tumour therapy [328]. Poly (ethylene glycol)-block-poly(D, L-lactide) (mPEG-PDLLA) can be loaded with PTX, available as Genexol®-PM [328]. Genexol®-PM has undergone clinical trials and is an approved, commercially available for the treatment of non-small cell lung cancer, as well as breast cancer [328, 331-333].

Myriad devices and delivery systems produced have been developed to treat different tumour types. Gliadel® wafers are one such example; this was developed to prolong the survival of patients with glioblastoma (GBM). This system is used post-surgical resection, *via* intra brain cavity administration. The device is a mixture of degradable polymeric microparticles (*i.e.* polyanhydride microparticles) loaded with carmustine (BCNU), a drug approved by the FDA and UK Medicines and Healthcare products Regulatory Agency (MHRA) for GBM therapy. The polyanhydride polymers used are characterised by a crystalline structure, with a melting point between 50 and 90^{o}C, they are hydrophobic and exhibit slow degradation rate at body temperature [330]. This therapeutic system was developed to decrease the residual tumour cell burden in the brain adjacent to the resection cavity margins and exhibits sustained drug release, allowing the drug to bypass the BBB [324, 328, 334-336]. The Rahman laboratory (Queens Medical

Centre, University of Nottingham) also recently developed a paste system using thermo-responsive degradable polymers loaded with multiple therapeutics, which included Temozolomide (TMZ) and Etoposide (ETP) [342]. This paste has been applied by neurosurgical delivery (to the brain cavity) in order to achieve high local dose, low systemic concentrations and sustained delivery of the cytotoxic drugs directly to the CNS using an orthotopic high-grade glioma animal model [342]. Their study showed that this localised dual drug delivery system can achieve a significant extension of survival *in vivo*; this technology can offer a possible treatment of residual malignant glioma cells [337].

Drug-loaded biomaterial devices and formulations can be effective for the delivery of therapeutic agents (*i.e.* localised therapy), reduce toxicity caused by chemotherapeutic drugs, and improve short circulation time and fast clearance issues [324, 338]. Usually, chemotherapeutic drugs are delivered systemically in high dosages in order to maintain the therapeutic dosage through the BBB; however, they can cause several side effects (*e.g.* bone marrow suppression) in patients due to the metabolisation and clearance of these toxic drugs. Moreover, localised drug delivery has shown significant effectiveness due to high drug concentration of drugs in close proximity to the primary tumour site. Systemic deliveries can be ineffective for brain tumours such as GBM, because the concentration of chemotherapeutic drug drops with increasing distance from the tumour site [326, 339, 340]. Targeted drug delivery to specific areas of the CNS is a recurrent

challenge for the development of effective disease treatments such as spinal cord tumours, spinal cord injury and GBM as a result of the high proliferative rate and infiltrative nature of cancer cells that are often in inaccessible areas of the CNS, and the difficulties associated with distinguishing normal and cancer cells [324, 341].

Therapeutic agents such as chemical drugs, proteins and gene and immunotherapy vaccines for solid tumours (*e.g.* GBM) have shown great potential to target tumours systemically and locally [328, 342-344]. Some chemotherapeutic drugs used for brain cancer therapy have been approved for oral administration for treatment of newly diagnosed or recurrent malignant gliomas [333].

Some drugs have been encapsulated for systemic and local delivery, such as i) TMZ, which is a derivative of the alkylating agent dacarbazine [328], ii) Docetaxel (DTX), used in the treatment of many types of cancer [345]; however it cannot be restricted for brain cancer use, as an efflux membrane transporter of P-glycoprotein limits the cellular retention and distribution of this toxic substance, iii) ETP used for inhibition of topoisomerase II-deoxyribonucleic acid (DNA) [347], which prevents nucleoside transfer, synthesis of DNA and induces retardation of cell cycle progression, and iv) Methotrexate sodium salt (S.MTX), which is an antineoplastic antimetabolite with immunosuppressant properties and affects the inhibition of tetrahydrofolate dehydrogenase, preventing the formation of tetrahydrofolate, crucial for the formation of DNA [328, 345-348].

Most of the anticancer agents cited above are used widely used in the treatment of rheumatoid arthritis, psoriasis, as therapies for leukemia, lymphoma, and solid tumours such as breast cancer, lung cancer and glioblastoma. Some of these drugs are more effective against cancers outside the brain due to the retention of drugs in the BBB and BTB, which regulates the transportation of large and small molecules to the brain. Furthermore, other factors can decrease the effectiveness of glioma therapy such as the acidic pH of the tumour microenvironment, tumour volume and intratumoral distribution of cancer cells due to the high proliferation rate of these cells [339, 349-353].

Recent drug delivery systems developed for GBM treatment require scrutiny as they can potentially damage healthy neural cells, cannot control the infiltrative nature of GBM cells, they can exhibit high toxicity when administrated systematically, exhibit several side effects and can have poor therapeutic response, notwithstanding the short survival of patients after the initial diagnosis.

More effective strategies are urgently needed for GBM treatment with the aim of increasing patient survival. In this thesis, a family of PLA and PLGA spherical MPs of controlled size, and porous morphologies have been produced (shown in chapter 2. Spherical microparticles were selected according to their typifying morphologies, with three different levels of porosity targeted for PLA and PLGA MPs, and loaded with dye and chemotherapeutic drugs as demonstrated here, further below, in section 3.2.1.2. The MPs developed in this thesis serve as a proof-of-concept study for the development of local multi-therapy

formulations explored here. The hypotheses tested in developing this multi-therapy system are described below:

i) Quantification of chemotherapeutic drugs

Spherical MPs made with PLA and PLGA loaded with chemotherapeutic drugs can show potentially a difference on drug loading due the polymers nature (*i.e.* hydrophobicity) as well as their distinct morphology.

ii) Release profile of non-porous and porous spherical particles

Particles with high levels of porosity can exhibit a higher percentage of release than their non-porous counterparts due to the fast diffusion of media inside the porous structure and rapid degradation of porous particles.

ii) Development of multi-therapy systems

The combination of PLGA-PEG matrix mixed with DTX and spherical particles loaded with multiple-drugs would offer a controlled sustained localised intra-cavity delivery as a result of:

a) the melting point of the PLGA-PEG matrix at 37^{o}C

b) burst release from the PLGA-PEG matrix

c) slow release from the encapsulated PLGA and PLA spherical particles

d) controlled drug release from spherical particles with different morphologies

e) paste and tablets formulations would offer a localised intra-cavity multi-therapy delivery system and the drug would remain in the brain cavity

f) the system used for both formulations can obviate the dislodgment of both paste and tablets in the first post-surgical hours

The multi therapy system consisted of a PLGA/PEG matrix mixed with 50 µg/mL of DTX and spherical PLA and PLGA MPs encapsulated with DTX, S.MTX and ETP (50 µg/mL) for paste and tablets formulation at ratio of 1:10 and 200:1, respectively. Drug concentration was established subsequently encapsulation study of NB developed in this thesis. Both formulations were developed in order to overcome some issues related to the current GBM treatment such as: i) the high local dosage of the chemotherapeutic drugs which can cause toxicity to healthy neural cells and tissue, ii) expand the contact between the proposed formulation loaded with toxic drugs and the cancerous cells, iii) the poor response to standard-of-care GBM treatment from systemic administration, as shown in Figure 3.2.

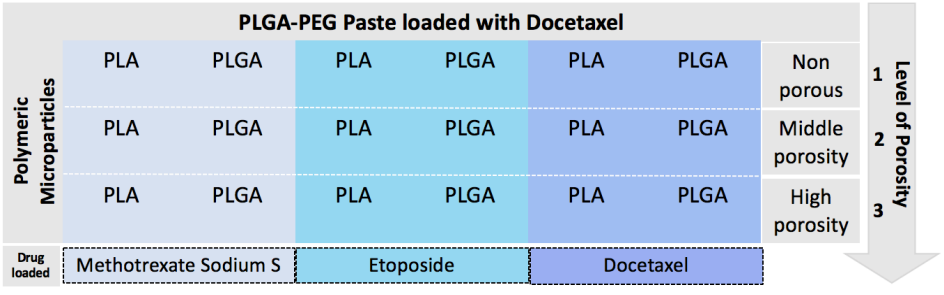


Figure 3.2: Summary of the local drug delivery systems investigated in this work as an initial screening study for localised therapy to overcome the poor prognosis of current GBM therapies.

3.2 Materials and Methods

3.2.1 Materials

The PLA, PLGA, PVA and organic solvents used here have been described in section 2.2.1. Poly (ethylene glycol) 400 (PEG_{400}) was purchased from Sigma-Aldrich, UK. Methotrexate sodium salt (BioChemPartner), Docetaxel trihydrate European Pharmacopeia (EP) reference standard (Sigma Aldrich) and Etoposide synthetic $\geq$ 98% were purchased from Sigma Aldrich and used as received. Dulbecco's modified Eagle's medium (DMEM), foetal bovine serum (FBS), Hank's balanced salt solution (HBSS), penicillin-streptomycin were purchased from Sigma Aldrich, UK. CellTiter 96® AQ_{ueous} Non-Radioactive Cell Proliferation Assay (MTS reagent) was purchased from Promega, UK.

3.2.2 Particle Size Distribution

Dynamic Light Scattering (DLS)

Particles in suspension were loaded in a small cell (10 mL) with ultrapure water. The particle suspensions were auto diluted by addition of ultrapure water to the cell until the suspension reached a concentration between 8 and 12% and the data recorded as described in section 2.2.5.

3.2.3 Dye loading of the microparticles

Microparticles were produced by single emulsion technique. 1000µg/mL of Nile Blue was diluted in 50:50 DCM:DMSO (v/v) and

the solution was kept as a stock solution. Nile Blue was diluted in the organic phase (polymer and DCM) until reaching a concentration of 50 µg/mL. The organic phase was added drop wise with a syringe driver (World Precision Instrument) into 0.5% (w/v) of PVA solution (25 mL) under constant stirring (IKA RCT basic) over 24 h (speed 500 rpm). The suspension of particles was washed three times with DI and centrifuged, as previously described in section 2.2.2. After the washing process, the particles were dried under vacuum at room temperature for 24 h.

3.2.3.1 Quantification of particles loaded with dye

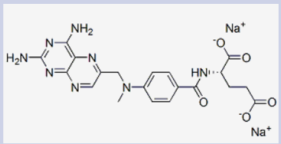
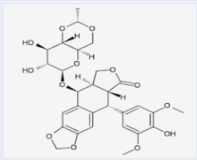
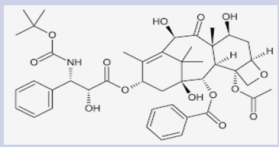
The loading of dyes within the microparticles was assessed by dissolving 1 mg of MPs in 50:50 DCM:DMSO (v/v) and an aliquot of 100µL MPs solution was kept and analysed by UV-vis spectroscopy. The UV detector was set at 615 nm (excitation) and 665 nm (emission). A calibration curve for Nile Blue in mixture of 50:50 DCM:DMSO (v/v) was constructed in the concentration range 0.5 – 100 µg/mL where the R^2 was 0.9888.

3.2.4 Drug encapsulation into microparticles

The microparticles were produced as before by a single emulsion technique. Stock solutions of methotrexate sodium salt (S. MTX), etoposide (ETP) and docetaxel (DTX) were diluted in DCM separately and the solution kept at concentration of 1000 µg/mL. The

chemotherapeutic drugs were weighed out by difference and the experimental work performed inside a fumehood. The S.MTX, ETP and DTX were diluted in the organic phase (polymer and DCM) to reach the final concentration at 50 µg/mL. The organic phase was added drop wise using a syringe driver (World Precision Instrument) into 0.5% (w/v) of PVA solution (25 mL) under constant stirring (using an IKA RCT basic) during 4 h (speed 500 rpm). Particles were washed centrifuged and dried as described in section 2.2.2. The solvent waste produced during the preparation of microparticles encapsulated with the toxic drugs was disposed in the toxic waste container. The required personal protective equipments were worn during laboratory work according to COSHH and risk assessments conducted. A summary of chemotherapeutic drugs used in this work is given in table 3.1.

Table 3.1: Schematic representation of chemotherapeutic drugs used in this study and their log P.

Chemotherapeutic drug	Chemical structure	Log P
Methotrexate sodium salt		0.74
Etoposide		1.16
Docetaxel		2.4

3.2.4.1 Quantification and encapsulation efficiency of drug loaded particles

High performance liquid chromatography (HPLC) (Schimadzu) was used to detect and quantify the drug loaded into the polymeric microparticles. First, 1 mg of dried particles was dissolved in H_2O:MeCN 50:50 (water:acetonitrile) for samples loaded with docetaxel. Methanol was used as an organic solvent to solubilise the samples loaded with sodium methotrexate and etoposide. After solubilisation, the samples were passed through a 0.45 µm filter. HPLC was performed using a C18 column (50 x 2 mm, 110 Å). The mobile phase was a 40:60 (v/v) mixture of H_2O:MeCN (v/v) for samples loaded with sodium methotrexate and docetaxel, and $C_2H_7NO_2$:MeCN (v/v) at pH 4.7 for samples loaded with etoposide. Calibration curves for sodium methotrexate, docetaxel and etoposide were constructed in the concentration ranges between 5 and 100 µg/mL where the R^2 was determined as 0.98108, 0.95338 and 0.97614, respectively. Equation 4 was used to define the drug concentration, where a and b were extracted from the calibration curve equation (y = ax +b):

$$\textbf{Drug Concentration: } \frac{\text{(Peak Area - b)}}{a} \qquad \text{Equation 4}$$

Following the determination of drug loading capacity, as shown in Equation 5, the drug content in the drug-loaded MPs and the encapsulation efficiency was calculated by Equation 5:

Drug Loading (%): (*mass of determined drug*) x 100

(*mass of polymer + drug*)

Equation 5

Following the determination of drug content in the dried drug-loaded MPs the encapsulation efficiency was calculated by Equation 6**:**

Encapsulation Efficiency **(%):** (*mass of determined drug*) x 100

(*mass of drug used in MP preparation*)

Equation 6

3.2.5 Polymer blend preparation

PLGA/PEG microparticles were prepared by mixing PLGA and PEG at a weight ratio of 95:5, respectively, with constant heat at 90^{o}C until both polymers were completely molten. The polymers were left to cool down and solidify at room temperature for 30 minutes, the solid polymer was then processed using a blender, and the particles were sieved to achieve a size range between 100-200 µm, as described in [291].

A stock solution of DTX at 1000 µg/mL was solubilised in milliQ water until reaching a concentration at 50 µg/mL. 100 µL of DTX solution at 50 µg/mL was withdrawn and mixed with PLGA/PEG

microparticles to form the paste formulation. Spherical polymeric PLGA and PLA microparticles were loaded separately with S.MTX, ETP and DTX at concentration of 50 μg/mL as described in section 3.2.4.

3.2.6 Paste formulation preparation

3.2.6.1 Paste formulation without drug

PLGA/PEG microparticles were weighed out (12.5 mg), solubilised in 100 μL of MilliQ water and the stock solution kept at 10 °C (solution A). The spherical polymeric microparticles were weighed out (0.005 g), solubilised in 200 μL of MilliQ water and the stock solution kept at 10 °C (solution B). Solution A was mixed with solution B (40 μL of A and 10 μL of B), and 150 μL of MilliQ water added to the final formulation. The paste formulation was then dried out for 30 min in an incubator at 37°C.

3.2.6.2 Paste formulation loaded with toxic drugs

Docetaxel (DTX) was weighed out by difference, solubilised in MilliQ water and kept as stock solution at concentration of 1000 μg/mL (DTX solution). PLGA/PEG microparticles were weighed out (0.0125 g), solubilised in 100 μL of MilliQ water and the stock solution kept at 10 °C (solution A). The spherical polymeric microparticles loaded with the chemotherapeutic drugs were weigh out (0.005 g), solubilised in 200 μL of MilliQ water and the stock solution kept at 10 °C (solution

B). Solution A was taken in 40 µL and mixed with 10 µL of DTX solution (DTX-A solution). Then, 10 µL of solution B was added and milliQ water (140 µL) was added to the formulation to reach a final concentration of DTX at 50 µg/mL. The paste formulation was dried out as described in section 3.2.6.1.

3.2.7 Tablet formulations preparation

3.2.7.1 Tablet formulation without drug

PLGA/PEG microparticles were weighed out (0.05 g) (Solid mixtrure A). The spherical polymeric microparticles were weighed out (0.005 g), solubilised in 200 µL of MilliQ water and the stock solution kept at 10 °C (Solution A). The solid mixture A was mixed with 10 µL of solution B and 190 µL of MilliQ water was added to the final formulation. The polymeric formulation was placed in a PTFE mould (12 mm deep x 6 mm diameter) and left to dried out for 2h in an incubator at 37 °C.

3.2.7.2 Tablet formulation loaded with toxic drug

DTX was weighed out by difference, solubilised in MilliQ water and kept as stock solution at concentration of 1000 µg/mL (DTX solution). PLGA/PEG microparticles were weighed out (0.05 g) (Solid mixtrure A). The spherical polymeric microparticles were weighed out (0.005 g), solubilised in 200 µL of MilliQ water and the stock solution was

kept at 10 °C (Solution A). The solid mixture A was mixed with 10 µL of solution B and 10 µL of DTX solution. Then, 190 µL of MilliQ water was added to the final formulation to reach the concentration of DTX solution at 50 µg/mL. The polymeric formulation was dried out as described in section 3.2.7.1.

3.2.8 Release study of loaded Nile Blue and chemotherapeutic drug

3.2.8.1 Release study with loaded polymeric microparticles

An *in vitro* release study of MPs loaded with Nile Blue (NB) was conducted using the dialysis method. After encapsulation of dye or drug and removal of solvents, microparticles (1mg) were dispersed in Dulbecco's phosphate buffered solution containing 1% Tween 80. The suspension was placed in a dialysis device (3500 kDa molecular weight cut-off) and immersed in 3 mL of buffer (pH 7.4). The dialysed samples (1mL) were removed from the device at predetermined time intervals and an equal amount of fresh media (buffer) was replaced. The amount of dye released was determined by UV-vis spectroscopy as described in section 3.2.3.1. The amounts of S.MTX, ETP and DTX were measured as described in section 3.2.4.2. All this work was performed in triplicates.

3.2.8.2 Release study with loaded paste and tablets formulation

An *in vitro* release study of paste and tablets loaded with Nile Blue and chemotherapeutic drugs was conducted using the dialysis method.

Each formulation was placed in a dialysis device, as described in section 3.2.8.1. The amount of dye released was determined by UV-vis, as described in section 3.2.3.1. The amounts of S.MTX, ETP and DTX were measured as described in section 3.2.4.2. All this work was performed in triplicates.

3.2.8.3 Release solution from loaded paste and tablets formulation for in vitro study using U87 cells

Each formulation was placed in 1 mL of DMEM solution supplemented with 10% of FBS. Samples were withdrawn at different time points over 30 days and cells studies performed, as described in section 3.2.9.1. All this work was performed in triplicates.

3.2.9 Cell culture

In vitro assays were performed using a human brain cancer cell line (U87) obtained from American Type Culture Collection (ATCC). Cells were maintained in DMEM supplemented with 10% FBS and 1% penicillin streptomycin at 37^{o}C with a 5% of CO_2 humidified atmosphere.

3.2.9.1 Cell viability

The cytotoxicity of the polymeric microparticles (MPs), free drug and polymeric formulations, as paste and tablets, were evaluated with U87 cells and an MTS assay. Cells were seeded at 5x10^{3} cells per well in 96-well plates and incubated overnight. Initially, polymeric microparticles without loading were tested varying their concentration

between 5 and 750 µg/mL. Free drug (*i.e.* S.MTX, DTX and ETP) was tested at 50 µg/mL during 2, 5 and 24 h period. The polymeric formulations (*i.e.* paste and tablet) loaded with chemotherapeutic drugs were left for over 30 days in 1mL of DMEM solution, as described in section 3.2.8.3 and tested subsequently with U87 cells (150µL). Cells were incubated for 24 h at 37°C with a 5% of CO_2 humidified atmosphere. The treatment was removed, cells were rinsed three times with HBSS, fresh medium then added to the wells (130 µL), incubated with 20 µL of MTS reagent for 3 h as indicated in the manufacturer's protocol and the absorbance determined at 490nm.

3.2.10 Statistical analysis

All experiments were performed in triplicates and values are expressed as mean $\pm$ standard deviation (SD). Statistical significant differences between the treatments were evaluated with analysis of variance (ANOVA) and Bartlett's test significant difference (LSD) using GraphPad Prism, with alpha < 0.05 and <0.0001 being the probability of error .

3.3 Results

3.3.1 Development and physicochemical characterisation of dye and drug-loaded polymeric microparticles with variable porosity

3.3.1.1 Size of microparticles with and without loading of dye and chemotherapeutic drugs

PLA and PLGA spherical MPs with different levels of porosity were produced *via* single emulsion processing. Particles of varying morphology were loaded with Nile Blue (NB), S.MTX, ETP or DTX at a concentration of 50 µg/mL, and the diameter size range of PLA and PLGA particles was measured by DLS, as shown in Figures 3.3 and 3.4, respectively. Spherical PLA MPs encapsulated with NB exhibited different sizes and size distribution; a broad peak for particle type A, between 40 and 85 µm, particle type B exhibited a triple peak between 40 and 65 µm, 70 and 75 µm and a third peak above 80 µm, whilst particle type C exhibited a broad peak between 40 and 85µm. PLA MPs loaded with S.MTX exhibited a broad double peak for particle type A up to 35 µm and from 50 to 60 µm, particle type B exhibited a broad peak between 40 and 65µm, whilst particle type C exhibit a broad peak between 40 and 80 µm. PLA MPs loaded with ETP exhibited triple narrow peaks for particle type A, between 45 and 50 µm, 55 and 59 µm and 61 and 65 µm, whilst particle types B and C showed broad peaks between 40 and 75 µm and 50 and 95 µm, all respectively. The PLA MPs encapsulated with DTX exhibit one broad peak up to 75 µm and a second narrow peak between 80 and 85 µm for

particle type A, particle type B exhibited a broad peak between 40 and 65μm and a second peak between 70 and 75μm, approximately whilst particle type C exhibited a broad peak between 35 and 85μm, as shown in Figure 3.3.

Spherical PLGA MPs encapsulated with NB exhibited a broad peak for particle type A' between 40 and 75 μm, particle type B' had a broad peak between 50 and 70 μm, whilst particle type C' exhibited a broad peak between 10 and 70 μm. PLGA MPs loaded with S.MTX exhibited four narrow peaks for particle type A' between 55 and 60 μm, 60 and 65 μm, 70 and 75 μm and a fourth peak between 75 and 80 μm, particle type B' also exhibited narrow peaks between 45 and 50 μm, 55 and 60 μm, 60 and 65 μm and a fourth peak between 65 and 70 μm, whilst particle type C' exhibited a broad peak up to 65 μm. PLGA particles loaded with ETP exhibited two broad peaks for particle type A' between 42.5 and 70 μm and 75 and 95 μm; particle type B' exhibited two broad peaks between 42.5 and 50 μm and 52.5 and 65 μm, whilst particle type C' had a broad peak between 25 and 70 μm, all respectively. The PLGA MPs encapsulated with DTX showed a single broad peak for all types of morphologies which particle type A' exhibited a peak between 15 and 65 μm, particle type B' exhibited a peak between 20 and 75 μm and particle type C' exhibited a peak between 10 and 63 μm, as shown in Figure 3.4.

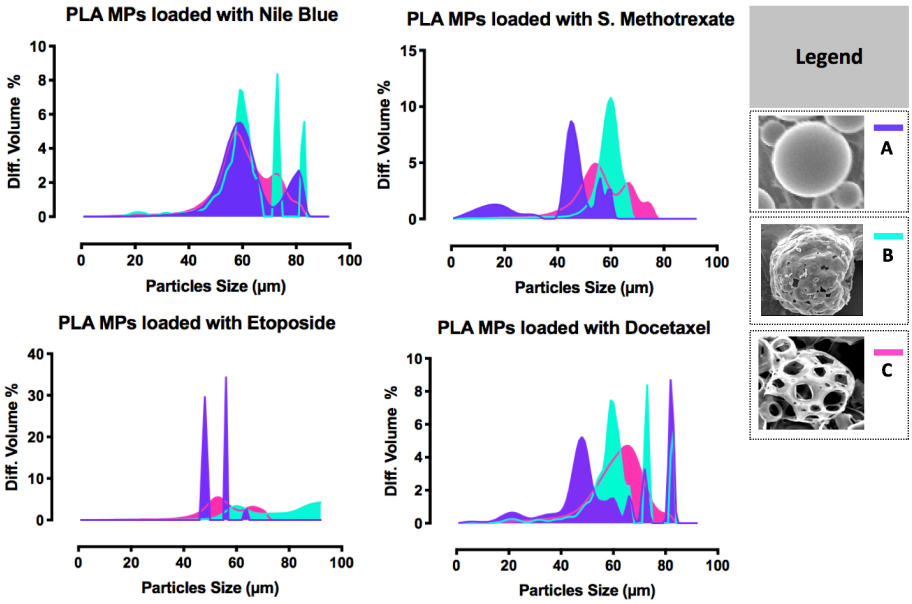


Figure 3.3: Size distribution of PLA spherical microparticles with variable morphologies, and encapsulated with Nile Blue, SMTX, ETP or DTX, as determined by DLS (n=3).

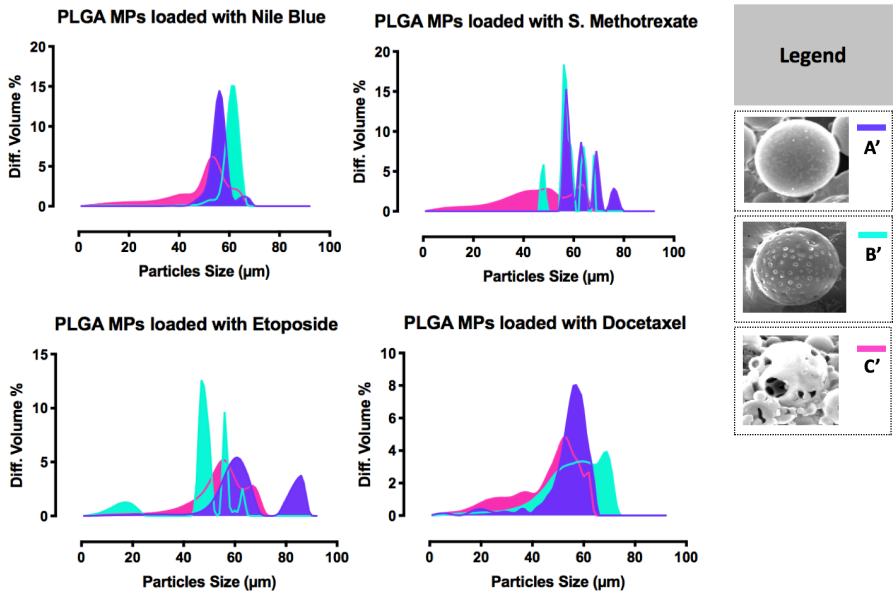


Figure 3.4: Size distribution of PLGA spherical microparticles with variable morphologies, and encapsulated with Nile Blue, SMTX, ETP or DTX, as determined by DLS (n=3).

3.3.1.2 Quantification of dye and chemotherapeutic drug content in the polymeric microparticles

PLA and PLGA microparticles of varying their morphology were encapsulated within different concentrations of NB, between 10 and 115 μg/mL, in order to establish the detectable concentration of dye for further studies by UV-vis. Table 3.2 presents the concentration of NB encapsulated into spherical polymeric microparticles. PLA particles encapsulated with theoretical concentration of NB between 10 and 22.5 μg/mL exhibited UV-vis concentration between 0.18 and 0.46 μg/mL, whilst particles encapsulated with NB at 50 μg/mL exhibited UV-vis concentration above 1.00 μg/mL. Furthermore, PLGA particles encapsulated with theoretical concentration of NB between 10 and 22.5 μg/mL exhibited UV-vis concentration range between 0.20 and 3.15 μg/mL, whilst particles encapsulated with NB at 50 μg/mL exhibited UV-vis concentration between 6.37 and 21.36 μg/mL.

Table 3.2: Amount of dye encapsulated in the spherical polymeric microparticles with variable morphology and dye concentration, determined using UV-vis spectroscopy (n=1).

Particles Type	Theoretical Concentration (µg/mL)	UV-Vis Concentration (µg/mL)	Encapsulation Efficiency (%)
A	10	0.18	1.80
	22.5	0.40	1.80
	50	1.05	2.11
	75	2.40	3.17
	115	4.95	4.30
B	10	0.33	3.35
	22.5	0.41	1.84
	50	1.87	3.74
	75	4.23	5.64
	115	10.58	9.20
C	10	0.26	2.66
	22.5	0.46	2.06
	50	2.30	5.60
	75	5.26	7.02
	115	13.34	11.60
A'	10	0.20	1.90
	22.5	0.42	1.87
	50	6.37	12.73
	75	11.10	14.80
	115	20.20	17.56
B'	10	0.60	6.00
	22.5	3.15	14.00
	50	21.36	42.73
	75	26.00	34.62
	115	55.04	47.86
C'	10	0.31	3.12
	22.5	0.35	1.58
	50	6.58	13.17
	75	8.67	11.57
	115	18.44	16.03

Table 3.3 presents the physicochemical characterisation (*i.e.* dye loading and amount of dye encapsulated in the polymeric MPs at concentration of 50 µg/mL) as a proof-of-concept study for subsequent drug encapsulation with S.MTX, ETP or DTX at concentration of 50

μg/mL by the single emulsion process, as described in section 3.2.4. PLA MPs exhibited a final dye concentration calculated from the calibration curve of NB between 8.02 and 3 μg/mL, corresponding to dye encapsulations of 16.4 ± 2.8%, 10.4 ±1.5% and 6.0 ± 0.78% for particles A, B and C, all respectively. PLGA MPs exhibited a dye concentration between 6.92 and 3.30 μg/mL, corresponding to dye encapsulations of 13.8 ± 3.2%, 21.6 ± 5.4% and 6.6 ± 2.1% for particles A, B and C, all respectively.

Table 3.3: Amount of dye encapsulated in the spherical polymeric microparticles with variable morphology, determined using UV-vis spectroscopy (n=3).

Polymeric Micro particles	Dye Concentration (μg/mL)	Amount of Dye (%)
A	8.02 ± 1.2	16.04 ± 2.8
B	5.2 ± 0.8	10.4 ± 1.5
C	3 ± 0.08	6 ± 0.78
A'	6.92 ± 1.75	13.84 ± 3.2
B'	10.8 ± 2.45	21.6 ± 5.4
C'	3.30 ± 0.53	6.6 ± 2.1

PLA and PLGA MPs encapsulated with S.MTX, ETP and DTX exhibited drug concentration below 10, 6 and 31 μg/mL, respectively. The MPs encapsulated with S.MTX evidenced a low amount of encapsulated drug, with the highest relative amount of drug observed for particles A' and B', as indicated by the red arrows (Table 3.4). The polymeric MPs encapsulated with ETP also exhibited a low amounts of encapsulated drug; however the non-porous PLA particles (type A) and highly porous PLGA particles (type C') exhibited a high drug

encapsulation, as shown in Table 3.3. The MPs encapsulated with DTX exhibited higher drug encapsulation in comparinson with the MPs encapsulated with S.MTX and ETP; with particles types B and B' exhibiting far higher drug encapsulation at 48 ± 26.3% and 62 ± 40%, respectively, compared with the other particle morphologies, as demonstrated by the red arrows in Table 3.4.

Table 3.4: Amount of chemotherapeutic drug encapsulated in the spherical polymeric microparticles varying their morphology as determined by HPLC (n=3).

Drug Encapsulated	Polymeric Micro particles	Drug Concentration (µg/mL)	Amount of Drug (%)
Methotrexate Sodium Salt	A	9 ± 4.8	8.80 ± 6
	B	5.06 ± 2.11	13 ± 11
	C	4.81 ± 2.02	11 ± 2.8
	A'	3.4 ± 0.035	6.81 ± 0.06 ←
	B'	2.3 ± 0.91	5 ±1.70 ←
	C'	2 ± 0.64	3.72 ± 1.16
Etoposide	A	5 ± 0.55	9.01 ± 0.9 ←
	B	3.45 ± 0.5	7 ± 0.96
	C	4 ± 2.54	8 ± 5.01
	A'	5.06 ± 2.8	10.13 ± 5.6
	B'	4 ± 2.21	8 ± 4.42
	C'	5.2 ± 1.81	11.82 ± 2.20 ←
Docetaxel	A	28 ± 20	56 ± 41
	B	24 ± 13	48 ± 26.3 ←
	C	26 ± 17	51.3 ± 33.06
	A'	5 ± 1	10.34 ± 2
	B'	31 ± 20	62 ± 40 ←
	C'	26 ± 19	52 ± 39

3.3.1.3 Study of the In vitro dye and drug release study from the polymeric microparticles as function of time

The release profile of dye and chemotherapeutic drugs was assessed in order to determine the relationship between particle porosity and the release profile across different particle morphologies.

Initially, NB was encapsulated and the release profile tested as a proof-of-concept ahead of further studies with known cytotoxic drugs. Particle types A, B and C exhibited similar release profiles when encapsulated with dye. Particle types A and B exhibited higher release rates over 30 days at ~30%, as shown in Figure 3.5. PLA MPs encapsulated with S.MTX exhibited a similar release rate, at ~20% for particle types A and B, whilst particle type C achieved a percentage of drug release above 60% over a 30-day period. The PLA MPs encapsulated with ETP exhibited a similar percentage of drug release between 20% and 30%. PLA MPs encapsulated with DTX exhibited a release profile above 80, 25 and 15% for particle types A, B and C, all respectively, as shown in Figure 3.5.

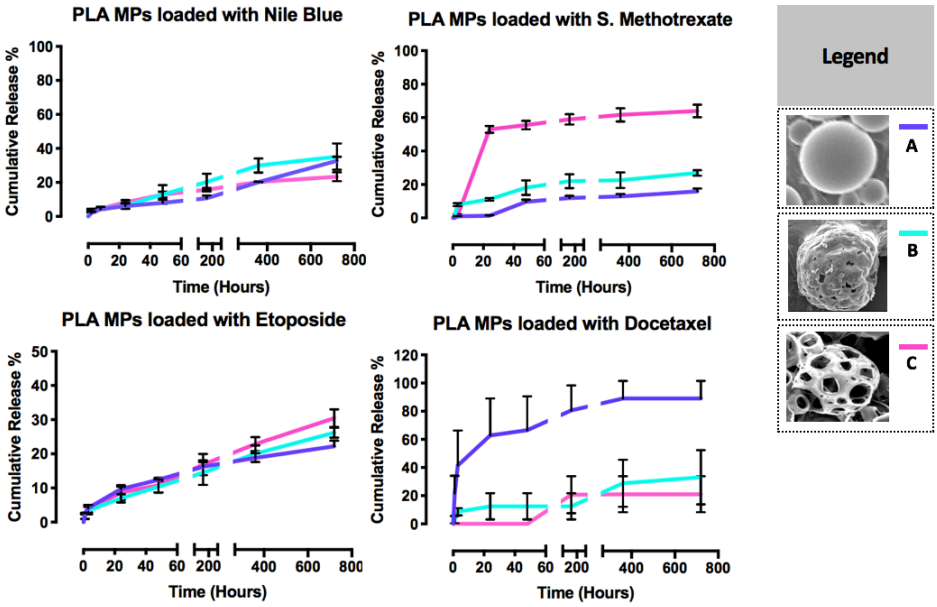


Figure 3.5: In vitro cumulative release profile of active agents encapsulated in PLA particles. Release study of spherical PLA microparticles encapsulated with Nile Blue, S.MTX, ETP or DTX as function of time. Error bars represent a confidence interval of 95%. (n=3) ($p<0.05$: NB and ETP release, $p>0.05$: S.MTX and DTX release one-way ANOVA with Bartlett's test).

PLGA MPs were also encapsulated with dye, S.MTX, ETP or DTX, and their release profiles assessed over 30 days. PLGA MPs encapsulated with dye exhibited cumulative release, above 60% for particle type A', whilst particle types B' and C' exhibited similar release profiles, attaining over 80% release. MPs encapsulated with S.MTX showed a similar release to particle types B' and C', which attained a cumulative release of 20%, whilst particle type A' exhibited a cumulative release of 40%. Type A' and B' PLGA MPs encapsulated with ETP had a cumulative release between 10 and 15%, whilst particle type C' exhibited release in excess of 20%. PLGA MPs encapsulated with DTX had higher cumulative release when compared with PLGA MPs encapsulated with S.MTX and ETP; with particle type A' and B' attaining a cumulative release above 95% and particle type C' attaining a cumulative release above 40%, as shown in Figure

3.6.

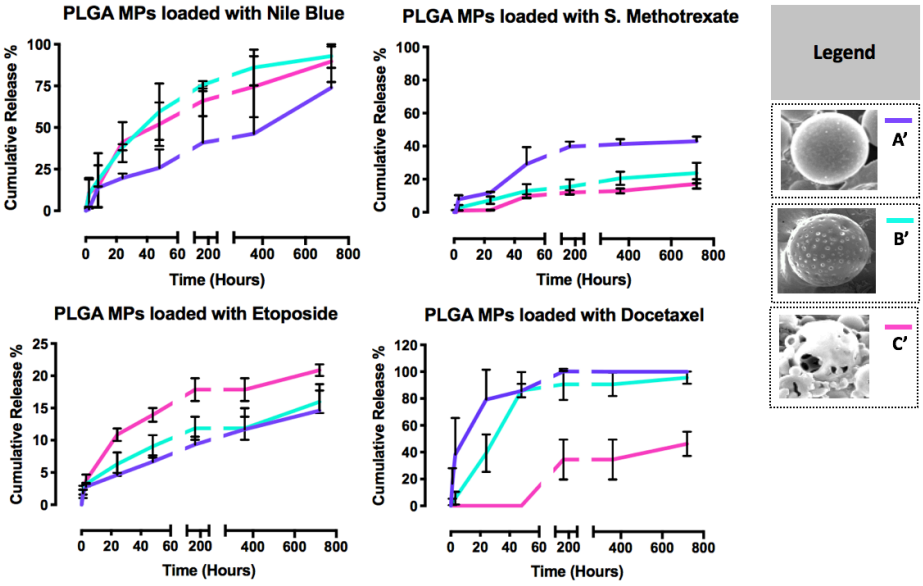


Figure 3.6: In vitro cumulative release profile of active agents loaded into PLGA microparticles. Release study of spherical PLGA microparticles encapsulated with Nile Blue, S.MTX, ETP and DTX as function of time. Error bars represent a confidence interval of 95%. (n=3) ($p<0.05$: NB, S.MTX and ETP release; $p>0.05$ DTX release one-way ANOVA with Bartlett's test).

3.3.2 Development of a degradable polymeric paste formulation as a proof of concept for a local multi therapy system for GBM

Local therapy systems have been used for GBM treatments in order to reduce systemic drug toxicity, attain therapeutic dosage proximal to the tumour site, and allow small and large molecules to bypass the BBB and BTB. The issues related with GBM treatment are highlighted earlier, in section 1.3.2.5, and are an initial concern for the development of GBM therapies. Furthermore, localised treatments have been developed to overcome the main challenges of systemic delivery, as discussed in section 2.3.2.5. In this work, a polymeric paste was developed using a thermo-responsive polymeric system based on PLGA-PEG MPs, incorporating an aqueous solution of DTX

at 50 μg/mL, and PLA and PLGA spherical MPs with varying morphology encapsulated with S.MTX, ETP or DTX, as described in section 3.2.4. This formulation was developed in order to offer a novel approach for multi-drug therapy as a proof of concept technology towards a local drug delivery system for GBM therapy.

3.3.2.1 In vitro dye and drug release study from the paste formulation as function of time

PLA and PLGA spherical MPs were initially encapsulated with dye and incorporated within a thermo-responsive PLGA-PEG matrix to develop a proof of concept system. PLA and PLGA spherical MPs were later encapsulated with NB and cytotoxic drugs, and the cumulative release assessed *in vitro*, determined by UV-vis and HPLC. PLA MPs encapsulated with dye exhibited a cumulative release below 20% for particle types A and C, whilst particle type B attained a release above 50% over the 30-days study duration, as shown in Figure 3.7. PLA MPs encapsulated with S.MTX and ETP exhibited similar release profiles even though the particles have different levels of porosity themselves. Particles encapsulated with S.MTX exhibited cumulative release between 20 and 30%, whilst PLA MPs encapsulated with ETP exhibited a cumulative release between 7.5 and 10%, as summarised below in Figure 3.7.

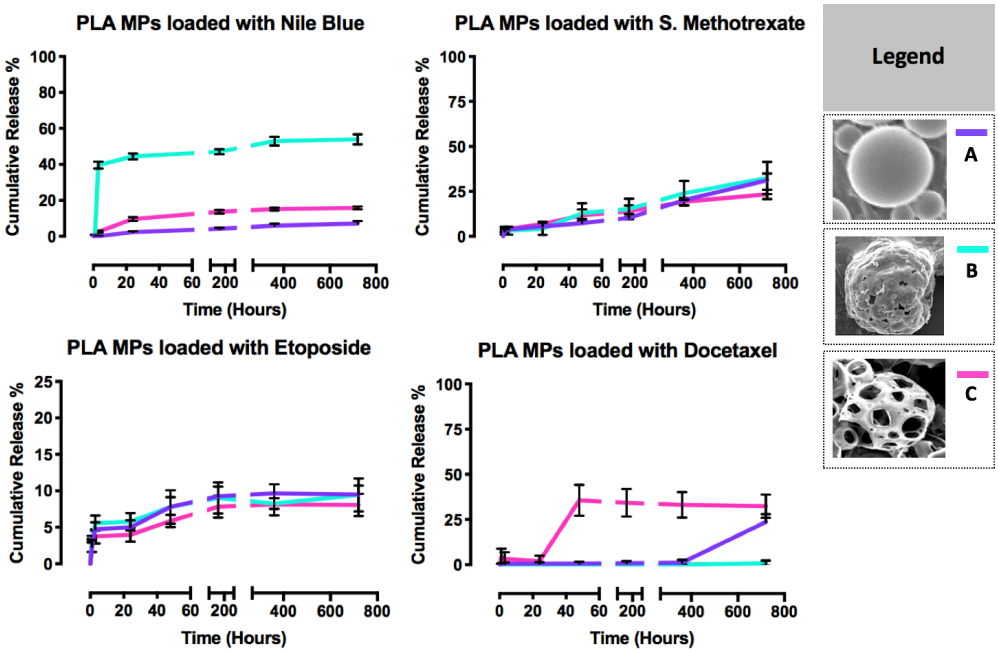


Figure 3.7: In vitro cumulative release profile of active agents loaded into paste formulation Release study of polymeric paste containing blank (non-drug loaded) PLGA/PEG matrix and PLA microparticles loaded with Nile Blue, S MTX, ETP and DTX. Error bars represent a confidence interval of 95%. (n=3) ($p<0.05$: S.MTX and ETP release; $p>0.05$: NB and DTX release one-way ANOVA with Bartlett's test).

PLGA MPs encapsulated with dye exhibited similar release profiles for particle type B' and C' which reached a cumulative release below 20%, whilst particle type A' exhibited an initial burst release at 80%, reaching 100% of dye release after just 24 h, as shown in Figure 3.8. PLGA MPs encapsulated with S.MTX showed a similar release profile, however particle type B' showed a cumulative release below 35%, whilst particle types A' and C' exhibited release of 52 and 48%, both respectively. Particles encapsulated with ETP exhibited similar profiles with particle types A', B' and C' having release of 12, 14 and 13% over the 30-day period of investigation, all respectively. PLGA spherical MPs encapsulated with DTX exhibited similar release profile when compared with PLGA MPs encapsulated with dye. Particle type A' attained release of 48% over 5 h of study and 93% over a 48 h

period, whilst particle types B' and C' exhibited cumulative release below 20% over the 30-day of study, as shown in Figure 3.8.

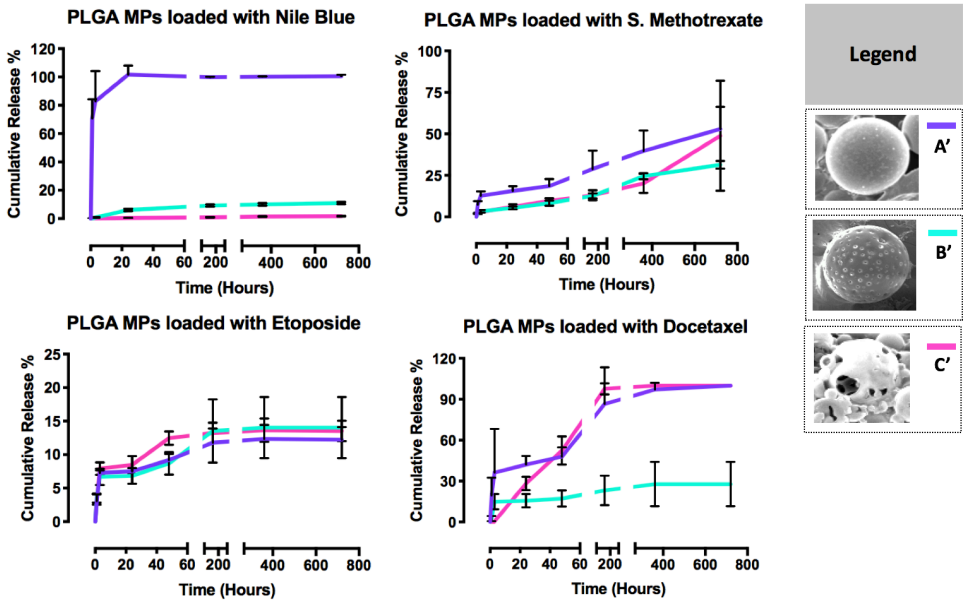


Figure 3.8: In vitro cumulative release profile of active agents loaded into paste formulation. Release study of polymeric paste containing blank PLGA/PEG matrix and PLGA spherical particles of varying morphology loaded with Nile Blue, S MTX, ETP and DTX. Error bars represent a confidence interval of 95%. (n=3) ($p<0.05$: S.MTX and ETP release; $p>0.05$: NB and DTX release one-way ANOVA with Bartlett's test).

3.3.2.2 In vitro U87 cell viability measured after treatment with non encapsulated microparticles, free drug and paste formulation with high loading efficiency .

Cellular viability was determined to assess the toxicity of the polymeric particles alone. Cells were treated with the paste therapy developed in this work as a screening strategy for the development of novel therapies against GBM. Particle toxicity was determined by varying their concentration between 5 and 750 µg/mL. U87 cells (GBM cells) were treated for 24h with the polymeric particles in suspension followed by a washing step then MTS assay, as described in section 3.2.9.1. PLGA and PLA spherical particles and PLGA-PEG MPs did not show any significant decrease in terms of cell viability

between the lowest and highest particle concentrations tested, as shown in Figure 3.10. The free drug was also tested in order to evaluate potential cytotoxic effect on U87 cells during 24 h of treatment. U87 cells treated with DTX showed the lowest cell viability at 68% when compared with S.MTX and ETP at 82 and 83%, as shown in Figure 3.11.

The paste formulations developed included five different types and were tested in order to evaluate the efficacy of the treatment against proliferation and growth of U87 cells over a 30-day period. Therapy 1 contained 25 µg/mL PLGA-PEG MPs (*e.g.* matrix) incorporated with DTX solution at 50 µg/mL. The other four formulations as described below in Figure 3.9, utilised the same proportion of PLGA-PEG mixed with DTX. However, these other therapies included a second therapeutic component in order to impair cell proliferation as shown in Figure 3.9.

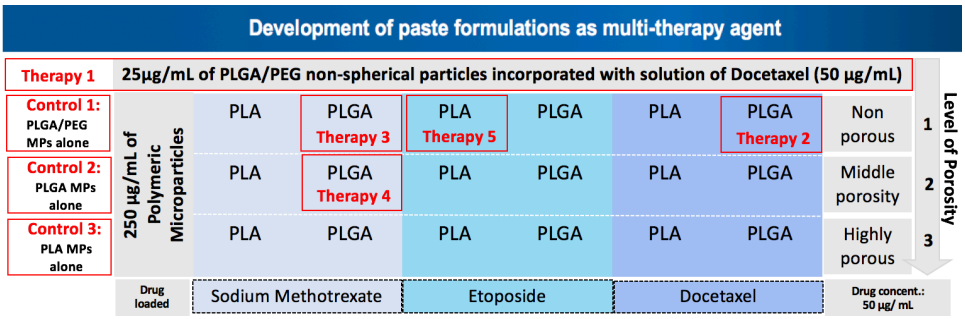


Figure 3.9: Multi-therapy system developed as a paste formulation for localised treatment against GBM cells proliferation and growth.

In general, the five therapies selected above to treat the U87 cells result in cell viability above 78%, whilst U87 cells treated with therapy 3 have the lowest cell viability at 55% over the 30-days of investigation period. Furthermore, results from therapies 2 and 5 are

significantly difference against control 1 and control 2, as shown in Figure 3.12 and Figure 3.13.

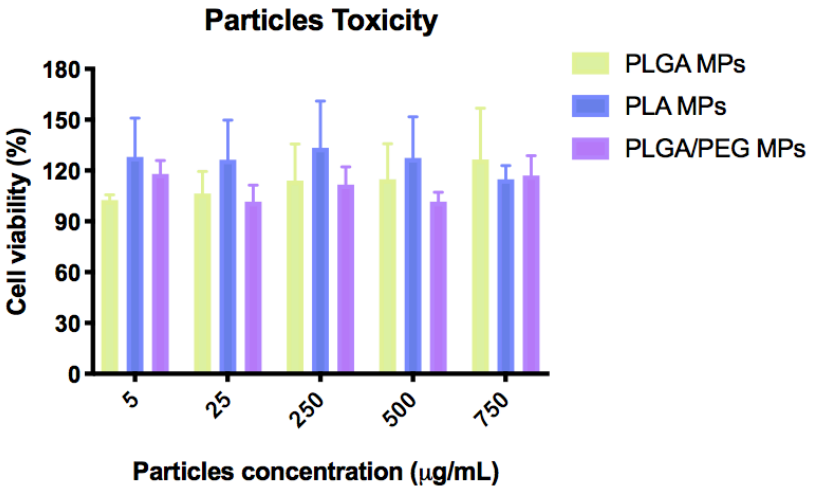


Figure 3.10: Cytotoxicity evaluation of the polymeric microparticles alone. U87 cells were assessed for viability after seeding onto non loaded particles. Error bars represent a confidence interval of 95%. (n=3) ($p<0.05$: PLGA MPs vs. PLGA/PEG MPs one-way ANOVA with Bartlett's test).

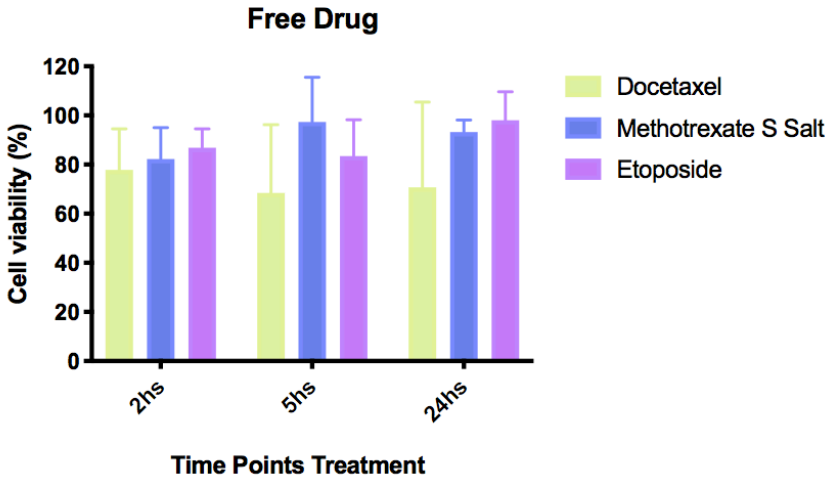


Figure 3.11: Cell viability of free drug. U87 cells were assessed for viability after seeding onto free drug solution at 50µg/mL. Error bars represent a confidence interval of 95%. (n=3) (no significant difference was shown: one-way ANOVA with Bartlett's test).

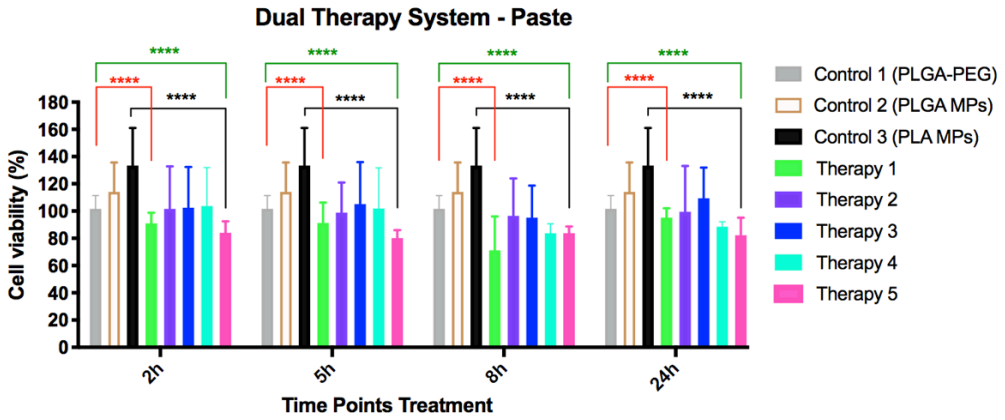


*Figure 3.12: Cytotoxicity of active agents released from PLGA/PEG paste. U87 cells were assessed for viability after seeding onto pre-selected paste loaded with chemotherapeutic drug to determine cytotoxic properties of released agents over 24h. Error bars represent a confidence interval of 95%. (n=3) (****p<0.0001 one-way ANOVA with Bartlett's test).*

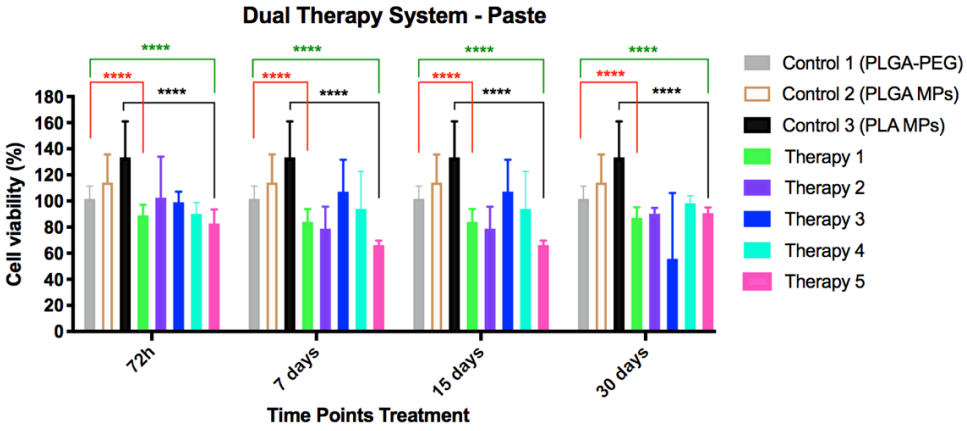


*Figure 3.13: Cytotoxicity of active agents released from PLGA/PEG paste. U87 cells were assessed for viability after seeding onto pre-selected paste loaded with chemotherapeutic drug to determine cytotoxic properties of released agents from 72 h up to 30 days. Error bars represent a confidence interval of 95%. (n=3) (****p<0.0001 one-way ANOVA with Bartlett's test).*

3.3.3 Development of tablet formulations as a local multi-therapy system for GBM

Therapeutic tablets were developed due to the necessity to improve the therapeutic efficacy of paste formulations, highlighted in this work in section 3.3.2, including: i) how the porosity of the particles could improve the efficacy of treatment against GBM cells, ii) which type of polymer would improve the incorporation of drug and release to result in increase cell death and iii) whether the treatment efficacy was related to the amount of particles encapsulated with the chemotherapeutic drugs.

3.3.3.1 In vitro study of the tablets in buffered solution over time

Tablets were developed and assesed *in vitro* in buffered solutions over a 30-day period to evaluate the incorporation of PLGA-PEG matrix with the PLA and PLGA microparticles as well as the behaviour of these polymers at 37°C in simulated physiological conditions.

Non-porous and porous PLA particle (types A and B, respectively) and non-porous and porous PLGA particle (types A' and B', respectively) were incorporated in PLGA-PEG MPs in order to create a multi-therapy system as a pharmaceutical tablet. The tablets were tested initially over 24 h and no significant difference between particle features between time point 0 and 24 h were observed, as summarised in Figures 3.14 and 3.15. Tablets were also assessed between 7 and 30 days, when a moderate difference in particle behaviour correlated with their degradation over 7 days was evident, compared with time point 0

(for types A, B, A', and B'), however a significant difference in particle morphology was evident at 15 days when particles showed significant blend with the PLGA-PEG matrix. Over the 30-day period of investigation, the surface of tablets contained MPs became progressively covered by a thickening polymer film, as shown in Figures 3.15 and 3.16.

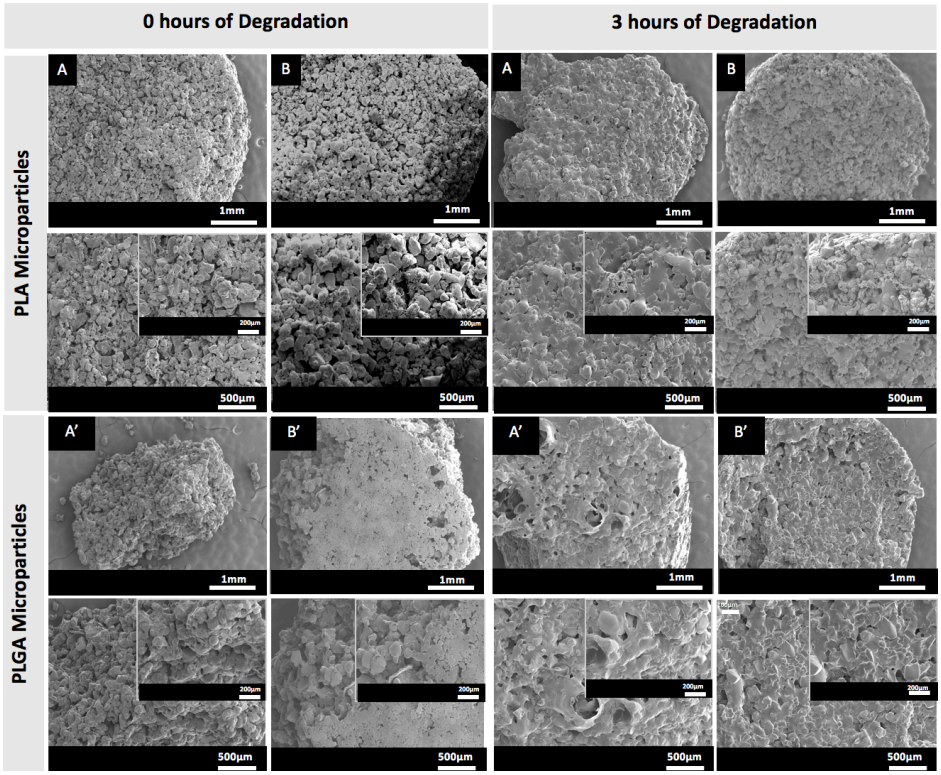


Figure 3.14: Analysis of PLA and PLGA particles mixed with PLGA/PEG matrix forming a pharmaceutical tablet in buffered solution assessed at time point zero and at 3h by SEM (Scale bars: 1mm, 500µm and 200µm - insets).

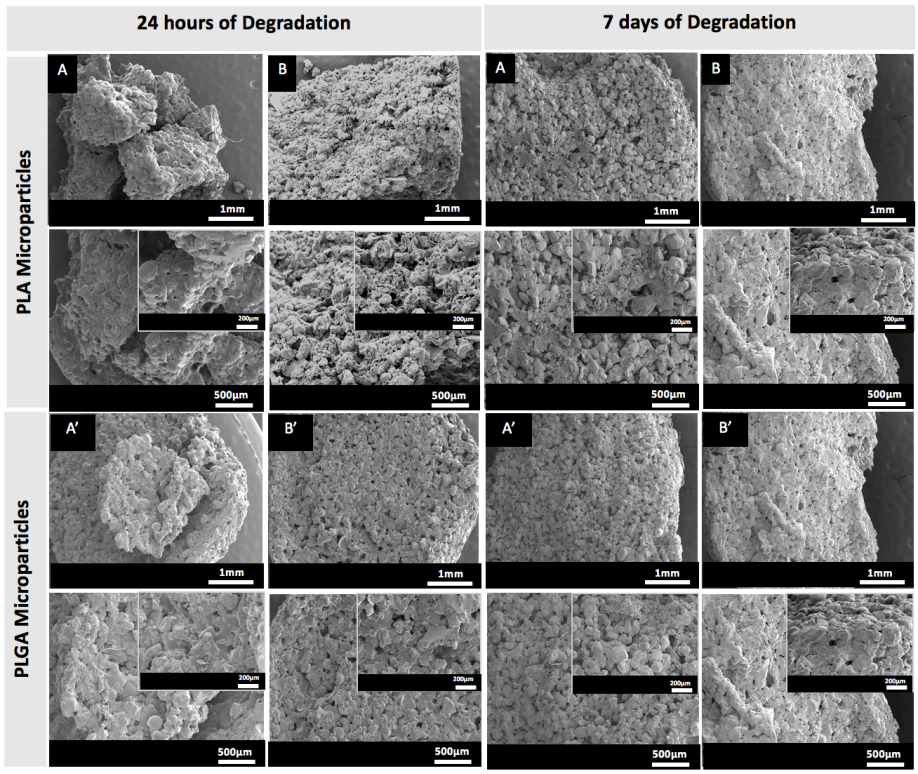


Figure 3.15: Analysis of PLA and PLGA particles mixed with PLGA/PEG matrix forming a pharmaceutical tablet in buffered solution assessed after 24 h and 7-day periods by SEM (Scale bars: 1mm, 500µm and 200µm-insets).

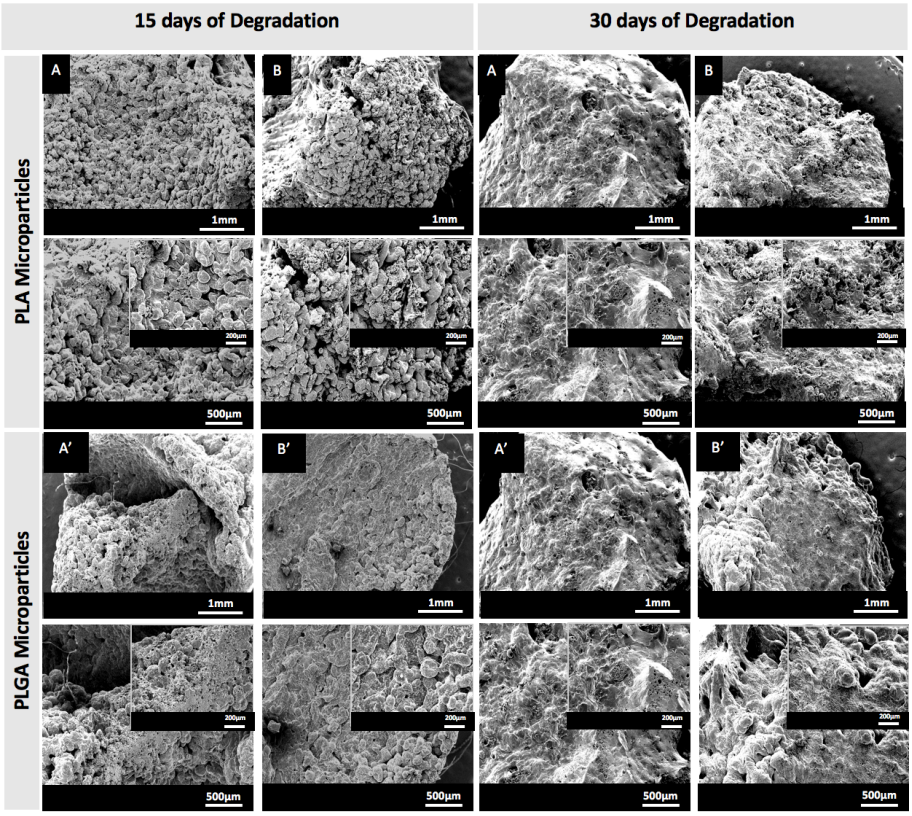


Figure 3.16: Analysis of PLA and PLGA particles mixed with PLGA/PEG matrix forming a pharmaceutical tablet in buffered solution assessed at 15- and 30-day periods by SEM (Scale bars: 1mm, 500µm and 200µm-insets)

3.3.3.2 In vitro dye and drug release study from the tablet formulations as function of time

PLA and PLGA spherical MPs with varying morphology were encapsulated initially with dye and incorporated within a PLGA-PEG matrix in order to mimic the release study of particles encapsulated with chemotherapeutic drugs over a 30-day period. PLA and PLGA particles were encapsulated with S.MTX and incorporated into PLGA-PEG matrix mixed with DTX at 50 μg/mL. The dye and drugs released over time were determined by UV-vis spectroscopy and HPLC, respectively.

Non-porous PLA MPs (type A) exhibited a similar dye release profile to non-porous and medium porosity PLGA MPs (types A' and B'), which attaining a cumulative release of 3.36%, 0.43%, and 1.93%, all respectively. However, the medium porosity PLA MPs (type B) exhibited a significant cumulative release of 12.5% over 15 days when compared the other formulations (*i.e.* particle types A, A' and B' particles) , as shown in Figure 3.13. PLA and PLGA MPs encapsulated with S.MTX exhibited a similar release profile; however particle types A' and B' presented a higher cumulative release at 100% and 89%, in comparison with particle types A and B, which had a cumulative release of 82% and 73% over the 30-day investigation period, respectively. The PLGA-PEG matrix was incorporated with DTX and mixed with PLA and PLGA MPs. The PLGA-PEG matrix system

mixed with DTX exhibited burst release in the first hour of study, with cumulative release to 100%, as shown in Figure 3.17.

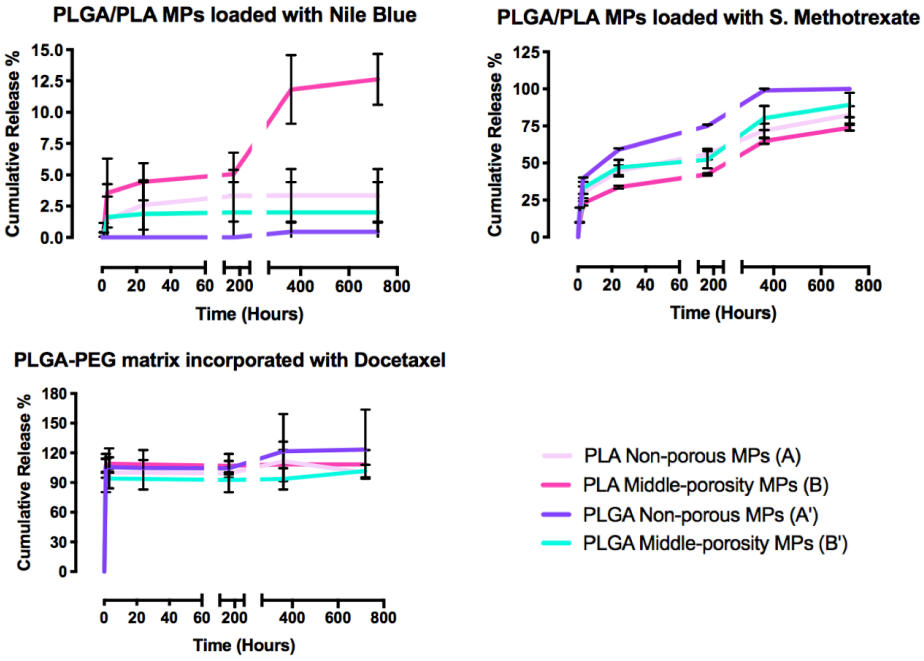


Figure 3.17: In vitro cumulative release profile of active agents loaded into the tablet formulations. Measurement of active components released from spherical microparticles (i.e. Nile Blue and S.MTX) and PLGA/PEG matrix (i.e. DTX) over the 30-day study. Error bars represent a confidence interval of 95%.(n=3) ($p<0.05$: PLGA/PLA S.MTX and PLGA-PEG DTX release; $p>0.05$: PLGA/PLA NB release one-way ANOVA with Bartlett's test).

3.3.3.3 In vitro study of U87 cells with selected tablet treatments over time

U87 cells were initially treated with polymeric microparticles to assess the lack of toxicity from polymeric particles by MTS assay, as described in section 3.2.9.1. Tablets were formulated in order to overcome the issues related with the paste treatments investigated in section 3.2.3.2 to control the proliferation of U87 cells. Tablet therapies were developed from a mixture of PLGA-PEG matrix incorporated with DTX and with PLA or PLGA MPs with varying morphologies and encapsulated with S.MTX. The five formulations

were developed as follows: Therapy 1, constituting 50 mg of PLGA-PEG matrix incorporated with DTX at 50 µg/mL and the other four formulations included a second therapeutic component in order to impair cell proliferation as summarised in Fig. 3.18.

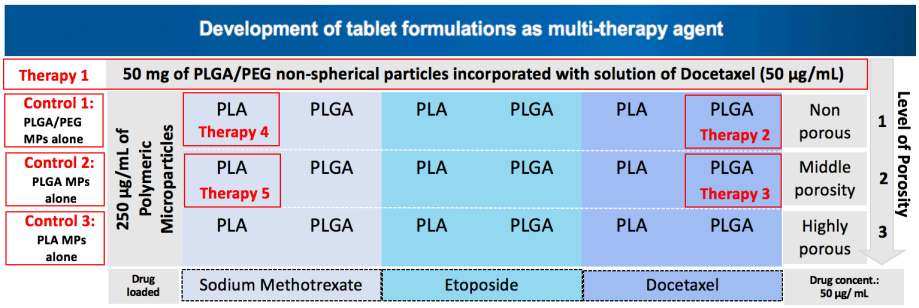


Figure 3.18: Multi-therapy system developed as a tablet formulation for localised treatment to control GBM cells proliferation and growth.

Therapies 1, 2, 3, 4 resulted in cell viabilities, between 65 and 111% however, these therapies exhibited significantly decreased cell viability between 8 and 23% when cells were treated with drug released solution over a 30-day period, as shown in Figure 3.20 (Dual Therapy Sytem – Tablets). Therapy 2 exhibited a significant difference versus Control 2 (PLGA MPs alone), whilst Therapies 4 and 5 exhibited a significant difference versus Control 3 (PLA MPs alone). Furthermore, Therapy 5 exhibited a significant difference versus Control 1 (PLGA-PEG MPs alone), and a continuous reduction in cell viability over time where the lowest cell viability reached 14% for Therapy 5 only when cells were treated with drug released solution over the 30-day period, as shown in Figures 3.19 and 3.20 (Dual Therapy System – Tablets).

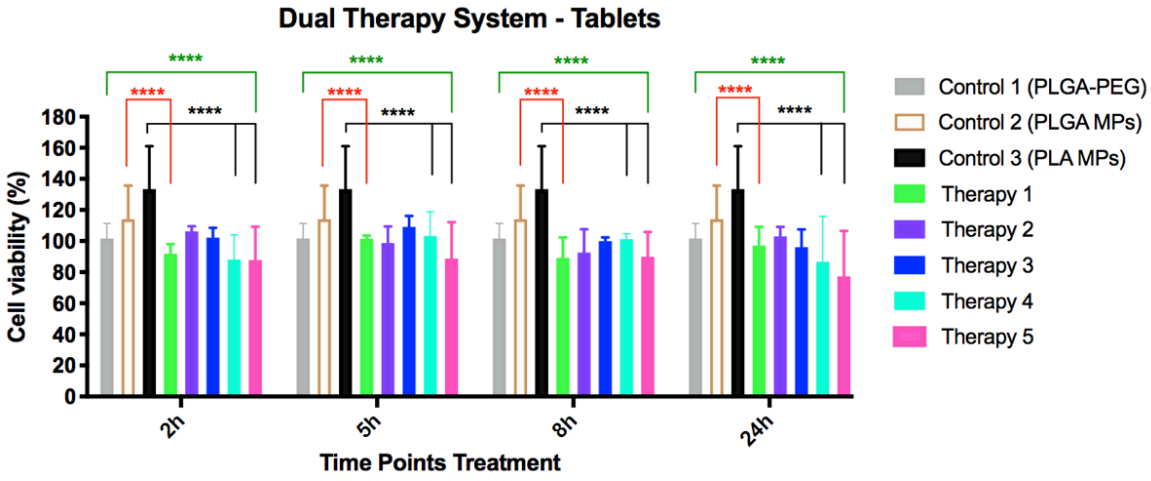


*Figure 3.19: Cytotoxicity of active agents released from tablet - based formulations. U87 cells were assessed for viability after seeding onto pre-selected tablets loaded with chemotherapeutic drug to determine cytotoxic properties of released agent over 24h. Error bars represent a confidence interval of 95%. (n=3) (**** p<0.0001 one-way ANOVA with Bartlett's test).*

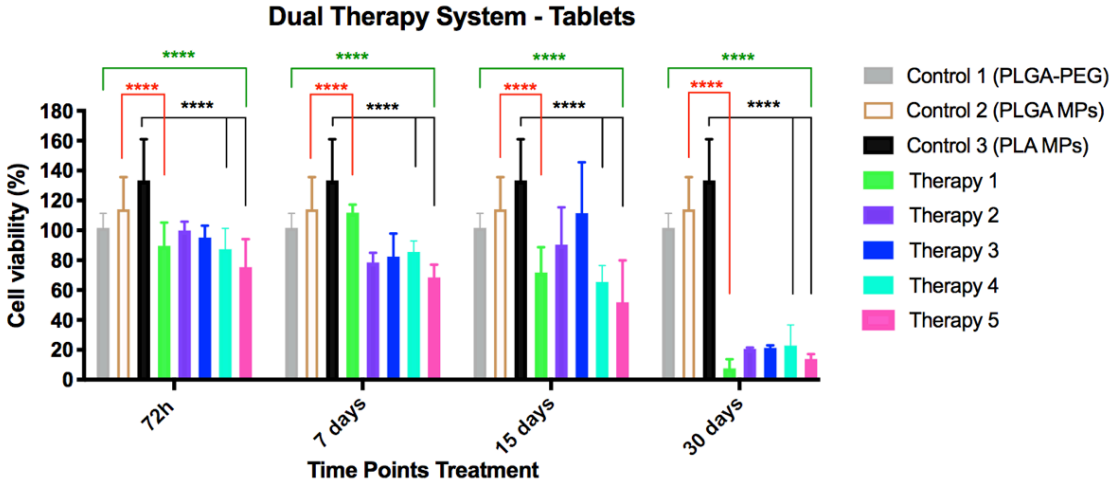


*Figure 3.20: Cytotoxicity of active agents released from tablets formulations. U87 cells were assessed for viability after seeding onto pre-selected tablets loaded with chemotherapeutic drug to determine cytotoxic properties of released agent from 72h up to 30 days. Error bars represent a confidence interval of 95%. (n=3) (**** p<0.0001 one-way ANOVA with Bartlett's test).*

3.4 Discussion

Polymeric micro- and nanoparticles have been explored worldwide for targeted therapeutics and can enable the controlled release of drugs over sustained periods of time in cancer therapy, as well as other diseases. Polymeric microparticles can protect drugs against the body

environment which may otherwise also result in particle degradation and undesired drug release [216, 338]. Particle porosity and size distribution are one of the major factors that determine release kinetics and application, and release kinetics which is related to the surface area of the particles [130].

In this work, PLA and PLGA microparticles have been developed with varying morphology and encapsulated with four different components, including a model dye (Nile Blue, NB), S.MTX, ETP and DTX, as shown in Tables 3.3 and 3.4. The size distribution of the particles encapsulated with these components was measured in section 3.3.1.1 and for all given formulations encapsulated with dye and chemotherapeutic agents did not cause difference in particles size compared to control samples; which was between 40 and 80 μm. Results with particles encapsulated with NB were useful as proof of concept data for assessing the effect of loading on particle size, and were subsequently useful in developing further studies here based on MPs with chemotherapeutic agents encapsulated.

Biomedical markets have expanded more than 10% annualy since the early 21st century and PLA and PLGA are some of the main FDA approved polymers used to address current biomedical needs [354, 355]. Microparticles made with PLA and PLGA have been extensively studied to deliver a large variety of medicinal agents, including micro and macro molecules, as well as hydrophilic and hydrophobic drugs due to low aqueous solubility of PLA and PLGA. The hydrophobicity of drugs influences their encapsulation into polymeric macroparticles

and polymer hydrophobicity can influence the release rate of the encapsulated drugs [216]. Encapsulation of hydrophobic drugs is an alternative to systemic delivery, addressing therapeutic dosage, local delivery, and decreases in systemic toxicity. Drug-loaded PLA and PLGA microparticles have been applied *in vitro* and *in vivo* for cancer therapy, and exist in products, such as Atridox® - a polymeric microparticle developed for periodontal treatment and Sandostatin® for acromegaly, and Lupron depot® - for prostate cancer [216, 356]. Block co-polymeric microparticles (*i.e.* PLGA-PEG-PLGA microparticles) encapsulated with paclitaxel have been developed to treat esophageal cancer, and OncoGel^{TM} has reached the clinical trial phase for efficacy evaluation of its efficacy against GBM [216, 357].

It is well known that PLGA has the ability to enpasulate both hydrophilic and hydrophobic agents; however PLA-based microparticles are more hydrophibic, having a higher ratio of non-polar to polar groups than PLGA in its repeat unit, and, are consequently more appropriate for the incorporation of hydrophobic drugs. A crucial step in in this thesis was the development of an encapsulation system for a hydrophobic dye (*i.e.* NB) as a proof-of-concept, prior to advancing with the encapsulation studies with chemotherapeutic drugs and *in vitro* drug release studies as function of time. PLA and PLGA MPs with varying morphology were encapsulated with dye and chemotherapeutic agents at a target concentration of 50 μg/mL. The particles encapsulated with NB exhibited a dye concentration between

3.0 and 10.8 μg/mL, varying between PLA and PLGA MPs. This result did not corroborate with the hypotheses that PLGA MPS could enable higher drug loading due the presence of glycolide in the chemical chain when compared with PLA MPs, suggesting that the drug loading profile can be affected by the logP of the NB. Furthermore, those chemotherapeutic agents with a similar logP value to NB may exhibit comparable encapsulation profiles [358].

PLA and PLGA MPs have been used extensively as a drug carriers for cancer treatment and their porosity can determine the release kinetics as well as the amount of drug encapsulated into the MPs during processing. Polymeric MPs with varying morphology were encapsulated with S.MTX, ETP or DTX in order to overcome the high toxicity of chemotherapeutic drugs and avoid the high concentration of drugs otherwise necessary to reach the therapeutic target when delivered systemically. MPs encapsulated with S.MTX exhibited a lower encapsulation efficiency in comparison to particles encapsulated with ETP and DTX. This result corroborates with the findings of Chew *et al* [338], where the hydrophilicity and hydrophobicity of the drug can determine the entrapment efficiency. Furthermore, it has been proven that the single emulsion method can retain lipophilic drugs successfully by direct incorporation of hydrophobic drugs into the organic phase, as developed here in this study.

Particle morphology and porosity level of these polymeric MPs can be a determining factor for the release kinetics of drugs. It is expected that particles with highly porous structures would exhibit a faster release

profile when compared with their non-porous counterparts due the rapid diffusion of media inside the polymeric matrix, as well as particle degradation. However, the results found corroborate partially with the hypotheses established in this study as the cumulative release profile varied between non porous, medium porosity and highly porous particles, suggesting that the diffusion rate of chemotherapeutic drugs can be influenced by their hydrophobicity and elution from the polymeric matrix. Furthermore, particle size and surface modifications with chemical attachments (*e.g* linkers, antibodies) can influence the release profiles of therapeutics immediately after implantation and over several months [221, 354, 359, 360].

Modelling of controlled release of drugs from polymeric devices has been adressed in order to investigate the diffusional relase and erosion mechanisms from polymers, as well as from pharmaceutical forms such as films, cylinders devices, tablets and dispersed powders [379-380]. Most models are typically based on Fickian diffusion theory and have been developed to predict the permeability of lipophilic drugs through hydrophilic enviroments, sink and dissolution conditions, as well as the absorption and elimintation of drugs from the body [381-382]. Models of particular relevance are the zero and first order kinectics [383], the Roseman and Higuchi model [384-385], the Hixson-Crowell model [382], the Korsmeyer-Peppas model, Baker-Lonsdale model and Hopfenberg model. However, the mathematical models cited above involves multiple physical and chemical phenomena such as dissolution parameters, radius of a spherical matrix

during the release study, total amount of drug when the pharmaceutical dosage form is exhausted [386], media viscosity, tuortuosity factor and porosity of the matrix over time [387]. These multiple parameters make modelling challenging to apply to the formulations developed in this thesis [386].

The method chosen to express the release kinectics in this work was a statistical method based on the analysis of variances, as a model-independent method, which tests ratio the relationships between parameters obtained from the release against formulations developed in association of spherical polymeric microparticles and polymeric matrix.

It is well known that a wide range of active compounds can be incorporated in degradable polymeric microspheres for local treatment of GBM. Microparticles encapsulated with paclitaxel, 5-Fluorouracil (5-FU) and carboplatin have been developed and pressed into disks for direct implantation in the brain tumour resection cavity [161, 335, 361, 362]. Other chemotherapeutic agents such as Etanidazole and Temozolomide have been loaded in PLGA microfiber disks, sheets, foams, wafers and spherical particles with different geometries and sizes to obtain standard pharmacokinetic and diffusion profiles into the brain, as well as preliminary efficacy results *in vitro* and *in vivo* [134, 161, 363-365]. The median overall survival of 5-FU treatment between groups has not been show to be significantly different, and the polymeric based formulations available in the market have not yet shown patient survival longer than 2 months [92, 175, 366-368].

PLA and PLGA MPs with different levels of porosity were encapsulated with chemotherapeutic agents in order to overcome the burst release caused by the non-porous PLGA spherical particles and the late release profile caused by the non porous PLA spherical particles as shown in Chapter 2 PLA and PLGA MPs loaded with NB were initially tested over a 30-day period in PBS solution at 37°C. PLA MPs encapsulated with NB, S.MTX, ETP or DTX exhibited a sustained release over a 30–day period. However, the cumulative release of PLA MPs was below 40% apart for particle types C and A encapsulated with S.MTX and DTX, as shown in Figure 3.5. The results presented in this section for particle types A encapsulated with DTX are distinct from those reported in the literature where porous particles usually show a superior percentage of drug released in comparison to non-porous particles [170]. The PLGA MPs developed in this thesis also exhibited a sustained release of NB and other chemotherapeutic agents. However, PLGA MPs encapsulated with NB and DTX exhibited higher cumulative release over 30-days in comparinson with NB and DTX PLA MPs. Furthermore, PLGA MPs encapsulated with NB and DTX reached a cumulative release above 80% over 15 days and 24 h respectively. However, non-porous and medium porosity particles encapsulated with DTX exhibited a superior percentage of drug released when compared with highly porous particles (*i.e.* particle type C') which is contrary to reports in literature [170]. This study demonstrated that PLA MPs loaded with NB and ETP, and PLGA MPs loaded with NB, S.MTX and ETP, of varying

morphology, did exhibit statistically differences in terms of their release profiles, as shown in Figure 3.6. These findings corroborate with the slow release profile from PLGA and PLA spherical particles and controllable cumulative release from spherical particles with different morphologies as described in the initial hypotheses (section 1.3), suggesting that the sustained release of active components is influenced by the diffusion rate and penetration depth of PBS solution into the particles, polymer type (and hydrophobicity), particle size, drug hydrophobicity and interaction of the spherical polymeric particles with the polymeric matrix [161].

Current brain tumour treatments include radiotherapy combined with localised drug delivery systems incorporated with polymeric materials as have been described in section 1.3.2.1. However these treatments have limitations, such as i) the low drug loading capacity of microparticles; ii) they are typically single drug systems, iii) poor drug diffusion through the brain cortex, iv) they typically exhibit fast drug release, v) implant dislodgement [161, 164, 369].

The standard localised treatment available in the market for GBM is the Gliadel® wafer, a drug delivery implant containing microparticles mixed homogenously with Carmustine (BCNU). The particles are compressed into small disks with a recommended dose of 61.6 mg of BCNU represented by 8 wafers [134, 161, 221] . The wafers are placed post surgically into the brain tumour cavity, and the system releases the therapeutic continuously for approximately for three weeks. However,

the majority of *in vivo* mammalian models studies have shown that the active components are taken up the first 5-7 days [161, 370].

Novel therapies systems have been developed in order to overcome the recurrence of GBM cells despite tumour resection followed by Gliadel® implant, and subsequent radiotherapy combined with TMZ chemotherapy [161]. However, only 8% of the patients treated with this therapy survive longer than 2.5 years and no long-term survivors are reported [161, 371]. Even though the scientific community has developed a significant number of studies using microparticles and nanoparticles as carriers for localised and systemic drug delivery systems, GBM remains incurable.

The thermo-responsive polymeric particle formulations developed by the Rahman laboratory (Queens Medical Center, Univeristy of Nottingham), *i.e.* PLGA/PEG microparticles of 100-200 μm diameter for GBM treatment have demonstrated improvement [144]. Their microparticles were mixed with a solution of trichostatin A (TSA), ETP or methotrexate (MTX) [144]. The paste formulation was developed in order to mould the chemotherapy carrying delivery device to the resection cavity in the brains of sheep cadavers and determine the localised drug release from the PLGA/PEG matrix [134]. Their formulation showed a lack of toxicity from blended PLGA/PEG alone *in vitro* and *in vivo* and demonstrated sustained drug release between 18 and 28 days [144].

Unfortunately, the formulation studies associated with development of polymeric microparticles and localised drug delivery for brain tumour

treatment have not improved much since the development of Glidel® wafers, mainly because of the difficulty in finding a standard polymer to control the drug release over time, which does not cause toxicity and the difficulty in achieving sufficient brain drug penetration by diffusion, to efficaciously target infiltrative GBM cells.

In this thesis a new method is proposed, and a novel paste system that which integrates spherical polymeric microparticles with a size range between 40 and 80 μm varying in their morphology and is shown to encapsulate three different chemotherapeutic agents, which were S.MTX, DTX and ETP. These microparticles were mixed with blended PLGA/PEG matrix and an aqueous solution of DTX in order to create a sustained release paste formulation, which could show a lack of toxicity to neuro oncological cells from the microparticles alone and could impair GBM cell proliferation using the treatment proposed in the *in vitro* work.

The microparticles were encapsulated with active components and mixed with the PLGA/PEG matrix to create a paste system, as described in section 3.2.6.2 in order to assess the *in vitro* release profiles over a 30-day period. The PLA microparticles in general demonstrated a sustained release over time. However, porous PLA particles encapsulated with NB exhibited faster release when compared with the non-porous PLA particles. The similar release profile was found for PLA particles encapsulated with DTX. Furthermore, PLGA microparticles exhibited a sustained release over-30 days period and particle type A' exhibited faster release profile when compared with

medium and highly porous PLGA particles. These results suggest that the morphology of the spherical particles is not a determining factor in altering the drug release profile, and other aspects must be considered such as the hydrophobicity of the drug, the interaction of the drug with the polymeric matrix and diffusion of media through the polymeric matrix. On the other hand, the mixture of PLGA-PEG matrix and PLA/PLGA MPs (paste formulation) confirm the hypotheses investigated in this work, suggesting that the multi-therapy formulation prolonged drug release from the polymeric matrix over time as a relationship between fast release rates from blended PLGA-PEG matrix and slow release from spherical PLA and PLGA particles. The controlled sustained release delivery developed in this work exhibited controlled can prolong the time of localised therapeutic treatment against GBM cells.

The polymeric MPs, free drug, and paste developed in this study were tested *in vitro,* as described in section 3.2.3.2. Polymeric MPs tested under various concentrations exhibited a lack of toxicity towards U87 cells, while the free drugs (*i.e.* DTX, S.MTX and ETP) resulted in cell viability above 70% over 24 h of treatment. These findings corroborate reports in the available literature, where the polymeric MPs alone exhibit lack of toxicity [134, 175], and suggests that the DTX is the most effective drug between those compared. Nevertheless, some treatments using S.MTX and ETP combined with DTX were developed in this thesis in order to prove the therapeutic efficiency of the treatments against GBM cells.

Paste therapies were tested over a 30-day period and resulted in cell viability above 70% for the control therapy containing only DTX (therapy 1), whilst therapy 3 resulted in cell viability above 55%, indicating that the multi-drug therapy encapsulated in polymeric spherical microparticles and PLGA/PEG matrix can prolong treatment over a 30-days period against GBM cell proliferation and growth and that S.MTX is suitable for GBM cells. Even though methotrexate possesses challenges, such as poor availability and dose dependent effects, the encapsulation in particles can overcome some of these current issues [216].

Drug selectivity against tumour cells, side effects, dose response and chemo resistance of cancer cells due to long and constant periods of treatment are major challenges in GBM treatment. Furthermore, the location of the tumour in the brain cortex, which does not allow a complete resection of all tumour cells due to the possible adverse neurological deficits (*i.e.* motor, sensory and cognitive) and loss of functional areas of the brain, is a persistent challenge [161]. The new formulations developed herein have been designed to overcome some of the issues highlighted above.

Tablet formulations were developed with two types of spherical particle morphologies; which were non-porous and porous -PLA and -PLGA particles, downselected from the formulations developed in Chapter 2. The tablet formulation in buffered solution exhibited a slight changed on day 7 of the *in vitro* study where the PLGA/PEG matrix started to create a thin film on the tablet surface. The tablets

were covered by a significantly thicker film by the end of the 30-day study. This result suggests that the presence of poly(ethylene glycol) (PEG) in the formulation should improve the co-polymer degradation due to the high solubility of PEG in hydrophilic solutions [372].

Microparticles loaded with NB exhibited sustained release over time, however medium porous PLA particles (particle type B) exhibited a significant cumulative release after 15 days, whilst medium porous PLGA particles (particle type B') exhibited a relatively low release percentage, the same was observed for non-porous PLA and PLGA particles (particle types A and A', respectively) during the study. The particles encapsulated with S.MTX demonstrated sustained release across all formulations studied here; however non-porous PLGA particles (particle type A') exhibited relatively higher percentage of cumulative release over the 30-day period in comparinson to the formulation groups B' and C'. Moreover, PLGA/PEG matrix mixed with DTX solution exhibited an initial burst release. The results demonstrate that the tablet formulation based on PLA/PLGA MPs in PLGA-PEG matrix, developed in this work, prolongs the period of drug release for GBM therapy when compared with PLGA/PEG matrix alone. These findings validate the hypothesis established in this study; a mixture of polymeric spherical particles within a PLGA/PEG matrix could prolong the cumulative release of chemotherapeutic drugs, and against the background of the literature literature, in which the presence of PEG in the formulation can cause rapid drug diffusion found in the PLGA-PEG matrices [134, 338].

Novel, specific and more effective therapy systems must be developed to reach the goal of eradicating GBM, as previously discussed. The work in this thesis demonstrates that the polymeric microparticles developed can promote the sustained release of chemotherapeutic drugs and gives new perspective and a pathway toward improved local delivery treatments for GBM. A novel therapeutic approach has been developed herein, using polymeric spherical microparticles encapsulated with S.MTX mixed with 50 mg of PLGA/PEG matrix with DTX in order to overcome the initial burst release from the PLGA/PEG matrix, and prolong GBM treatment *in vitro* with a sustained, controlled release system using a suitable drug to impair the proliferation of GBM cells.

The polymeric MPs alone did not demonstrate a toxic response when tested with U87 cells, as discussed in section 3.2.3.2, however some treatments established in this work, such as therapies 4 and 5, decreased cell viability over time. The multi-therapy agent tablets (therapies 4 and 5) developed in this work appear promising as successful chemotherapy agents for *in vivo* and *ex vivo* study, in which the drug could remain in the brain cavity, avoiding dislodgement (*i.e.* of paste and tablets) in the first hours post-surgery, following established local delivery systems for GBM cells [175, 190, 244].

3.5 Conclusion

Porous polymeric MPs with varying morphologies using PLA and PLGA have been developed. PLA and PLGA are attractive for use as

therapeutic delivery vehicles they are both FDA approved polymers, used worldwide in biomedical applications, with established biocompatibility and degradability. The MPs developed here were loaded with NB (dye), as well therapeutic drugs such as S.MTX, ETP and DTX, which are currently used for various cancer types. These three cytotoxic drugs are under *in vitro* and *in vivo* investigation as potential therapies for GBM [346 – 348].

Polymeric microparticles were encapsulated with NB in order to develop a proof-of-concept study for an encapsulation system with a dye concentration of 50 μg/mL. The PLA and PLGA spherical MPs exhibited limited encapsulation efficiency suggesting that the nature of polymer (*i.e.* hydrophobic or hydrophilic), the interaction of the dye with the polymer and nature of the dye can influence the amount of the dye encapsulated. Furthermore, any toxic drug encapsulated in the PLA and PLGA MPs would show similar encapsulation efficiency profiles if they presented an approximate logP value to NB.

Particles encapsulated with the cytotoxic drugs exhibited a suitable sustained and controlled drug delivery; where the PLA MPs had a slower cumulative release in general when compared to PLGA MPs. These findings correlate well with literature, where PLGA can promote a higher cumulative release as well as improved encapsulation efficiency (for some drugs) due the more hydrophilic nature of the PLGA caused by the presence of glycolide in the chemical chain.

The particles developed in section 3.2.1 were used to achieve a multi-therapy system for local drug delivery against GBM. The multi-therapy

system included either spherical PLA MP or PLGA MPs, both of varying morphology, encapsulated with chemotherapeutic drugs. Further, these were mixed with a thermo-responsive polymeric matrix with DTX (*i.e.* PLGA/PEG matrix). Initial studies included a release study of dye over 30-days as a proof-of-concept towards particles encapsulated with the chemotherapeutic drugs. Particles alone, free drug, and formulation-based therapies developed in this thesis were tested *in vitro* on U87 cells. Polymeric MPs demonstrated a lack of toxicity, whilst DTX resulted in cell viability of below 70%. The study demonstrated a sustained and controlled release of the dye and chemotherapeutic drugs, suggesting that the particles alone do not cause cell toxicity and that DTX is a candidate drug for GBM therapy. Furthermore, the paste system can potentially delay the onset of tumour recurrence formation by efficacious targeting of residual infiltrative GBM cells.

The paste developed in this thesis represents an importamt contribution towards the development of formulations for improved control of GBM cell proliferation; a search of the literature reveals little evidence of improvement since the development of Gliadel® wafers, the established post-surgical therapy. A novel therapeutic approach was developed using polymeric spherical microparticles encapsulated with S.MTX mixed within a thermoresponsive PLGA/PEG matrix in order to overcome the initial burst release from the PLGA/PEG matrix alone, and to prolong GBM treatment *in vitro* with a sustained controlled release system, using a suitable drug to impair the

proliferation of GBM cells. The tablet formulations encapsulated with S.MTX exhibited a sustained release whilst the PLGA/PEG matrix mixed with DTX exhibited an initial burst release over 80%. These findings corroborate with the literature, indicating that this system can be used for sustained and controlled release of chemotherapeutic agents against GBM. The multi-therapy technology (*i.e.* tablet formulation made with PLA spherical particles encapsulated with S.MTX and mixed with PLGA/PEG matrix and DTX solution developed here) was also tested *in vitro* with U87 cells and demonstrated a controlled reduction of cell viability over time (therapies 4 and 5). These findings in this chapter suggest that the multi-therapy technology developed herein improved the otherwise poor solubility of S.MTX in an aqueous environment and warrant further *in vivo* testing as chemotherapy toward the prevention, or at least delay of tumour the development and recurence.

CHAPTER 4. Final Conclusions and Future Prospects

4.1 Technologies to develop spherical microparticles and the biological application

Biomaterials have gained considerable attention over the last few years with wide application such as tissue engineering, drug delivery devices and gene delivery. A variety of polyesters (*e.g.* PLA, PLGA, PCL) and PEG have been used to develop biomedical devices and biomaterials with suitable biocompatibility, low toxicity and appropriate mechanical properties. Polymeric materials as drug delivery systems are expanded here in this thesis as micro- and nano-particles, with controlled pore structure and different morphologies, produced by different processing methods as described in Chapter 2. Emulsion processing is most commonly used to produce micro- and nano-particles due the rapid formation of particles with some control over shape and size (*e.g.* physical properties).

It is well known that the size and level of porosity of microparticles can be controlled by the processing method and porogen used during particle production. Reports in the literature demonstrated that by altering particles morphology, porosity, and the interconnectivity between pores, can modify the drug release profiles, and augment drug release due to enhanced diffusion of media throughout the porous structure and influence the degradation of the polymeric matrix.

Polymeric based systems (*i.e.* microparticles) are useful for the design, of novel biomedical devices, to encapsulate different drugs of varying hydrophobicity. Microparticles can modulate drug release over time, and in some cases be loaded with cells and other biological moieties,

which can provide an appropriate niche for cells proliferation and differentiation.

4.2 Local drug delivery systems and GBM treatment

Glioblastoma is a well known aggressive primary brain cancer of central nervous system (CNS) and trypifies in a median survival of less than 2 years after initial diagnosis. Current treatment adopted for GBM involves surgical resection in a effort to remove the cancerous cells and necrosis area, followed by chemotherapy strategies and radiotherapy, all of which are focused on prolonging patients survival and their quality of life. The treatment strategies adopted in the clinic vary from patient to patient according to their clinical settings condition and age.

Current clinically available treatments have high levels of failure due to several factors, such as the blood-brain-barrier (BBB) and brain-tumor-barrier (BTB), the high systemic dosage to access the therapeutic window at the site, causing high toxicity and side effects, the size and location of the tumor, rapid drug clearance and non-specificity of the chemotherapeutic drugs.

The research community have developed different strategies to improve drug delivery systems for GBM treatment in order to reduce side effects and maintain the drug in the brain cavity for longer time periods. Polymeric microparticles have become a standard carrier for cancer treatment and are one of the choices for the development of local drug delivery devices for GBM treatment. Despite the efforts of the research community, patient survival has not improved much and

GBM remains incurable. However, new treatment strategies are under pre-clinical investigation and some researchers have developed sustained release systems that have been explored *in vitro*, with different types of chemotherapeutic drugs over 3-4 weeks, exhibiting prolonged drug release intra cavity when compared with Gliadel® wafers [144].

There is a critical need to develop improved local drug delivery systems is a critical need for GBM treatment to overcome the limitations of systemic delivery (*i.e.* high toxicity and side effects). New strategies must be adopted to avoid cell resistence and recurrence, non-specificity of the chemotherapeutic drugs, dislodgement of polymeric devices, and to improve drug penetration through the brain.

4.3 Development of PLA and PLGA microparticles of varying morphologies and porosities

Polymeric microparticles (PMPs) with controllable size and shape can be produced by judicious choice of processing method, as described previously. The type of polymer, molecular weight, co-polymer composition and nature of any excipients added to the particles also influence particle size and shape.

Development of drug delivery particles has attracted significant attention from pharmaceutical industry over the last decade. Some of the methods used to produce these particles include single emulsion and double emulsion techniques, as previously, encapsulation also

depends on the hydrophobicity and hydrophilicity of the active component, as well as the types of polymer type.

Polymeric microparticles are the gold standard material for drug delivery devices, which can encapsulate different types of agents such as drugs of various hydrophilicity, and have used for various biomedical applications. It is well known that the physical features of the particles is a limiting aspect for their biomedical application, and it is crucial to investigate the physical and chemical properties of the polymeric microparticles applied *in vitro* and *in vivo*.

Chapter 2 detailed the successful development of new PLA and PLGA microparticles of controlled and varying morphology (*i.e.* size and porosity) achieved *via* single emulsion process was presented. The particles produced were fully characterised in terms of their size, porosity, pore size distribution, density, surface area, and their *in vitro* degradation in physiological conditions. Particle morphology (size and pore structure) could be tailored by adjusting the formulations and processing methods established in this work, including the use of a porogen mixed into the organic solvent. Polymeric microparticles exhibited showed the same level of porosity between their external and internal regions, and the particles sized varied up to 320 μm in diameter for PLA microparticles, and between 20 and 80 μm in diameter for PLGA microparticles. The level of porosity of the polymeric microparticles was confirmed by image analysis of Cryo-SEM images. The particles exhibited homogeneous porosity with pores size up to 7.6 μm. The difference between the level of porosity and

interconnectivity of pores was further evidenced using the BET surface area analysis technique. Non-porous particles exhibited lower gas adsorption suggesting that the gas adsorption was restricted to monolayer adsorption, which may be due to absence of pores and low adsorbate molecular diameter. The behaviour of microparticles varying in their morphology was assessed in buffered solution. Porous PLA particles exhibited change in their morphology 7 and 15 days, whilst porous PLGA particles exhibited morphological change within in the first hours of the study (3 h and 24 h). The degradation of PLA and PLGA particles is predominantly *via* simple hydrolysis process, and influenced by polymer composition, and rate of diffusion of media throughout the particles structure.

This work provided evidence for the development of polymeric particles with controlled shape and size. A family of non-porous and porous spheres was investigated using two degradable polymers (PLA and PLGA) these were taken forward for investigation as drug delivery vehicles towards multi-therapy delivery systems against GBM.

4.4 Multi-therapy system and the efficacy of the local treatment

It is well known from the literature that biomaterials devices made with polymeric microparticles have the ability to prolong the half-life of drugs to achieve controlled sustained drug release, increase the stability of drugs in the biological environment, overcome the poor solubility of hydrophobic drugs, and improve the transport of drugs through biological barriers such as the BBB and BTB. Many devices with appropriate biocompatibility and low toxicity have been

developed to treat different types of tumours, including GBM. Gliadel® wafers are one of these examples discussed in this work.

Current treatments against GBM include the systemic delivery of chemotherapeutic drugs in high dosages in order to maintain the therapeutic dosage through the BBB, as described in section 3.1. It has been proven that systemic delivery is ineffective for brain tumours because the concentration of chemotherapeutic drug drops with increasing distance from the tumour site and the drugs are nonspecific to GBM cells.

Targeted drug delivery to specific areas of the CNS is a recurrent challenge in the development of effective GBM treatment as a result of the high proliferative rate and invasive nature of cancer cells that are often inaccessible (to surgery), and the difficulties associated with distinguishing normal and cancer cells. However, there is a critical demand to improve the efficacy of treatment and survival of the patients with GBM.

Chapter 3, detailed the development of polymeric microparticles with varying morphology that could be loaded with a model dye and active components (*e.g.* model dye and chemotherapeutic drugs) *via* the single emulsion processing route (developed in Chapter 2). Particles loaded with these components were developed and fully characterised in terms of their size and pore structure, and their dye and drug loading quantified (using UV-vis and HPLC), *in vitro* release studies were conducted, particle degradation under biological conditions assessed and an *in vitro* cell study undertaken to assess particle toxicity and the

efficacy of treatment against U87 cell. PLA and PLGA particles loaded with NB exhibited a size range between 30 and 85 μm in diameter, whilst microparticles loaded with S.MTX, ETP and DTX exhibited a broad size range between 10 to 90 μm in comparinson to dye loaded particles. PLA particles encapsulated with dye had reduced incorporation of active component in comparinson to PLGA particles. PLA and PLGA particles of varying morphology were also encapsulated with S.MTX, ETP and DTX; few particles exhibited an acceptable encapsulation efficiency as demonstrated in section 3.2.1.2. Selected particles were subsequently tested *in vitro* in a release study to investigate the relationship between the level of particle porosity and the drug release profile. The study demonstrated minimal difference between the non-porous and porous particles release profiles, aside from PLA particles encapsulated with S.MTX, and PLGA particles encapsulated with DTX.

Polymeric microparticles varying in their morphology were mixed into a thermoresponsive PLGA-PEG matrix in order to develop a local multi-therapy system in the form of a polymeric paste as well as an alternative tablet form. The results demonstrated that the paste and tablet formulations prolonged drug release from the polymeric matrix over time as a consequence of the balance between the burst drug release from the PLGA-PEG matrix and the slow release from the PLA and PLGA microparticles. Control microparticles alone were not toxic to GBM cells. The therapies developed and evaluated here show

potential as local multi-therapy agents against GBM, to prevent or delay the development of tumour resistance.

4.5 Future perspectives

The last few years have witnessed an extraordinary expansion in drug delivery research for cancer therapy, in particular expressly when conventional chemotherapeutic agents fail to show clinical relevance in the treatment of tumours, due to their high toxicity and/or chemoresistance. Research focused on local delivery strategies using multi-therapy agents seem promissing against GBM, as investigated in this thesis. The effect of local delivery system developed here should be taken forward for further *in vivo* and *ex vivo* investigation pending ethical approval (*e.g.* in sheep brain models) to show their effectiveness as local delivery system in this more pertinent setting. The drug release and particle behaviour should be further evaluated under other physiological conditions such as acidic environment to mimic the pH of cancer cells (≈5.8-7.0). Further research should assess the mechanical properties and the dissolution profile of the polymeric tablets under normal and acidic pH. The hope is that further studies can identify the ideal conditions and create an efficient local multi-therapy system against GBM, which will ultimately improve the drug delivery across the BBB/BTB and prolong patients survival.

REFERENCES

1. Sarce Thomann, F., *Hygrothermal modelling as a top-down design tool for mesoporous desiccants*. 2016, University of Nottingham.
2. Hall, C. and W.D. Hoff, *Water transport in brick, stone and concrete*. 2011: CRC Press.
3. Rescignano, N., et al., *Use of alginate, chitosan and cellulose nanocrystals as emulsion stabilizers in the synthesis of biodegradable polymeric nanoparticles.* Journal of colloid and interface science, 2015. **445**: p. 31-39.
4. Li, X., et al., *Nanoparticles by spray drying using innovative new technology: The Büchi Nano Spray Dryer B-90.* Journal of Controlled Release, 2010. **147**(2): p. 304-310.
5. Hossain, K.M.Z., U. Patel, and I. Ahmed, *Development of microspheres for biomedical applications: a review.* Progress in Biomaterials. **4**(1): p. 1-19.
6. Fan, J.-B., et al., *Nanoporous microspheres: from controllable synthesis to healthcare applications.* Journal of Materials Chemistry B, 2013. **1**(17): p. 2222-2235.
7. Shen, J., et al., *In vitro-in vivo correlation of parenteral risperidone polymeric microspheres.* Journal of Controlled Release, 2015. **218**: p. 2-12.
8. Rocha-García, D., et al., *Gelatin-based porous silicon hydrogel composites for the controlled release of tramadol.* European Polymer Journal, 2018. **108**: p. 485-497.
9. Chvatal, A., et al., *Formulation and comparison of spray dried non-porous and large porous particles containing meloxicam for pulmonary drug delivery.* International journal of pharmaceutics, 2019. **559**: p. 68-75.
10. Weiser, J.R. and W.M. Saltzman, *Controlled release for local delivery of drugs: barriers and models.* Journal of Controlled Release, 2014. **190**: p. 664-673.
11. Kumari, A., S.K. Yadav, and S.C. Yadav, *Biodegradable polymeric nanoparticles based drug delivery systems.* Colloids and Surfaces B: Biointerfaces, 2010. **75**(1): p. 1-18.
12. Pandey, S.K., et al., *Anti-cancer evaluation of quercetin embedded PLA nanoparticles synthesized by emulsified nanoprecipitation.* International journal of biological macromolecules, 2015. **75**: p. 521-529.
13. Parveen, S., R. Misra, and S.K. Sahoo, *Nanoparticles: a boon to drug delivery, therapeutics, diagnostics and imaging.* Nanomedicine: Nanotechnology, Biology and Medicine, 2012. **8**(2): p. 147-166.
14. Beck-Broichsitter, M., O.M. Merkel, and T. Kissel, *Controlled pulmonary drug and gene delivery using polymeric nano-carriers.* Journal of controlled release, 2012. **161**(2): p. 214-224.
15. Rosalia, R.A., et al., *CD40-targeted dendritic cell delivery of PLGA-nanoparticle vaccines induce potent anti-tumor responses.* Biomaterials, 2015. **40**: p. 88-97.
16. Huh, A.J. and Y.J. Kwon, *"Nanoantibiotics": a new paradigm for treating infectious diseases using nanomaterials in the antibiotics resistant era.* Journal of Controlled Release, 2011. **156**(2): p. 128-145.
17. Sahiner, N., S.S. Suner, and R.S. Ayyala, *Mesoporous, degradable hyaluronic acid microparticles for sustainable drug delivery application.* Colloids and Surfaces B: Biointerfaces, 2019. **177**: p. 284-293.
18. Asikainen, S., et al., *Hydrolysis and drug release from poly (ethylene glycol)-modified lactone polymers with open porosity.* European Polymer Journal, 2019. **113**: p. 165-175.

19. Prabhakaran, M.P., et al., *Electrospraying technique for the fabrication of metronidazole contained PLGA particles and their release profile.* Materials Science and Engineering: C, 2015. **56**: p. 66-73.
20. Anselmo, A.C., et al., *Elasticity of nanoparticles influences their blood circulation, phagocytosis, endocytosis, and targeting.* ACS nano, 2015. **9**(3): p. 3169-3177.
21. Shapira-Furman, T., et al., *Biodegradable wafers releasing Temozolomide and Carmustine for the treatment of brain cancer.* J Control Release, 2019. **295**: p. 93-101.
22. Beyatricks, K., *Recent trends in microsphere drug delivery system and its therapeutic applications–A review.* Critical review in pharmaceutical sciences, 2013. **2**(1): p. 1-14.
23. Beck-Broichsitter, M., et al., *Modified vibrating-mesh nozzles for advanced spray-drying applications.* European Journal of Pharmaceutics and Biopharmaceutics, 2015. **92**: p. 96-101.
24. Andrade, F., et al., *Nanotechnology and pulmonary delivery to overcome resistance in infectious diseases.* Advanced drug delivery reviews, 2013. **65**(13): p. 1816-1827.
25. Bertrand, N. and J.-C. Leroux, *The journey of a drug-carrier in the body: an anatomo-physiological perspective.* Journal of Controlled Release, 2012. **161**(2): p. 152-163.
26. Rezwan, K., et al., *Biodegradable and bioactive porous polymer/inorganic composite scaffolds for bone tissue engineering.* Biomaterials, 2006. **27**(18): p. 3413-3431.
27. Acosta, N., et al., *Physical Stability studies of semi-solid formulations from natural compounds loaded with chitosan microspheres.* Marine drugs, 2015. **13**(9): p. 5901-5919.
28. Lim, H.-P., B.-T. Tey, and E.-S. Chan, *Particle designs for the stabilization and controlled-delivery of protein drugs by biopolymers: A case study on insulin.* Journal of Controlled Release, 2014. **186**: p. 11-21.
29. Mukhopadhyay, P., et al., *pH-sensitive chitosan/alginate core-shell nanoparticles for efficient and safe oral insulin delivery.* International journal of biological macromolecules, 2015. **72**: p. 640-648.
30. Sinha, V., et al., *Poly-ε-caprolactone microspheres and nanospheres: an overview.* International journal of pharmaceutics, 2004. **278**(1): p. 1-23.
31. Goulart, C.O., et al., *Evaluation of biodegradable polymer conduits–poly (l-lactic acid)–for guiding sciatic nerve regeneration in mice.* Methods, 2015.
32. Vert, M., *After soft tissues, bone, drug delivery and packaging, PLA aims at blood.* European Polymer Journal, 2015. **68**: p. 516-525.
33. Elsawy, M.A., et al., *Hydrolytic degradation of polylactic acid (PLA) and its composites.* Renewable and Sustainable Energy Reviews, 2017. **79**: p. 1346-1352.
34. Zhou, W., et al., *Controlled release of clodronate from PLA/PCL complex microsphere.* Materials Letters, 2015. **152**: p. 293-297.
35. Gurler, E.B., et al., *Encapsulated melatonin in polycaprolactone (PCL) microparticles as a promising graft material.* Materials Science and Engineering: C, 2019.
36. Armentano, I., et al., *Biodegradable polymer matrix nanocomposites for tissue engineering: a review.* Polymer degradation and stability, 2010. **95**(11): p. 2126-2146.
37. Luciani, A., et al., *PCL microspheres based functional scaffolds by bottom-up approach with predefined microstructural properties and release profiles.* Biomaterials, 2008. **29**(36): p. 4800-4807.
38. Dhanaraju, M.D., et al., *Preparation and characterization of injectable microspheres of contraceptive hormones.* International journal of pharmaceutics, 2003. **268**(1): p. 23-29.

39. Beck-Broichsitter, M., J. Nicolas, and P. Couvreur, *Design attributes of long-circulating polymeric drug delivery vehicles.* European Journal of Pharmaceutics and Biopharmaceutics, 2015. **97**: p. 304-317.
40. Andreani, T., et al., *Preparation and characterization of PEG-coated silica nanoparticles for oral insulin delivery.* International journal of pharmaceutics, 2014. **473**(1): p. 627-635.
41. Wu, J., et al., *Binding characteristics between polyethylene glycol (PEG) and proteins in aqueous solution.* Journal of Materials Chemistry B, 2014. **2**(20): p. 2983-2992.
42. Kim, K.K. and D.W. Pack, *Microspheres for drug delivery*, in *BioMEMS and Biomedical Nanotechnology*. 2006, Springer. p. 19-50.
43. Fleming, R., *The Spray Process of Drying.* Industrial & Engineering Chemistry, 1921. **13**(5): p. 447-449.
44. Maged, A., A.A. Mahmoud, and M.M. Ghorab, *Nano spray drying technique as a novel approach to formulate stable econazole nitrate nanosuspension formulations for ocular use.* Molecular pharmaceutics, 2016. **13**(9): p. 2951-2965.
45. Li, Y., et al., *Properties of chitosan-microencapsulated orange oil prepared by spray-drying and its stability to detergents.* Journal of agricultural and food chemistry, 2013. **61**(13): p. 3311-3319.
46. Shi, A.-m., et al., *Rheological properties of suspensions containing cross-linked starch nanoparticles prepared by spray and vacuum freeze drying methods.* Carbohydrate polymers, 2012. **90**(4): p. 1732-1738.
47. Parikh, D.M., *Handbook of pharmaceutical granulation technology*. 2009: CRC Press.
48. Liu, W., X. Chen, and C. Selomulya, *On the spray drying of uniform functional microparticles.* Particuology, 2015. **22**: p. 1-12.
49. Li, D., et al., *Electrospinning: a simple and versatile technique for producing ceramic nanofibers and nanotubes.* Journal of the American Ceramic Society, 2006. **89**(6): p. 1861-1869.
50. Keshani, S., et al., *Spray drying: an overview on wall deposition, process and modeling.* Journal of Food Engineering, 2015. **146**: p. 152-162.
51. Kadota, K., et al., *Preparation of composite particles of hydrophilic or hydrophobic drugs with highly branched cyclic dextrin via spray drying for dry powder inhalers.* Powder Technology, 2015.
52. Sosnik, A. and K.P. Seremeta, *Advantages and challenges of the spray-drying technology for the production of pure drug particles and drug-loaded polymeric carriers.* Advances in Colloid and Interface Science, 2015.
53. Carr, R.L., *Classifying flow properties of solids.* 1965.
54. Chawla, A., et al., *Production of spray dried salbutamol sulphate for use in dry powder aerosol formulation.* International Journal of Pharmaceutics, 1994. **108**(3): p. 233-240.
55. Braig, V., et al., *Can spray freeze-drying improve the re-dispersion of crystalline nanoparticles of pure naproxen?* International journal of pharmaceutics, 2019. **564**: p. 293-298.
56. Pham, D.-D., E. Fattal, and N. Tsapis, *Pulmonary drug delivery systems for tuberculosis treatment.* International journal of pharmaceutics, 2015. **478**(2): p. 517-529.
57. Kunda, N.K., et al., *Dry powder pulmonary delivery of cationic PGA-co-PDL nanoparticles with surface adsorbed model protein.* International journal of pharmaceutics, 2015. **492**(1): p. 213-222.
58. Silva, A.S., M.T. Tavares, and A. Aguiar-Ricardo, *Sustainable strategies for nano-in-micro particle engineering for pulmonary delivery.* Journal of Nanoparticle Research, 2014. **16**(11): p. 1-17.
59. Lu, W., et al., *Inhalable co-amorphous budesonide-arginine dry powders prepared by spray drying.* International journal of pharmaceutics, 2019.

60. Brinkmann-Trettenes, U., S. Barnert, and A. Bauer-Brandl, *Single step bottom-up process to generate solid phospholipid nano-particles.* Pharmaceutical development and technology, 2014. **19**(3): p. 326-332.
61. Jaworek, A. and A. Sobczyk, *Electrospraying route to nanotechnology: an overview.* Journal of Electrostatics, 2008. **66**(3): p. 197-219.
62. Dimer, F.A., et al., *Inhalable resveratrol microparticles produced by vibrational atomization spray drying for treating pulmonary arterial hypertension.* Journal of Drug Delivery Science and Technology, 2015. **29**: p. 152-158.
63. Baba, K. and K. Nishida, *Steroid nanocrystals prepared using the Nano Spray Dryer B-90.* Pharmaceutics, 2013. **5**(1): p. 107-114.
64. Beber, T., et al., *Submicron polymeric particles prepared by vibrational spray-drying: Semisolid formulation and skin penetration/permeation studies.* European Journal of Pharmaceutics and Biopharmaceutics, 2014. **88**(3): p. 602-613.
65. Baumgarten, P.K., *Electrostatic spinning of acrylic microfibers.* Journal of colloid and interface science, 1971. **36**(1): p. 71-79.
66. Medeiros, E.S., et al., *Solution blow spinning: A new method to produce micro - and nanofibers from polymer solutions.* Journal of applied polymer science, 2009. **113**(4): p. 2322-2330.
67. Murase, S.K., et al., *Electrosprayed poly (butylene succinate) microspheres loaded with indole derivatives: A system with anticancer activity.* European Polymer Journal, 2015. **71**: p. 196-209.
68. Kim, M.K., et al., *Effect of shear viscosity on the preparation of sphere-like silk fibroin microparticles by electrospraying.* International journal of biological macromolecules, 2015. **79**: p. 988-995.
69. Zhang, F., et al., *Mechanisms and control of silk-based electrospinning.* Biomacromolecules, 2012. **13**(3): p. 798-804.
70. Almería, B., et al., *Controlling the morphology of electrospray-generated PLGA microparticles for drug delivery.* Journal of colloid and interface science, 2010. **343**(1): p. 125-133.
71. Baldino, L., S. Cardea, and E. Reverchon, *Supercritical Assisted Electrospray: An Improved Micronization Process.* Polymers, 2019. **11**(2).
72. Tapia-Hernández, J.A., et al., *Micro-and Nanoparticles by Electrospray: Advances and Applications in Foods.* Journal of agricultural and food chemistry, 2015. **63**(19): p. 4699-4707.
73. Ki, C.S., et al., *Development of 3-D nanofibrous fibroin scaffold with high porosity by electrospinning: implications for bone regeneration.* Biotechnology letters, 2008. **30**(3): p. 405-410.
74. Park, S.Y., et al., *Electrospun silk fibroin scaffolds with macropores for bone regeneration: an in vitro and in vivo study.* Tissue Engineering Part A, 2010. **16**(4): p. 1271-1279.
75. Kawakami, M., et al., *Chondrocyte distribution and cartilage regeneration in silk fibroin sponge.* Bio-medical materials and engineering, 2011. **21**(1): p. 53-61.
76. Wang, Y., et al., *Stem cell-based tissue engineering with silk biomaterials.* Biomaterials, 2006. **27**(36): p. 6064-6082.
77. Quinlan, E., et al., *Controlled release of vascular endothelial growth factor from spray - dried alginate microparticles in collagen–hydroxyapatite scaffolds for promoting vascularization and bone repair.* Journal of tissue engineering and regenerative medicine, 2017. **11**(4): p. 1097-1109.
78. Rad, R.T., et al., *Tadalafil nanocomposites as a dry powder formulation for inhalation, a new strategy for pulmonary arterial hypertension treatment.* European Journal of Pharmaceutical Sciences, 2019.
79. Lee, Y.-H., M.-Y. Bai, and D.-R. Chen, *Multidrug encapsulation by coaxial tri-capillary electrospray.* Colloids and Surfaces B: Biointerfaces, 2011. **82**(1): p. 104-110.

80. Gao, J., et al., *Facile preparation of hierarchically porous polymer microspheres for superhydrophobic coating.* Nanoscale, 2014. **6**(2): p. 1056-1063.
81. Malik, S.A., et al., *Electrospray Synthesis and Properties of Hierarchically Structured PLGA TIPS Microspheres for use as Controlled Release Technologies.* Journal of Colloid and Interface Science, 2016.
82. Bognitzki, M., et al., *Nanostructured fibers via electrospinning.* Advanced Materials, 2001. **13**(1): p. 70-72.
83. McCann, J.T., M. Marquez, and Y. Xia, *Highly porous fibers by electrospinning into a cryogenic liquid.* Journal of the American Chemical Society, 2006. **128**(5): p. 1436-1437.
84. Medeiros, E.S., et al., *Effect of relative humidity on the morphology of electrospun polymer fibers.* Canadian Journal of Chemistry, 2008. **86**(6): p. 590-599.
85. Behrens, A.M., et al., *In situ deposition of PLGA nanofibers via solution blow spinning.* ACS Macro Letters, 2014. **3**(3): p. 249-254.
86. Van de Witte, P., et al., *Phase separation processes in polymer solutions in relation to membrane formation.* Journal of Membrane Science, 1996. **117**(1): p. 1-31.
87. Barton, B., P. Graham, and A. McHugh, *Dynamics of spinodal decomposition in polymer solutions near a glass transition.* Macromolecules, 1998. **31**(5): p. 1672-1679.
88. Witt, J.A., D.R. Mumm, and A. Mohraz, *Bijel reinforcement by droplet bridging: a route to bicontinuous materials with large domains.* Soft Matter, 2013. **9**(29): p. 6773-6780.
89. Chen, J., S.R. Kline, and Y. Liu, *From the depletion attraction to the bridging attraction: The effect of solvent molecules on the effective colloidal interactions.* The Journal of chemical physics, 2015. **142**(8): p. 084904.
90. Rajendran, M. and A. Bhattacharya, *Production of rare-earth orthoferrite ceramic fibres by aqueous sol-gel blow spinning process.* Journal of the European Ceramic Society, 2004. **24**(1): p. 111-117.
91. Medeiros, E.L.G., et al., *Porous Bioactive Nanofibers via Cryogenic Solution Blow Spinning and Their Formation into 3D Macroporous Scaffolds.* ACS Biomaterials Science & Engineering, 2016. **2**(9): p. 1442-1449.
92. Alvarez, G. S., et. al., *Antibiotic-loaded silica nanoparticle-collagen composite hydrogels with prolonged antimicrobial activity for wound infection prevention.*J. Mater. Chem. B, 2014. **2**: p. 4660-4670.
93. Marefati, A., et al., *Fabrication of encapsulated oil powders from starch granule stabilized W/O/W Pickering emulsions by freeze-drying.* Food Hydrocolloids, 2015. **51**: p. 261-271.
94. Tadros, T.F., *Encyclopedia of Colloid and Interface Science*. 2013: Springer.
95. Binks, B.P., J. Dong, and N. Rebolj, *Equilibrium phase behaviour and emulsion stability in silicone oil+ water+ AOT mixtures.* Physical Chemistry Chemical Physics, 1999. **1**(9): p. 2335-2344.
96. Kabalnov, A. and J. Weers, *Macroemulsion stability within the Winsor III region: theory versus experiment.* Langmuir, 1996. **12**(8): p. 1931-1935.
97. Julio, L.M., et al., *Chia seed oil-in-water emulsions as potential delivery systems of ω-3 fatty acids.* Journal of Food Engineering, 2015. **162**: p. 48-55.
98. Etienne, G., et al., *Cross-talk between emulsion drops: how are hydrophilic reagents transported across oil phases?* Lab on a Chip, 2018. **18**(24): p. 3903-3912.
99. Tadros, T., et al., *Formation and stability of nano-emulsions.* Advances in colloid and interface science, 2004. **108**: p. 303-318.
100. Rao, J.P. and K.E. Geckeler, *Polymer nanoparticles: preparation techniques and size-control parameters.* Progress in Polymer Science, 2011. **36**(7): p. 887-913.

101. Kumbar, S., A. Kulkarni, and T. Aminabhavi, *Crosslinked chitosan microspheres for encapsulation of diclofenac sodium: effect of crosslinking agent.* Journal of microencapsulation, 2002. **19**(2): p. 173-180.
102. Agnihotri, S.A., N.N. Mallikarjuna, and T.M. Aminabhavi, *Recent advances on chitosan-based micro-and nanoparticles in drug delivery.* Journal of controlled release, 2004. **100**(1): p. 5-28.
103. Simmons, E., et al., *A comparison of the microparticles produced when two disposable-bag oxygenators and a disc oxygenator are used for cardiopulmonary bypass.* J Thorac Cardiovasc Surg, 1972. **63**(4): p. 613-21.
104. Lee, B.K., et al., *Fabrication of drug-loaded polymer microparticles with arbitrary geometries using a piezoelectric inkjet printing system.* Int J Pharm, 2012. **427**(2): p. 305-10.
105. Marco Salviato, M.Z., Marino Quaresimin *Nanoparticle debonding strength: A comprehensive study on interfacial effects* International Journal of Solids and Structures 2013. **50**: p. 3225-3232.
106. Macosko, C.W., *Rheology Principles, Measurements, and Applications* 1994: Wiley-VCH.
107. Ajayan, P.M., Schadler, L. S., & Braun, P. V, *Nanocomposite science and technology*. 2006: John Wiley & Sons.
108. Myerson, J.W., et al., *Non-affinity factors modulating vascular targeting of nano- and microcarriers.* Adv Drug Deliv Rev, 2016. **99**(Pt A): p. 97-112.
109. Tscheka, C., et al., *Macrophage uptake of cylindrical microparticles investigated with correlative microscopy.* Eur J Pharm Biopharm, 2015. **95**(Pt A): p. 151-5.
110. Hu, X., et al., *Nanoporous CD-MOF particles with uniform and inhalable size for pulmonary delivery of budesonide.* Int J Pharm, 2019. **564**: p. 153-161.
111. Zhou, Q.T., et al., *Inhaled formulations and pulmonary drug delivery systems for respiratory infections.* Adv Drug Deliv Rev, 2015. **85**: p. 83-99.
112. Frey, F., F. Ziebert, and U.S. Schwarz, *Stochastic Dynamics of Nanoparticle and Virus Uptake.* Phys Rev Lett, 2019. **122**(8): p. 088102.
113. Anselmo, A.C., et al., *Elasticity of nanoparticles influences their blood circulation, phagocytosis, endocytosis, and targeting.* ACS Nano, 2015. **9**(3): p. 3169-77.
114. Belyaev, A.V., *Hydrodynamic repulsion of spheroidal microparticles from micro-rough surfaces.* PLoS One, 2017. **12**(8): p. e0183093.
115. Champion, J.A. and S. Mitragotri, *Shape induced inhibition of phagocytosis of polymer particles.* Pharm Res, 2009. **26**(1): p. 244-9.
116. Morga, M., et al., *Spheroidal Microparticle Monolayers Characterized by Streaming Potential Measurements.* Langmuir, 2017. **33**(38): p. 9916-9925.
117. Yamada, M., et al., *Using elongated microparticles to enhance tailorable nanoemulsion delivery in excised human skin and volunteers.* J Control Release, 2018. **288**: p. 264-276.
118. Raphael, A.P., et al., *Elongate microparticles for enhanced drug delivery to ex vivo and in vivo pig skin.* J Control Release, 2013. **172**(1): p. 96-104.
119. Salinas, R.Y., et al., *Photoreceptor discs form through peripherin-dependent suppression of ciliary ectosome release.* J Cell Biol, 2017. **216**(5): p. 1489-1499.
120. Danilevich, V.N., et al., *New insight into formation of DNA-containing microparticles during PCR: the scaffolding role of magnesium pyrophosphate crystals.* J Biomol Struct Dyn, 2016. **34**(3): p. 625-39.
121. Molday, R.S. and A.F.X. Goldberg, *Peripherin diverts ciliary ectosome release to photoreceptor disc morphogenesis.* J Cell Biol, 2017. **216**(5): p. 1227-1229.
122. Steinmetz, N.F., et al., *Virus-templated silica nanoparticles.* Small, 2009. **5**(7): p. 813-6.

123. Hayashi, K., et al., *Cellulose-based molecularly imprinted red-blood-cell-like microparticles for the selective capture of cortisol.* Carbohydr Polym, 2018. **193**: p. 173-178.
124. Tanimoto, S., I. Nishii, and S. Kanaoka, *Biomineralization-inspired fabrication of chitosan/calcium carbonates core-shell type composite microparticles as a drug carrier.* Int J Biol Macromol, 2019. **129**: p. 659-664.
125. Zhou, F.L., et al., *Co-electrospraying of tumour cell mimicking hollow polymeric microspheres for diffusion magnetic resonance imaging.* Mater Sci Eng C Mater Biol Appl, 2019. **101**: p. 217-227.
126. Geng, Y., et al., *Shape effects of filaments versus spherical particles in flow and drug delivery.* Nat Nanotechnol, 2007. **2**(4): p. 249-55.
127. Liu, Y., et al., *The shape of things to come: importance of design in nanotechnology for drug delivery.* Ther Deliv, 2012. **3**(2): p. 181-94.
128. Muro, S., et al., *Control of endothelial targeting and intracellular delivery of therapeutic enzymes by modulating the size and shape of ICAM-1-targeted carriers.* Mol Ther, 2008. **16**(8): p. 1450-8.
129. Macosko, C.W., *Rheology: principles, measurements, and applications*. 1994: Wiley-vch.
130. Braz, A.L. and I. Ahmed, *Manufacturing processes for polymeric micro and nanoparticles and their biomedical applications.* 2017.
131. Lee, B.K., Y. Yun, and K. Park, *PLA micro-and nano-particles.* Advanced drug delivery reviews, 2016. **107**: p. 176-191.
132. Basra, A.S., *Basra, Arrandeep Singh., and University of Nottingham. Theses. Pharmacy. Size-tuneable Biodegradable Polymeric Nanoparticles for Controlled Drug Delivery* in *Pharmacy School*. 2015, University of Nottingham United Kingdom
133. Gayer, C., et al., *Development of a solvent-free polylactide/calcium carbonate composite for selective laser sintering of bone tissue engineering scaffolds.* Mater Sci Eng C Mater Biol Appl, 2019. **101**: p. 660-673.
134. Rahman, C.V., et al., *Adjuvant chemotherapy for brain tumors delivered via a novel intra-cavity moldable polymer matrix.* PLoS One, 2013. **8**(10): p. e77435.
135. Gervelas, C., et al., *Direct lung delivery of a dry powder formulation of DTPA with improved aerosolization properties: effect on lung and systemic decorporation of plutonium.* J Control Release, 2007. **118**(1): p. 78-86.
136. N'Guessan, A., et al., *Dexamethasone palmitate large porous particles: A controlled release formulation for lung delivery of corticosteroids.* Eur J Pharm Sci, 2018. **113**: p. 185-192.
137. Pham, D.D., et al., *Formulation of pyrazinamide-loaded large porous particles for the pulmonary route: avoiding crystal growth using excipients.* Int J Pharm, 2013. **454**(2): p. 668-77.
138. Sinha, V.R. and A. Trehan, *Biodegradable microspheres for protein delivery.* J Control Release, 2003. **90**(3): p. 261-80.
139. Ma, X., et al., *Adsorption of heavy metal ions using hierarchical CaCO3-maltose meso/macroporous hybrid materials: adsorption isotherms and kinetic studies.* J Hazard Mater, 2012. **209-210**: p. 467-77.
140. Kozielski, K.L., et al., *Cancer-selective nanoparticles for combinatorial siRNA delivery to primary human GBM in vitro and in vivo.* Biomaterials, 2019. **209**: p. 79-87.
141. Kim, H., et al., *Highly porous large poly (lactic-co-glycolic acid) microspheres adsorbed with palmityl-acylated exendin-4 as a long-acting inhalation system for treating diabetes.* Biomaterials, 2011. **32**(6): p. 1685-1693.
142. Lee, Y.S., et al., *Development of porous PLGA/PEI 1.8 k biodegradable microspheres for the delivery of mesenchymal stem cells (MSCs).* Journal of Controlled Release, 2015. **205**: p. 128-133.

143. Kim, M.R., Y.T. Lim, and K.Y. Cho, *Biodegradable Microparticles with Surface Dimples as a Bi‐Modal Imaging Contrast Agent.* Macromolecular rapid communications, 2013. **34**(5): p. 406-410.
144. Fernandez-Pineiro, I., et al., *Development and characterisation of chondroitin sulfate- and hyaluronic acid-incorporated sorbitan ester nanoparticles as gene delivery systems.* Eur J Pharm Biopharm, 2018. **125**: p. 85-94.
145. Kim, S.Y., J.-Y. Hwang, and U.S. Shin, *Preparation of nano/macroporous polycaprolactone microspheres for an injectable cell delivery system using room temperature ionic liquid and camphene.* Journal of colloid and interface science, 2016. **465**: p. 18-25.
146. Cheng, S.I. and D.C. Stuckey, *Protein recovery from surfactant precipitation.* Biotechnology progress, 2011. **27**(6): p. 1614-1622.
147. Kuzmov, A. and T. Minko, *Nanotechnology approaches for inhalation treatment of lung diseases.* Journal of Controlled Release, 2015. **219**: p. 500-518.
148. Zhu, B., et al., *Delivery of theophylline as dry powder for inhalation.* asian journal of pharmaceutical sciences, 2015. **10**(6): p. 520-527.
149. Garcia Contreras, L., et al., *Pharmacokinetics of inhaled rifampicin porous particles for tuberculosis treatment: Insight into rifampicin absorption from the lungs of guinea pigs.* Molecular pharmaceutics, 2015. **12**(8): p. 2642-2650.
150. Lee, C., et al., *Treatment of bleomycin-induced pulmonary fibrosis by inhaled tacrolimus-loaded chitosan-coated poly (lactic-co-glycolic acid) nanoparticles.* Biomedicine & Pharmacotherapy, 2016. **78**: p. 226-233.
151. Lee, W.-H., et al., *Inhalation of nanoparticle-based drug for lung cancer treatment: Advantages and challenges.* asian journal of pharmaceutical sciences, 2015. **10**(6): p. 481-489.
152. Kraft, K.S. and K. Somerville, *Diketopiperazine microparticles with defined isomer contents*. 2012, Google Patents.
153. Mann, A.E., *Method and composition for treating hyperglycemia*. 2013, Google Patents.
154. Kim, H., et al., *Albumin-coated porous hollow poly (lactic-co-glycolic acid) microparticles bound with palmityl-acylated exendin-4 as a long-acting inhalation delivery system for the treatment of diabetes.* Pharmaceutical research, 2011. **28**(8): p. 2008-2019.
155. Schoubben, A., et al., *Powder, capsule and device: an imperative ménage à trois for respirable dry powders.* International journal of pharmaceutics, 2015. **494**(1): p. 40-48.
156. Hoppentocht, M., et al., *Technological and practical challenges of dry powder inhalers and formulations.* Advanced drug delivery reviews, 2014. **75**: p. 18-31.
157. Tong, Z., et al., *CFD–DEM investigation of the effect of agglomerate–agglomerate collision on dry powder aerosolisation.* Journal of Aerosol Science, 2016. **92**: p. 109-121.
158. Sai, M., et al., *Research on the preparation and characterization of chitosan grafted polyvinylpyrrolidone gel membrane with iodine.* Journal of Applied Polymer Science, 2015. **132**(14).
159. Nagy, G., et al., *Controlled release of methotrexate from functionalized silica-gelatin aerogel microparticles applied against tumor cell growth.* Int J Pharm, 2019. **558**: p. 396-403.
160. GLOBOCAN. 2018 [cited 2019 13th May 2019].
161. Bastiancich, C., et al., *Anticancer drug-loaded hydrogels as drug delivery systems for the local treatment of glioblastoma.* J Control Release, 2016. **243**: p. 29-42.
162. Fischer, I., et al., *Angiogenesis in gliomas: biology and molecular pathophysiology.* Brain pathology, 2005. **15**(4): p. 297-310.

163. Ulrich, T.A. and S. Kumar, *18 Mechanobiology in Health and Disease in the Central Nervous System.* 2011.
164. Wei, X., et al., *Brain tumor-targeted drug delivery strategies.* Acta Pharm Sin B, 2014. **4**(3): p. 193-201.
165. Ferlay, J., et al., *Estimates of worldwide burden of cancer in 2008: GLOBOCAN 2008.* International journal of cancer, 2010. **127**(12): p. 2893-2917.
166. Bray, F., et al., *Global cancer statistics 2018: GLOBOCAN estimates of incidence and mortality worldwide for 36 cancers in 185 countries.* CA: a cancer journal for clinicians, 2018. **68**(6): p. 394-424.
167. Dolecek, T.A., et al., *CBTRUS statistical report: primary brain and central nervous system tumors diagnosed in the United States in 2005–2009.* Neuro-oncology, 2012. **14**(suppl_5): p. v1-v49.
168. Grossman, S.A. and J.F. Batara. *Current management of glioblastoma multiforme*. in *Seminars in oncology*. 2004. Elsevier.
169. Bastiancich, C., et al., *Drug combination using an injectable nanomedicine hydrogel for glioblastoma treatment.* International journal of pharmaceutics, 2019. **559**: p. 220-227.
170. Stupp, R., et al., *Radiotherapy plus concomitant and adjuvant temozolomide for glioblastoma.* New England Journal of Medicine, 2005. **352**(10): p. 987-996.
171. López-Dávila, V., A.M. Seifalian, and M. Loizidou, *Organic nanocarriers for cancer drug delivery.* Current opinion in pharmacology, 2012. **12**(4): p. 414-419.
172. Ghosh, D., S. Nandi, and S. Bhattacharjee, *Combination therapy to checkmate glioblastoma: clinical challenges and advances.* Clinical and translational medicine, 2018. **7**(1): p. 33.
173. Sottoriva, A., et al., *Intratumor heterogeneity in human glioblastoma reflects cancer evolutionary dynamics.* Proceedings of the National Academy of Sciences, 2013. **110**(10): p. 4009-4014.
174. Inda, M.M., et al., *Tumor heterogeneity is an active process maintained by a mutant EGFR-induced cytokine circuit in glioblastoma.* Genes Dev, 2010. **24**(16): p. 1731-45.
175. Tseng, Y.Y., et al., *Concurrent Chemotherapy of Malignant Glioma in Rats by Using Multidrug-Loaded Biodegradable Nanofibrous Membranes.* Sci Rep, 2016. **6**: p. 30630.
176. Brandes, A.A. and M.V. Fiorentino, *The role of chemotherapy in recurrent malignant gliomas: an overview.* Cancer Invest, 1996. **14**(6): p. 551-9.
177. Bush, N.A., S.M. Chang, and M.S. Berger, *Current and future strategies for treatment of glioma.* Neurosurg Rev, 2017. **40**(1): p. 1-14.
178. Rahman, R., *Biomaterial-based local drug delivery to brain tumors.* Ther Deliv, 2014. **5**(12): p. 1243-5.
179. Ohgaki, H. and P. Kleihues, *Epidemiology and etiology of gliomas.* Acta Neuropathol, 2005. **109**(1): p. 93-108.
180. Lathia, J.D., et al., *Cancer stem cells in glioblastoma.* Genes Dev, 2015. **29**(12): p. 1203-17.
181. Hadjipanayis, C.G. and E.G. Van Meir, *Brain cancer propagating cells: biology, genetics and targeted therapies.* Trends Mol Med, 2009. **15**(11): p. 519-30.
182. Chen, J., et al., *A restricted cell population propagates glioblastoma growth after chemotherapy.* Nature, 2012. **488**(7412): p. 522-6.
183. Binda, E., et al., *Drug Delivery in an Orthotopic Tumor Stem Cell-Based Model of Human Glioblastoma.* Methods Mol Biol, 2019. **1869**: p. 197-205.
184. Vescovi, A.L., R. Galli, and B.A. Reynolds, *Brain tumour stem cells.* Nat Rev Cancer, 2006. **6**(6): p. 425-36.

185. Johnson, D.R., et al., *2016 Updates to the WHO Brain Tumor Classification System: What the Radiologist Needs to Know.* Radiographics, 2017. **37**(7): p. 2164-2180.
186. Furnari, F.B., et al., *Malignant astrocytic glioma: genetics, biology, and paths to treatment.* Genes Dev, 2007. **21**(21): p. 2683-710.
187. Shergalis, A., et al., *Current Challenges and Opportunities in Treating Glioblastoma.* Pharmacol Rev, 2018. **70**(3): p. 412-445.
188. Tosoni, A., et al., *Relapsed Glioblastoma: Treatment Strategies for Initial and Subsequent Recurrences.* Curr Treat Options Oncol, 2016. **17**(9): p. 49.
189. Jain, R.K., *Transport of molecules, particles, and cells in solid tumors.* Annu Rev Biomed Eng, 1999. **1**: p. 241-63.
190. Affronti, M.L., et al., *Overall survival of newly diagnosed glioblastoma patients receiving carmustine wafers followed by radiation and concurrent temozolomide plus rotational multiagent chemotherapy.* Cancer, 2009. **115**(15): p. 3501-11.
191. van den Bent, M.J., et al., *Adjuvant procarbazine, lomustine, and vincristine chemotherapy in newly diagnosed anaplastic oligodendroglioma: long-term follow-up of EORTC brain tumor group study 26951.* J Clin Oncol, 2013. **31**(3): p. 344-50.
192. Buckner, J.C., et al., *Radiation plus Procarbazine, CCNU, and Vincristine in Low-Grade Glioma.* N Engl J Med, 2016. **374**(14): p. 1344-55.
193. Jiang, Y., et al., *Enhanced Antiglioma Efficacy of Ultrahigh Loading Capacity Paclitaxel Prodrug Conjugate Self-Assembled Targeted Nanoparticles.* ACS Appl Mater Interfaces, 2017. **9**(1): p. 211-217.
194. Ramachandran, R., et al., *Theranostic 3-Dimensional nano brain-implant for prolonged and localized treatment of recurrent glioma.* Sci Rep, 2017. **7**: p. 43271.
195. Querido, A., *On the permeability of the blood-brain barrier.* Arch Neerl Physiol Homme Anim, 1948. **28**(3-4): p. 432-43.
196. Friedemann, U., *Blood-brain barrier.* Physiological Reviews, 1942. **22**(2): p. 125-145.
197. Abbott, N.J., et al., *Structure and function of the blood-brain barrier.* Neurobiol Dis, 2010. **37**(1): p. 13-25.
198. Liu, X., et al., *Development of a computational approach to predict blood-brain barrier permeability.* Drug Metab Dispos, 2004. **32**(1): p. 132-9.
199. Banks, W.A., *Characteristics of compounds that cross the blood-brain barrier.* BMC Neurol, 2009. **9 Suppl 1**: p. S3.
200. Clark, D.E., *In silico prediction of blood-brain barrier permeation.* Drug Discov Today, 2003. **8**(20): p. 927-33.
201. Bodor, N. and P. Buchwald, *Barriers to remember: brain-targeting chemical delivery systems and Alzheimer's disease.* Drug Discov Today, 2002. **7**(14): p. 766-74.
202. van Tellingen, O., et al., *Overcoming the blood-brain tumor barrier for effective glioblastoma treatment.* Drug Resist Updat, 2015. **19**: p. 1-12.
203. Miranda, A., et al., *Breaching barriers in glioblastoma. Part II: Targeted drug delivery and lipid nanoparticles.* Int J Pharm, 2017. **531**(1): p. 389-410.
204. Chacko, A.M., et al., *Targeted delivery of antibody-based therapeutic and imaging agents to CNS tumors: crossing the blood-brain barrier divide.* Expert Opin Drug Deliv, 2013. **10**(7): p. 907-26.
205. Agarwal, S., et al., *Vesicular systems employing natural substances as promising drug candidates for MMP inhibition in glioblastoma: A nanotechnological approach.* Int J Pharm, 2018. **551**(1-2): p. 339-361.
206. Wolburg, H., et al., *Localization of claudin-3 in tight junctions of the blood-brain barrier is selectively lost during experimental autoimmune encephalomyelitis and human glioblastoma multiforme.* Acta Neuropathol, 2003. **105**(6): p. 586-92.

207. Fabis, M.J., et al., *Loss of blood-brain barrier integrity in the spinal cord is common to experimental allergic encephalomyelitis in knockout mouse models.* Proc Natl Acad Sci U S A, 2007. **104**(13): p. 5656-61.
208. Yu, X., et al., *Design of Nanoparticle-Based Carriers for Targeted Drug Delivery.* J Nanomater, 2016. **2016**.
209. Hendricks, B.K., A.A. Cohen-Gadol, and J.C. Miller, *Novel delivery methods bypassing the blood-brain and blood-tumor barriers.* Neurosurg Focus, 2015. **38**(3): p. E10.
210. Schlageter, K.E., et al., *Microvessel organization and structure in experimental brain tumors: microvessel populations with distinctive structural and functional properties.* Microvasc Res, 1999. **58**(3): p. 312-28.
211. Ruan, S., et al., *Ligand-Mediated and Enzyme-Directed Precise Targeting and Retention for the Enhanced Treatment of Glioblastoma.* ACS Appl Mater Interfaces, 2017. **9**(24): p. 20348-20360.
212. Chen, Y. and L. Liu, *Modern methods for delivery of drugs across the blood-brain barrier.* Adv Drug Deliv Rev, 2012. **64**(7): p. 640-65.
213. Lu, W., et al., *Cationic albumin conjugated pegylated nanoparticle with its transcytosis ability and little toxicity against blood-brain barrier.* Int J Pharm, 2005. **295**(1-2): p. 247-60.
214. Liu, K., et al., *Paclitaxel and quercetin nanoparticles co-loaded in microspheres to prolong retention time for pulmonary drug delivery.* Int J Nanomedicine, 2017. **12**: p. 8239-8255.
215. Yoo, J.W., et al., *Bio-inspired, bioengineered and biomimetic drug delivery carriers.* Nat Rev Drug Discov, 2011. **10**(7): p. 521-35.
216. Mir, M., N. Ahmed, and A.U. Rehman, *Recent applications of PLGA based nanostructures in drug delivery.* Colloids Surf B Biointerfaces, 2017. **159**: p. 217-231.
217. Cabezas, L.I., et al., *Validation of a mathematical model for the description of hydrophilic and hydrophobic drug delivery from biodegradable foams: Experimental and comparison using indomethacin as released drug.* Industrial & Engineering Chemistry Research, 2014. **53**(21): p. 8866-8873.
218. Chew, S., V. Hinojosa, and M. Arriaga, *Bioresorbable polymer microparticles in the medical and pharmaceutical fields*, in *Bioresorbable Polymers for Biomedical Applications*. 2017, Elsevier. p. 229-264.
219. Dunne, M., O. Corrigan, and Z. Ramtoola, *Influence of particle size and dissolution conditions on the degradation properties of polylactide-co-glycolide particles.* Biomaterials, 2000. **21**(16): p. 1659-1668.
220. Shah, S.R., et al., *Verteporfin-loaded polymeric microparticles for intratumoral treatment of brain cancer.* Molecular pharmaceutics, 2019.
221. Brem, H., et al., *Placebo-controlled trial of safety and efficacy of intraoperative controlled delivery by biodegradable polymers of chemotherapy for recurrent gliomas. The Polymer-brain Tumor Treatment Group.* Lancet, 1995. **345**(8956): p. 1008-12.
222. Domb, A.J. and W. Khan, *Focal controlled drug delivery*. 2014: Springer.
223. Domb, A.J. and N. Kumar, *Biodegradable polymers in clinical use and clinical development*. 2011: John Wiley & Sons.
224. Proost, J.H., *13 Pharmacokinetic/Pharmacodynamic Modelling in Drug Targeting.* Methods and Principles in Medicinal Chemistry, 2001: p. 333.
225. Saka, R., P. Sathe, and W. Khan, *Brain local delivery strategy*, in *Brain Targeted Drug Delivery System*. 2019, Elsevier. p. 241-286.
226. Zhang, S., M. Xing, and B. Li, *Recent advances in musculoskeletal local drug delivery.* Acta biomaterialia, 2019.
227. Newman, M.R. and D.S. Benoit, *Local and targeted drug delivery for bone regeneration.* Current opinion in biotechnology, 2016. **40**: p. 125-132.
228. Ziemba, A.M. and R.J. Gilbert, *Biomaterials for local, controlled drug delivery to the injured spinal cord.* Frontiers in pharmacology, 2017. **8**: p. 245.

229. Vulic, K. and M.S. Shoichet, *Affinity-based drug delivery systems for tissue repair and regeneration.* Biomacromolecules, 2014. **15**(11): p. 3867-3880.
230. Sudhakar, Y., K. Kuotsu, and A. Bandyopadhyay, *Buccal bioadhesive drug delivery—a promising option for orally less efficient drugs.* Journal of controlled release, 2006. **114**(1): p. 15-40.
231. Hearnden, V., et al., *New developments and opportunities in oral mucosal drug delivery for local and systemic disease.* Advanced drug delivery reviews, 2012. **64**(1): p. 16-28.
232. Langer, R. and J. Folkman, *Polymers for the sustained release of proteins and other macromolecules.* Nature, 1976. **263**(5580): p. 797.
233. Vinay, R. and V. KusumDevi, *Potential of targeted drug delivery system for the treatment of bone metastasis.* Drug delivery, 2016. **23**(1): p. 21-29.
234. Dwivedi, P., et al., *Engineered multifunctional biodegradable hybrid microparticles for paclitaxel delivery in cancer therapy.* Materials Science and Engineering: C, 2019.
235. Howell, S., *Pharmacologic principles of intraperitoneal chemotherapy for the treatment of ovarian cancer.* International Journal of Gynecologic Cancer, 2008. **18**(Suppl 1): p. 20-25.
236. Santhosh, K.T., A. Alizadeh, and S. Karimi-Abdolrezaee, *Design and optimization of PLGA microparticles for controlled and local delivery of Neuregulin-1 in traumatic spinal cord injury.* Journal of Controlled Release, 2017. **261**: p. 147-162.
237. Caplin, J.D. and A.J. García, *Implantable antimicrobial biomaterials for local drug delivery in bone infection models.* Acta biomaterialia, 2019.
238. Preisig, D., et al., *Mucoadhesive microparticles for local treatment of gastrointestinal diseases.* European Journal of Pharmaceutics and Biopharmaceutics, 2016. **105**: p. 156-165.
239. Andrews, G.P., T.P. Laverty, and D.S. Jones, *Mucoadhesive polymeric platforms for controlled drug delivery.* European Journal of Pharmaceutics and Biopharmaceutics, 2009. **71**(3): p. 505-518.
240. Fan, Y., et al., *Local release of rapamycin by microparticles delays islet rejection within the anterior chamber of the eye.* Scientific reports, 2019. **9**(1): p. 3918.
241. Morishita, M. and K. Park, *Biodrug delivery systems: fundamentals, applications and clinical development*. 2016: CRC Press.
242. Fisher, R., L. Pusztai, and C. Swanton, *Cancer heterogeneity: implications for targeted therapeutics.* British journal of cancer, 2013. **108**(3): p. 479.
243. Ganz, D.E., et al., *Tissue transport affects how treatment scheduling increases the efficacy of chemotherapeutic drugs.* Journal of theoretical biology, 2018. **438**: p. 21-33.
244. Debinski, W., *Drug cocktails for effective treatment of glioblastoma multiforme.* Expert review of neurotherapeutics, 2008. **8**(4): p. 515-517.
245. Stupp, R., et al., *High-grade glioma: ESMO Clinical Practice Guidelines for diagnosis, treatment and follow-up.* Annals of oncology, 2014. **25**(suppl_3): p. iii93-iii101.
246. Yoon, H.J., et al., *Differential diagnosis of oligodendroglial and astrocytic tumors using imaging results: the added value of perfusion MR imaging.* Neuroradiology, 2017. **59**(7): p. 665-675.
247. Chaichana, K.L., L. Pinheiro, and H. Brem, *Delivery of local therapeutics to the brain: working toward advancing treatment for malignant gliomas.* Therapeutic delivery, 2015. **6**(3): p. 353-369.
248. Parrish, K., J.N. Sarkaria, and W.F. Elmquist, *Improving drug delivery to primary and metastatic brain tumors: strategies to overcome the blood–brain barrier.* Clinical Pharmacology & Therapeutics, 2015. **97**(4): p. 336-346.
249. Brem, H. and P. Gabikian, *Biodegradable polymer implants to treat brain tumors.* Journal of controlled release, 2001. **74**(1-3): p. 63-67.

250. DiMeco, F., et al., *Local delivery of mitoxantrone for the treatment of malignant brain tumors in rats.* Journal of neurosurgery, 2002. **97**(5): p. 1173-1178.
251. Walter, K.A., et al., *Interstitial taxol delivered from a biodegradable polymer implant against experimental malignant glioma.* Cancer research, 1994. **54**(8): p. 2207-2212.
252. Lesniak, M.S., et al., *Local delivery of doxorubicin for the treatment of malignant brain tumors in rats.* Anticancer research, 2005. **25**(6B): p. 3825-3831.
253. Bow, H., et al., *Local delivery of angiogenesis-inhibitor minocycline combined with radiotherapy and oral temozolomide chemotherapy in 9L glioma.* Journal of neurosurgery, 2014. **120**(3): p. 662-669.
254. Yohay, K., et al., *Efficacy of local polymer-based and systemic delivery of the anti-glutamatergic agents riluzole and memantine in rat glioma models.* Journal of neurosurgery, 2014. **120**(4): p. 854-863.
255. Bianco, J., et al., *On glioblastoma and the search for a cure: where do we stand?* Cellular and Molecular Life Sciences, 2017. **74**(13): p. 2451-2466.
256. Dazzi, C., et al., *A sequential chemo-radiotherapeutic treatment for patients with malignant gliomas: a phase II pilot study.* Anticancer research, 2000. **20**(1B): p. 515-518.
257. Kozielski, K.L., et al., *Cancer-selective nanoparticles for combinatorial siRNA delivery to primary human GBM in vitro and in vivo.* Biomaterials, 2019.
258. Zhang, W., et al., *A coupled field study of subsurface fracture flow and colloid transport.* Journal of Hydrology, 2015. **524**: p. 476-488.
259. Masciopinto, C., R. La Mantia, and C.V. Chrysikopoulos, *Fate and transport of pathogens in a fractured aquifer in the Salento area, Italy.* Water Resources Research, 2008. **44**(1).
260. Ganesh, A.N., et al., *Colloidal aggregation: From screening nuisance to formulation nuance.* Nano today, 2018. **19**: p. 188-200.
261. Royer, J.R., et al., *Rheology and dynamics of colloidal superballs.* Soft Matter, 2015. **11**(28): p. 5656-5665.
262. Ni, R., et al., *Phase diagram of colloidal hard superballs: from cubes via spheres to octahedra.* Soft Matter, 2012. **8**(34): p. 8826-8834.
263. Egres, R.G. and N.J. Wagner, *The rheology and microstructure of acicular precipitated calcium carbonate colloidal suspensions through the shear thickening transition.* Journal of rheology, 2005. **49**(3): p. 719-746.
264. Danov, K.D., D.K. Danova, and P.A. Kralchevsky, *Hydrodynamic forces acting on a microscopic emulsion drop growing at a capillary tip in relation to the process of membrane emulsification.* Journal of colloid and interface science, 2007. **316**(2): p. 844-857.
265. Mendoza, A.J., et al., *Particle laden fluid interfaces: dynamics and interfacial rheology.* Advances in colloid and interface science, 2014. **206**: p. 303-319.
266. Miller, R. and L. Liggieri, *Bubble and drop interfaces*. 2011: CRC Press.
267. Fuller, G.G. and J. Vermant, *dynamics and rheology of complex fluid–fluid interfaces.* Soft Matter, 2011. **7**(17): p. 7583-7585.
268. Hong, Y., et al., *Preparation of porous polylactide microspheres by emulsion‐solvent evaporation based on solution induced phase separation.* Polymers for advanced technologies, 2005. **16**(8): p. 622-627.
269. Freiberg, S. and X. Zhu, *Polymer microspheres for controlled drug release.* International journal of pharmaceutics, 2004. **282**(1): p. 1-18.
270. Palmer, D., et al., *Printing particles: A high-throughput technique for the production of uniform, bioresorbable polymer microparticles and encapsulation of therapeutic peptides.* Chemical Engineering Science, 2017. **166**: p. 122-129.
271. Ekanem, E.E., et al., *Structured biodegradable polymeric microparticles for drug delivery produced using flow focusing glass microfluidic devices.* ACS applied materials & interfaces, 2015. **7**(41): p. 23132-23143.

272. Mo, L., et al., *Preparation and characterization of teniposide PLGA nanoparticles and their uptake in human glioblastoma U87MG cells.* International journal of pharmaceutics, 2012. **436**(1): p. 815-824.
273. Yang, Y.-Y., H.-H. Chia, and T.-S. Chung, *Effect of preparation temperature on the characteristics and release profiles of PLGA microspheres containing protein fabricated by double-emulsion solvent extraction/evaporation method.* Journal of Controlled Release, 2000. **69**(1): p. 81-96.
274. Qutachi, O., et al., *Injectable and porous PLGA microspheres that form highly porous scaffolds at body temperature.* Acta biomaterialia, 2014. **10**(12): p. 5090-5098.
275. Davoodi, P., et al., *Coaxial electrohydrodynamic atomization: microparticles for drug delivery applications.* Journal of Controlled Release, 2015. **205**: p. 70-82.
276. Han, W., et al., *Preparation of polyacrylonitrile-based porous hollow carbon microspheres.* Colloids and Surfaces A: Physicochemical and Engineering Aspects, 2017. **520**: p. 467-476.
277. Song, L., et al., *Design, preparation and enhanced photocatalytic activity of porous BiOCl/BiVO 4 microspheres via a coprecipitation-hydrothermal method.* Journal of Alloys and Compounds, 2017.
278. Deshmukh, O.S., et al., *Hard and soft colloids at fluid interfaces: Adsorption, interactions, assembly & rheology.* Advances in colloid and interface science, 2015. **222**: p. 215-227.
279. Hunter, T.N., et al., *The role of particles in stabilising foams and emulsions.* Advances in Colloid and Interface Science, 2008. **137**(2): p. 57-81.
280. Sacanna, S., W. Kegel, and A. Philipse, *Thermodynamically stable pickering emulsions.* Physical review letters, 2007. **98**(15): p. 158301.
281. Ramsden, W., *Separation of Solids in the Surface-Layers of Solutions and'Suspensions'(Observations on Surface-Membranes, Bubbles, Emulsions, and Mechanical Coagulation).--Preliminary Account.* Proceedings of the royal Society of London, 1903. **72**: p. 156-164.
282. Zhang, M.-J., et al., *Uniform microparticles with controllable highly interconnected hierarchical porous structures.* ACS applied materials & interfaces, 2015. **7**(25): p. 13758-13767.
283. Qu, J.-B., et al., *A novel stationary phase derivatized from hydrophilic gigaporous polystyrene-based microspheres for high-speed protein chromatography.* Journal of Chromatography A, 2009. **1216**(37): p. 6511-6516.
284. Nakayama, D., et al., *Simple and precise preparation of a porous gel for a colorimetric glucose sensor by a templating technique.* Angewandte Chemie, 2003. **115**(35): p. 4329-4332.
285. Zhao, X., et al., *Colloidal crystal beads as supports for biomolecular screening.* Angewandte Chemie International Edition, 2006. **45**(41): p. 6835-6838.
286. Wang, H., et al., *Enhanced encapsulation and bioavailability of breviscapine in PLGA microparticles by nanocrystal and water-soluble polymer template techniques.* European Journal of Pharmaceutics and Biopharmaceutics, 2017. **115**: p. 177-185.
287. Kauffman, K.J., et al., *Optimization of rapamycin-loaded acetalated dextran microparticles for immunosuppression.* International journal of pharmaceutics, 2012. **422**(1): p. 356-363.
288. Le Ray, A.-M., et al., *Vancomycin encapsulation in biodegradable poly (ε-caprolactone) microparticles for bone implantation. Influence of the formulation process on size, drug loading, in vitro release and cytocompatibility.* Biomaterials, 2003. **24**(3): p. 443-449.
289. Blanco-García, E., et al., *Development and characterization of anti-inflammatory activity of curcumin-loaded biodegradable microspheres with*

potential use in intestinal inflammatory disorders. International journal of pharmaceutics, 2017. **518**(1): p. 86-104.
290. Park, C.G., et al., *Enhanced ocular efficacy of topically-delivered dorzolamide with nanostructured mucoadhesive microparticles.* International journal of pharmaceutics, 2017. **522**(1): p. 66-73.
291. J, S.S., *Surgical delivery of drug releasing poly(lactic-co-glycolic acid)/poly(ethylene glycol) paste with in vivo effects against glioblastoma.* Ann R Coll Surg Engl, 2014. **96**: p. 495-501.
292. Xiang, A. and A.J. McHugh, *A generalized diffusion–dissolution model for drug release from rigid polymer membrane matrices.* Journal of membrane science, 2011. **366**(1): p. 104-115.
293. Leong, K. and R. Langer, *Polymeric controlled drug delivery.* Advanced Drug Delivery Reviews, 1988. **1**(3): p. 199-233.
294. Thomann, F.S., et al., *Hygrothermal simulation-informed design of mesoporous desiccants for optimised energy efficiency of mixed mode air conditioning systems.* Journal of Materials Chemistry A, 2015. **3**(33): p. 17290-17303.
295. Sel, O., et al., *Principles of hierarchical meso-and macropore architectures by liquid crystalline and polymer colloid templating.* Langmuir, 2006. **22**(5): p. 2311-2322.
296. Rolison, D.R., *Catalytic nanoarchitectures--the importance of nothing and the unimportance of periodicity.* Science, 2003. **299**(5613): p. 1698-701.
297. HAYNES, J., *ADSORPTION, SURFACE-AREA AND POROSITY-GREGG, SJ, SING, SW*. 1983, ROYAL SOC CHEMISTRY THOMAS GRAHAM HOUSE, SCIENCE PARK, MILTON ROAD ….
298. Ni, R., et al., *Exploring polyvinylpyrrolidone in the engineering of large porous PLGA microparticles via single emulsion method with tunable sustained release in the lung: in vitro and in vivo characterization.* Journal of Controlled Release, 2017. **249**: p. 11-22.
299. Xie, J., et al., *Electrohydrodynamic atomization for biodegradable polymeric particle production.* Journal of Colloid and Interface Science, 2006. **302**(1): p. 103-112.
300. Atkins, P., *Shriver and Atkins' inorganic chemistry*. 2010: Oxford University Press, USA.
301. Rouquerol, J., et al., *Adsorption by powders and porous solids: principles, methodology and applications*. 2013: Academic press.
302. Torquato, S. and Y. Jiao, *Dense packings of the Platonic and Archimedean solids.* Nature, 2009. **460**(7257): p. 876-879.
303. Damasceno, P.F., M. Engel, and S.C. Glotzer, *Predictive self-assembly of polyhedra into complex structures.* Science, 2012. **337**(6093): p. 453-457.
304. Erbil, H.Y., *Control of stain geometry by drop evaporation of surfactant containing dispersions.* Advances in colloid and interface science, 2015. **222**: p. 275-290.
305. Elbert, D.L., *Liquid–liquid two-phase systems for the production of porous hydrogels and hydrogel microspheres for biomedical applications: a tutorial review.* Acta biomaterialia, 2011. **7**(1): p. 31-56.
306. Wagner, C.S., et al., *Particle nanosomes with tailored silhouettes.* Soft Matter, 2012. **8**(6): p. 1928-1933.
307. Dang, J.M. and K.W. Leong, *Natural polymers for gene delivery and tissue engineering.* Advanced drug delivery reviews, 2006. **58**(4): p. 487-499.
308. Leong, K., et al., *DNA-polycation nanospheres as non-viral gene delivery vehicles.* Journal of controlled release, 1998. **53**(1): p. 183-193.
309. Serda, R.E., et al., *Multi-stage delivery nano-particle systems for therapeutic applications.* Biochimica et Biophysica Acta (BBA)-General Subjects, 2011. **1810**(3): p. 317-329.

310. Vanarase, A.U., J.G. Osorio, and F.J. Muzzio, *Effects of powder flow properties and shear environment on the performance of continuous mixing of pharmaceutical powders.* Powder technology, 2013. **246**: p. 63-72.
311. Allen, T., *Particle size measurement*. 2013: Springer.
312. Lowell, S., et al., *Characterization of porous solids and powders: surface area, pore size and density*. Vol. 16. 2012: Springer Science & Business Media.
313. Schneider, D., et al., *Transport properties of hierarchical micro–mesoporous materials.* Chemical Society Reviews, 2016. **45**(12): p. 3439-3467.
314. Gregg, S. and K. Sing, *Adsorption, surface area and porosity academic.* New York, 1982: p. 242-245.
315. Rolison, D.R., *Catalytic nanoarchitectures--the importance of nothing and the unimportance of periodicity.* Science, 2003. **299**(5613): p. 1698-1701.
316. Branton, P.J., P.G. Hall, and K.S. Sing, *Physisorption of alcohols and water vapour by MCM-41, a model mesoporous adsorbent.* Adsorption, 1995. **1**(1): p. 77-82.
317. Branton, P.J., K.S. Sing, and J.W. White, *Adsorption of carbon tetrachloride and nitrogen by 3.4 nm pore diameter siliceous MCM-41.* Journal of the Chemical Society, Faraday Transactions, 1997. **93**(13): p. 2337-2340.
318. Mylonaki, I., et al., *Imaging the porous structure in the core of degrading PLGA microparticles: The effect of molecular weight.* Journal of controlled release, 2018. **286**: p. 231-239.
319. Li, L. and S.P. Schwendeman, *Mapping neutral microclimate pH in PLGA microspheres.* Journal of Controlled Release, 2005. **101**(1-3): p. 163-173.
320. Liu, Y. and S.P. Schwendeman, *Mapping microclimate pH distribution inside protein-encapsulated PLGA microspheres using confocal laser scanning microscopy.* Molecular pharmaceutics, 2012. **9**(5): p. 1342-1350.
321. Busatto, C., et al., *Effect of particle size, polydispersity and polymer degradation on progesterone release from PLGA microparticles: Experimental and mathematical modeling.* International journal of pharmaceutics, 2018. **536**(1): p. 360-369.
322. Auras, R.A., et al., *Poly (lactic acid): synthesis, structures, properties, processing, and applications*. Vol. 10. 2011: John Wiley & Sons.
323. Qodratnama, R., *Controlling the rate of the release of proteins from microparticles for tissue engineering applications*. 2012, University of Nottingham.
324. Chen, J.C., L.M. Li, and J.Q. Gao, *Biomaterials for local drug delivery in central nervous system.* Int J Pharm, 2019. **560**: p. 92-100.
325. Fuhrmann, T., P.N. Anandakumaran, and M.S. Shoichet, *Combinatorial Therapies After Spinal Cord Injury: How Can Biomaterials Help?* Adv Healthc Mater, 2017. **6**(10).
326. Fuchs, K., et al., *Drug-eluting embolic microspheres for local drug delivery - State of the art.* J Control Release, 2017. **262**: p. 127-138.
327. Shin, S.W., *The current practice of transarterial chemoembolization for the treatment of hepatocellular carcinoma.* Korean J Radiol, 2009. **10**(5): p. 425-34.
328. Yang, J., et al., *Development of bioactive materials for glioblastoma therapy.* Bioact Mater, 2016. **1**(1): p. 29-38.
329. LaVan, D.A., T. McGuire, and R. Langer, *Small-scale systems for in vivo drug delivery.* Nat Biotechnol, 2003. **21**(10): p. 1184-91.
330. Tang, X., et al., *Polymeric biomaterials in tissue engineering and regenerative medicine*, in *Natural and Synthetic Biomedical Polymers*. 2014, Elsevier. p. 351-371.
331. Hu, Q., et al., *Glioma therapy using tumor homing and penetrating peptide-functionalized PEG-PLA nanoparticles loaded with paclitaxel.* Biomaterials, 2013. **34**(22): p. 5640-50.

332. Kim, T.Y., et al., *Phase I and pharmacokinetic study of Genexol-PM, a cremophor-free, polymeric micelle-formulated paclitaxel, in patients with advanced malignancies.* Clin Cancer Res, 2004. **10**(11): p. 3708-16.
333. Kim, D.W., et al., *Multicenter phase II trial of Genexol-PM, a novel Cremophor-free, polymeric micelle formulation of paclitaxel, with cisplatin in patients with advanced non-small-cell lung cancer.* Ann Oncol, 2007. **18**(12): p. 2009-14.
334. Chen, X., et al., *A partition-type tubular scaffold loaded with PDGF-releasing microspheres for spinal cord repair facilitates the directional migration and growth of cells.* Neural Regen Res, 2018. **13**(7): p. 1231-1240.
335. Floyd, J.A., A. Galperin, and B.D. Ratner, *Drug encapsulated polymeric microspheres for intracranial tumor therapy: A review of the literature.* Adv Drug Deliv Rev, 2015. **91**: p. 23-37.
336. Wait, S.D., et al., *Polymeric drug delivery for the treatment of glioblastoma.* Neuro Oncol, 2015. **17 Suppl 2**: p. ii9-ii23.
337. Smith, S., et al., *Overall survival in an orthotopic GBM model is significantly prolonged by neurosurgical delivery of PLGA/PEG interstitial chemotherapy.* Neuro-oncology, 2018. **20**(suppl_1): p. i6-i6.
338. Chew, S.A. and S. Danti, *Biomaterial-Based Implantable Devices for Cancer Therapy.* Adv Healthc Mater, 2017. **6**(2).
339. Ningaraj, N.S., *Drug delivery to brain tumours: challenges and progress.* Expert Opin Drug Deliv, 2006. **3**(4): p. 499-509.
340. Rich, J.N. and D.D. Bigner, *Development of novel targeted therapies in the treatment of malignant glioma.* Nat Rev Drug Discov, 2004. **3**(5): p. 430-46.
341. Wang, Z., et al., *Local delivery of minocycline from metal ion-assisted self-assembled complexes promotes neuroprotection and functional recovery after spinal cord injury.* Biomaterials, 2017. **112**: p. 62-71.
342. Drappatz, J., et al., *Phase I study of GRN1005 in recurrent malignant glioma.* Clin Cancer Res, 2013. **19**(6): p. 1567-76.
343. Jendrossek, V., C. Belka, and M. Bamberg, *Novel chemotherapeutic agents for the treatment of glioblastoma multiforme.* Expert Opin Investig Drugs, 2003. **12**(12): p. 1899-924.
344. Simpson, L. and E. Galanis, *Recurrent glioblastoma multiforme: advances in treatment and promising drug candidates.* Expert Rev Anticancer Ther, 2006. **6**(11): p. 1593-607.
345. Guo, J., et al., *Targeted Drug Delivery via Folate Receptors for the Treatment of Brain Cancer: Can the Promise Deliver?* J Pharm Sci, 2017. **106**(12): p. 3413-3420.
346. Venishetty, V.K., et al., *Increased brain uptake of docetaxel and ketoconazole loaded folate-grafted solid lipid nanoparticles.* Nanomedicine, 2013. **9**(1): p. 111-21.
347. Kuo, Y.C. and Y.C. Chen, *Targeting delivery of etoposide to inhibit the growth of human glioblastoma multiforme using lactoferrin- and folic acid-grafted poly(lactide-co-glycolide) nanoparticles.* Int J Pharm, 2015. **479**(1): p. 138-49.
348. Needle, M.N., et al., *Phase II study of daily oral etoposide in children with recurrent brain tumors and other solid tumors.* Med Pediatr Oncol, 1997. **29**(1): p. 28-32.
349. Fidler, I.J., et al., *The seed and soil hypothesis: vascularisation and brain metastases.* Lancet Oncol, 2002. **3**(1): p. 53-7.
350. Black, K.L. and N.S. Ningaraj, *Modulation of brain tumor capillaries for enhanced drug delivery selectively to brain tumor.* Cancer Control, 2004. **11**(3): p. 165-73.
351. Li, Y., et al., *Delivery of nanomedicines to extracellular and intracellular compartments of a solid tumor.* Adv Drug Deliv Rev, 2012. **64**(1): p. 29-39.
352. Jang, S.H., et al., *Drug delivery and transport to solid tumors.* Pharm Res, 2003. **20**(9): p. 1337-50.

353. Tannock, I.F. and D. Rotin, *Acid pH in tumors and its potential for therapeutic exploitation.* Cancer Res, 1989. **49**(16): p. 4373-84.
354. da Silva, D., et al., *Biocompatibility, biodegradation and excretion of polylactic acid (PLA) in medical implants and theranostic systems.* Chemical Engineering Journal, 2018. **340**: p. 9-14.
355. Avérous, L. and E. Pollet, *Biodegradable Polymers, Environmental Silicate Nano-Biocomposites.* Springer–Verlag London, 2012. **2**: p. 25-26.
356. Malik, K., et al., *Atrigel: A potential parenteral controlled drug delivery system.* Der Pharmacia Sinica, 2010. **1**(1): p. 74-81.
357. Wolinsky, J.B., Y.L. Colson, and M.W. Grinstaff, *Local drug delivery strategies for cancer treatment: gels, nanoparticles, polymeric films, rods, and wafers.* Journal of controlled release, 2012. **159**(1): p. 14-26.
358. Madsen, J., et al., *Nile Blue-based nanosized pH sensors for simultaneous far-red and near-infrared live bioimaging.* J Am Chem Soc, 2013. **135**(39): p. 14863-70.
359. Cohen, S., et al., *Controlled delivery systems for proteins based on poly(lactic/glycolic acid) microspheres.* Pharm Res, 1991. **8**(6): p. 713-20.
360. Langer, R., et al., *Isolations of a cartilage factor that inhibits tumor neovascularization.* Science, 1976. **193**(4247): p. 70-2.
361. Li, K.W., et al., *Polilactofate microspheres for Paclitaxel delivery to central nervous system malignancies.* Clin Cancer Res, 2003. **9**(9): p. 3441-7.
362. Emerich, D.F., et al., *Injectable chemotherapeutic microspheres and glioma I: enhanced survival following implantation into the cavity wall of debulked tumors.* Pharm Res, 2000. **17**(7): p. 767-75.
363. Ranganath, S.H. and C.H. Wang, *Biodegradable microfiber implants delivering paclitaxel for post-surgical chemotherapy against malignant glioma.* Biomaterials, 2008. **29**(20): p. 2996-3003.
364. Kumar Naraharisetti, P., et al., *In vivo performance of implantable biodegradable preparations delivering Paclitaxel and Etanidazole for the treatment of glioma.* Biomaterials, 2007. **28**(5): p. 886-94.
365. Ong, B.Y., et al., *Paclitaxel delivery from PLGA foams for controlled release in post-surgical chemotherapy against glioblastoma multiforme.* Biomaterials, 2009. **30**(18): p. 3189-96.
366. Menei, P., et al., *Local and sustained delivery of 5-fluorouracil from biodegradable microspheres for the radiosensitization of malignant glioma: a randomized phase II trial.* Neurosurgery, 2005. **56**(2): p. 242-8; discussion 242-8.
367. Menei, P., et al., *Stereotaxic implantation of 5-fluorouracil-releasing microspheres in malignant glioma.* Cancer, 2004. **100**(2): p. 405-10.
368. Tseng, Y.-Y., et al., *Sustainable release of carmustine from biodegradable poly [(D, L)-lactide-co-glycolide] nanofibrous membranes in the cerebral cavity: in vitro and in vivo studies.* Expert opinion on drug delivery, 2013. **10**(7): p. 879-888.
369. Feng, B., et al., *Delivery of sodium borocaptate to glioma cells using immunoliposome conjugated with anti-EGFR antibodies by ZZ-His.* Biomaterials, 2009. **30**(9): p. 1746-55.
370. Bota, D.A., et al., *Interstitial chemotherapy with biodegradable BCNU (Gliadel) wafers in the treatment of malignant gliomas.* Ther Clin Risk Manag, 2007. **3**(5): p. 707-15.
371. Smoll, N.R., K. Schaller, and O.P. Gautschi, *Long-term survival of patients with glioblastoma multiforme (GBM).* J Clin Neurosci, 2013. **20**(5): p. 670-5.
372. Chen, X., et al., *PLGA-PEG-PLGA triblock copolymeric micelles as oral drug delivery system: In vitro drug release and in vivo pharmacokinetics assessment.* J Colloid Interface Sci, 2017. **490**: p. 542-552.
373. Hwangbo, K-H., et al., *Facile fabrication of uniform golf-ball-shaped microparticles from various polymers*. Soft Matter, 2011. **7**: p.10874-10878.